Département de Biologie
Unité de Zoologie
Université de Fribourg (Suisse)

Mitochondrial tRNA import in the parasitic protozoon *Trypanosoma brucei* and its consequences on mitochondrial translation

THESE

présentée à la Faculté des Sciences de l'Université de Fribourg (Suisse)
pour l'obtention du grade de *Doctor rerum naturalium*

Fabien Charrière
de Riaz

Nr. 1544
Imprimerie Saint-Paul
2006

Acceptée par la Faculté des Sciences de l'Université de Fribourg (Suisse) sur la proposition de

Prof. Fritz Müller, Université de Fribourg, Président du Jury
Prof. André Schneider, Université de Fribourg, Directeur de thèse, Rapporteur
Prof. Patrick Linder, Université de Genève, Corapporteur

Fribourg, le 07 novembre 2006

Le Directeur de thèse

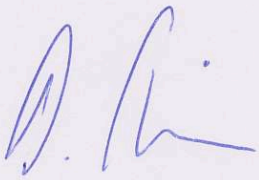

André Schneider

Le Doyen

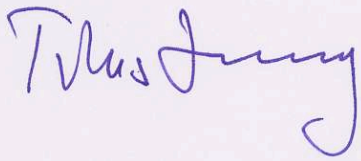

Titus Jenny

Table of contents

Summary

The protozoon parasite *Trypanosoma brucei* is the causing agent of human sleeping sickness. Besides its clinical importance *T. brucei* is also an excellent model for basic research since it has many unique features. The mitochondrion of *T. brucei*, for example, lacks tRNA genes. The tRNAs required for mitochondrial translation are therefore encoded in the nucleus and imported from the cytosol [1]. Thus, except for the initiator $tRNA^{Met}$ and $tRNA^{Sec}$, all trypanosomal tRNAs function in both the cytosol and the mitochondrion. An important consequence of mitochondrial tRNA import is that the imported tRNAs are of eukaryotic evolutionary origin. The mitochondrion however derives from a bacterial ancestor. Thus, we wanted to investigate how the bacterial-type translation system of the mitochondrion has adapted to eukaryotic-type tRNAs during evolution.

Due to the exclusive cytosolic localization of the trypanosomal initiator $tRNA^{Met}$, the only $tRNA^{Met}$ present in the mitochondrion of *T. brucei* is the imported eukaryotic elongator $tRNA^{Met}$. In bacteria and organelles, the translation initiation process requires the specific formylation of the initiator methionyl-$tRNA^{Met}$ by the methionyl-tRNA formyltransferase (MTF). The subsequent binding of the resulting initiator formylmethionyl-$tRNA^{Met}$ to the bacterial-type initiation factor 2 (IF2) promotes the interaction of the tRNA with the ribosome. In the mitochondrion of *T. brucei* a fraction of the imported elongator methionyl-$tRNA^{Met}$ is unexpectedly formylated by an extraordinary large MTF orthologue [2]. In the present work we identified the trypanosomal IF2 and we demonstrated that it is required for normal growth of the parasite. Furthermore, we showed that it recognizes the formylmethionylated imported elongator $tRNA^{Met}$, but not its unformylated counterpart. Hence, together with previous studies [1, 2], this work emphasizes the dual use of a cytosolic elongator $tRNA^{Met}$ as initiator and elongator in a mitochondrial translation system (Results A).

In order to be used in translation each tRNA needs to be attached to its cognate amino acid. The process of attachment is called aminoacylation and is catalyzed by

aminoacyl-tRNA synthetases. Since cytosolic and imported tRNAs of *T. brucei* derive from the same set of nuclear genes they are expected to be aminoacylated by the same enzymes. In agreement with this hypothesis, most trypanosomal aminoacyl-tRNA synthetases are represented by single genes. Interestingly however, the *T. brucei* genome contains two different genes for eukaryotic tryptophanyl-tRNA synthetases. We show in this work that both of these enzymes are essential for normal growth. Furthermore we demonstrate that the unexpected use of a second tryptophanyl-tRNA synthetase in *T. brucei* is caused by a mitochondria-specific editing event of the $tRNA^{Trp}$ which is required for the mitochondrial reassignment of the UGA codon to tryptophan (Results B).

In the part C of the results section some components involved in the insertion of serine and selenocysteine into trypanosomal proteins were characterized. In the context of the mitochondrial tRNA import it was shown that $tRNA^{Sec}$ is the second cytosol-specific tRNA in *T. brucei*.

In order to understand the connection between the mitochondrial tRNA import and protein translocation in *T. brucei* we used the RNA interference (RNAi) strategy to knock down the expression of the Tim17-22 and Tim8-13 homologues. These proteins are known to be components of the mitochondrial protein translocation machinery in other organisms. Morphological effects caused by their depletion are presented in the part D of the results.

Résumé

Le parasite protozoaire *Trypanosoma brucei* est l'agent pathogène responsable de la maladie du sommeil chez l'homme. En plus de son importance dans le domaine de la lutte contre les maladies tropicales, *T. brucei* est également un excellent modèle pour la recherche fondamentale car il présente beaucoup de caractéristiques qui lui sont propres. Par exemple, aucun ARN de transfert (ARNt) n'est codé dans le génome mitochondrial. Pour cette raison, les ARNts nécessaires au processus de traduction mitochondriale sont codés dans le noyau, puis importés depuis le cytosol [1]. Ainsi, mis à part l'initiateur $ARNt^{Met}$ et l'$ARNt^{Sec}$, tous les ARNts du trypanosome fonctionnent à la fois dans le cytosol et dans la mitochondrie. Une conséquence importante de l'import mitochondrial des ARNts réside dans le fait que les ARNts utilisés dans la mitochondrie de *T. brucei* ont une origine évolutionnaire eucaryote. Cependant la mitochondrie provient d'un ancêtre bactérien. C'est pourquoi nous avons voulu étudier comment le système de traduction mitochondriale, qui est de type bactérien, s'est adapté aux ARNts de type eucaryote durant l'évolution.

Etant donné que l'initiateur $ARNt^{Met}$ du trypanosome est localisé exclusivement dans le cytosol, le seul $ARNt^{Met}$ présent dans la mitochondrie de *T. brucei* est l'élongateur $ARNt^{Met}$ qui est importé depuis le cytosol. Dans les bactéries et les organelles, la formylation spécifique de l'initiateur methionyl-$ARNt^{Met}$ catalisée par la methionyl-ARNt formyltransferase (MTF) est nécessaire au processus d'initiation de la traduction. L'initiateur formylmethionyl-$ARNt^{Met}$ résultant de cette réaction se lie alors avec le facteur d'initiation 2 de type bactérien (IF2), ce qui favorise l'intéraction de l'ARNt avec le ribosome. Etonnamment, dans la mitochondrie de *T. brucei*, une partie de l'élongateur $ARNt^{Met}$ importé est formylée par un orthologue de MTF dont la taille est spécialement grande [2]. Durant ce travail de thèse, nous avons identifié IF2 chez *T. brucei* et démontré que cette protéine est nécessaire à la croissance normale du parasite. De plus, nous avons montré qu'IF2 ne reconnaît l'élongateur methionyl-$ARNt^{Met}$ que si ce dernier est formylé. Ainsi, en complément de précédentes études [1, 2], ce travail met l'accent sur le double rôle de l'élongateur

cytosolique ARNt^{Met} en tant qu'initiateur et élongateur dans un système de traduction mitochondriale (Résultats A).

Pour être fonctionnel pendant la traduction, chaque ARNt doit être attaché à son acide aminé. Le processus d'attachement, appelé aminoacylation, est catalisé par des aminoacyl-ARNt synthétases. Etant donné que chez *T. brucei* les ARNts cytosoliques et importés proviennent du même ensemble de gènes nucléaires, on s'attend à ce qu'ils soient aminoacylés par les mêmes enzymes. Le fait que la plupart des aminoacyl-ARNt synthétases du trypanosome sont représentées par des gènes uniques supporte cette hypothèse. Cependant, le génome du trypanosome contient deux différents gènes codant pour deux tryptophanyl-tRNA synthétases de type eucaryote. Nous montrons dans ce travail que ces deux enzymes sont essentielles pour une croissance normale. De plus nous démontrons que la nécessité d'une deuxième tryptophanyl-tRNA synthétase chez *T. brucei* est due à l'édition intra-mitochondriale de l'ARNt^{Trp} (tRNA editing) requise pour le ré-assignement du codon UGA en tryptophane (Résultats B).

Dans la partie C des résultats, certains composants impliqués dans l'insertion de la sérine et de la sélénocystéine dans les protéines ont été caractérisés. Dans le contexte de l'import mitochondrial des ARNts nous avons montré que l'ARNt^{Sec} est le second ARNt localisé exclusivement dans le cytosol du trypanosome.

Dans le but d'examiner le rapport entre l'import mitochondrial des ARNts et des protéines chez *T. brucei*, nous avons utilisé la technique de l'ARN interférence (RNAi) en vue de réduire sensiblement l'expression des homologues de Tim17-22 et Tim8-13. Ces protéines sont connues pour faire partie de l'appareil de translocation des protéines mitochondriales chez d'autres organismes. Les effets morphologiques causés par leur ablation sont présentés dans la partie D des résultats.

I. Introduction

A. Mitochondrial tRNA import

A.1. General introduction

The mitochondrial genome generally encodes only a small fraction of the organellar proteins, the vast majority of them being nucleus-encoded and imported from the cytosol. Nevertheless mitochondria contain a complete translation system based on rRNAs and tRNAs whose genetic origin is very often mitochondrial. However in plants, some fungi and protozoa, a variable number of tRNA genes are absent from the mitochondrial genome. In these organisms the lack is compensated for by import of a small fraction of the corresponding cytosolic tRNAs. The number of imported tRNAs extends from two in *Saccharomyces cerevisiae* [3, 4] to the complete set in trypanosomatids [1] and apicomplexans [5]. In *Trypanosoma brucei* the only cytosol-specific tRNAs are the initiator $tRNA^{Met}$ and $tRNA^{Sec}$ (part C of the results). The same tRNAs are probably also cytosol-specific in *Leishmania*. Furthermore it has been suggested that unlike in *T. brucei* a $tRNA^{Gln}$, the $tRNA^{Gln}$ (CUG), might be cytosol-specific [6].

The question of how proteins are translocated into mitochondria has been investigated in great details but the import process of negatively charged tRNAs across the hydrophobic mitochondrial membranes is still poorly understood. In the present chapter the targeting and machinery of mitochondrial tRNA import are reviewed.

A.2. Targeting

A.2.1. The import substrate

Conflicting results were found regarding the nature of the import substrate in trypanosomatids. Some 5'-extended precursor tRNAs were found in the mitochondrial fraction of *T. brucei* [7]. For example the dicistronic precursor containing $tRNA^{Ser}$(CGA) – $tRNA^{Leu}$(CAA) was found in both the cytosol and the mitochondrion of *T. brucei* [8]. In addition the dicistronic tRNA substrate was imported *in vitro* while the mature $tRNA^{Leu}$ was not [9]. Furthermore a sequence motif, which acts as an import signal was identified in the 5' extension of the precursor $tRNA^{Leu}$ [10]. In contrast to these results, *in vivo* studies showed that three different tRNAs were efficiently imported either expressed in their own genomic context or containing various lengths of the 5'flanking sequences from different tRNAs [11]. In the same study it was demonstrated that even heterologous tRNAs containing non trypanosomal flanking sequences were imported. Furthermore, a tagged version of $tRNA^{Leu}$(CAA) containing 0, 10, 59 or 216 nucleotides of its 5' flanking sequence was expressed in *T. brucei* and shown to be imported with the same efficiency than the WT $tRNA^{Leu}$(CAA) in all four cases [1]. Transfection of *Leishmania tarentolae* with constructs allowing expression of tagged $tRNA^{Ile}$ and $tRNA^{Gln}$ were performed to analyze the importance of the 5' flanking genomic sequence for *in vivo* localization [12]. Exchange or deletion of these flanking sequences changed neither their expression nor the extent of their mitochondrial ($tRNA^{Ile}$) and cytosolic ($tRNA^{Gln}$) localization. Finally in *L. tarentolae*, five different imported tRNAs were shown to be processed at their 5' and 3' ends before export from the nucleus [13]. The same study showed that *in vitro* the T7-transcribed mature $tRNA^{Ile}$ is imported more efficiently than its 5' extended precursor.

These data suggest that the precursors are not the *in vivo* import substrates. Primer extension analysis of mitochondrial tRNAs from *Leishmania tarentolae* and *Trypanosoma brucei* has shown that the band corresponding to precursor tRNA might be derived from circularized mature tRNA molecules. It has been suggested that these molecules could be produced by an endogenous RNA ligase *in vivo* or during mitochondrial isolation [14].

In summary these results suggest that the *in vivo* import substrate is the mature tRNA.

A.2.2. Targeting signals

Different *in vivo* and *in vitro* studies revealed the tRNA import signals in different species. These results have been reviewed by Bhattacharyya *et al* [15] (table 1).

Table 1: Import signals in tRNAs (updated from [15])

Organisms	**tRNA species**	**Location of signal**	**Evidence**	**Reference**
Trypanosoma brucei	$tRNA^{Met-e}(CAU)$	T arm	Point mutation	[16]
	$tRNA^{Leu}(CAA)$	5' flank	Deletion, point mutation	[10]
Leishmania spp	$tRNA^{Tyr}(GUA)$	D arm	Fragmentation, point mutation	[17]
	$tRNA^{Ile}(UAU)$	D arm		[12]
		V-T arm	Domain swap	[18]
	$tRNA^{Trp}(CCA)$	Anticodon	Fractionation	[13]
	$tRNA^{Thr}(AGU)$	V-loop	C→U editing	[19]
	$tRNA^{Glu}(UUC)$	Anticodon	Base insertion Base modification	[20]
Saccharomyces	$tRNA^{Lys}(CUU)$	Anticodon Acceptor stem	Point mutation	[21]
Tetrahymena	$tRNA^{Gln}(UUG)$	Anticodon	Point mutation	[22]
Arabidopsis	$tRNA^{Val}(AAC)$	Anticodon + D stem	Point mutation	[23]
		T-domain	Point mutation	[24]
	$tRNA^{Ala}(UGC)$	Acceptor stem	Point mutation	[25]
Tobacco	$tRNA^{Gly}(UCC)$	Anticodon + D-domain	Point mutation	[26]

From these findings it is clear that no universal signal exists. In some cases there are even several independent signals in the same tRNA, like in *Leishmania* $tRNA^{Ile}(UAU)$, yeast $tRNA^{Lys}(CUU)$ and *Arabidopsis* $tRNA^{Val}(AAC)$.

tRNA import has also been studied in the apicomplexan *Toxoplasma gondii* [5]. In this work the authors expressed the *T. gondii* WT $tRNA^{Met-i}$ and a variant containing the T-arm of $tRNA^{Met-e}$ in *Trypanosoma brucei*. After expression both tRNAs are retained in the cytosol. This was unexpected since the trypanosomal T-arm of $tRNA^{Met-e}$ rendered the trypanosomal $tRNA^{Met-i}$ importable [16]. Hence the import signals seem to be different in apicomlexans than in *T. brucei*, but one cannot exclude

that the expression in *T. gondii* itself would provide different results. Furthermore the $tRNA^{Gln}$ and $tRNA^{Trp}$ of *T. gondii* do not contain any thio-modified nucleotides in the cytosol and mitochondrion, respectively, which is also different from the situation in trypanosomatids [5, 20, 27].

The role of nucleotide modifications in tRNA import has been investigated in several studies. The mitochondrial and cytosolic forms of the $tRNA^{Lys}$, $tRNA^{Leu}$, $tRNA^{Tyr}$ of *T. brucei* were compared by direct enzymatic sequence analysis and were shown to be modified in the mitochondrion on a conserved cytidine residue [28]. A mutant form of the $tRNA^{Tyr}$ which cannot be modified was expressed in *T. brucei* and found in the mitochondrial fraction. This suggests that the modified cytidine is not required for import. However in *Leishmania*, the wobble position of the $tRNA^{Glu}$(UUC) and $tRNA^{Gln}$(UUG) was shown to contain a cytosol-specific thiomodification [20]. Interestingly the cytosolic fraction of $tRNA^{Glu}$(UUC) was less efficiently imported into isolated mitochondria than the corresponding *in vitro* transcript, which suggests that the thio-modification acts as a retention signal. Unfortunately however no data are available concerning the import efficiency of the $tRNA^{Glu}$(UUC) isolated from mitochondrial extract. Hence, one cannot conclude that the thiomodification alone is sufficient to prevent import and complementary *in vivo* experiments would therefore be of great interest. Similarly, native $tRNA^{Met\text{-}e}$ was isolated either from the cytosol or the mitochondrion of *T. brucei*, and tested for *in vitro* import [16]. The result was that only the mitochondrial form of the tRNA was imported suggesting that nucleotide modification(s) might play a role in targeting.

A.2.3. tRNA – tRNA interactions during import

In an *in vitro* system derived from *Leishmania,* tRNAs were shown to interact cooperatively or antagonistically for transfer into the mitochondrion [18, 29]. The tRNAs were classified in two classes: type I tRNAs, where the anticodon and D-arm serve as import signals, have a high intrinsic transfer efficiency. However type II tRNAs, with variable loop and T-arm as import signals, have a low intrinsic transfer efficiency. Furthermore, type I tRNAs stimulate the translocation of type II tRNAs, whereas type II inhibit the import of type I. However, so far this “ping-pong” mechanism of tRNA import has not been described in any other species.

A.2.4. Targeting factors

A number of cytosolic tRNA import factors have been described in yeast [30, 31]. First of all, *in vitro* import of the $tRNA^{lys}$(CUU) requires addition of the precursor form of the mitochondrial lysyl-tRNA synthetase (preMSK) and the cytosolic lysyl-tRNA synthetase [30, 32]. Aminoacylation of $tRNA^{lys}$(CUU) by the cytosolic enzyme was initially thought to be a prerequisite for import, but some poorly aminoacylated mutant *in vitro* transcripts were efficiently imported [21]. In the same work it was shown that the import correlates with the capacity of the tRNA to bind preMSK, suggesting that as long as the tRNA still binds to preMSK, aminoacylation is not necessary for import. However binding to preMSK is not sufficient for mitochondrial import of $tRNA^{lys}$(CUU). Recently, another cytosolic factor has been identified, the glycolytic enzyme enolase. This protein is required for *in vivo* import of $tRNA^{lys}$(CUU), since its depletion inhibits tRNA import [31]. Furthermore the addition of both recombinant preMSK and enolase proteins to the aminoacylated $tRNA^{lys}$(CUU) is sufficient to induce *in vitro* import. The authors also showed the requirement of the imported $tRNA^{lys}$(CUU) for proper mitochondrial translation, since the absence of enolase and subsequent inhibition of mitochondrial import affected mitochondrial translation. In yeast another nucleus-encoded tRNA ($tRNA^{Gln}$) was recently reported to be targeted to mitochondria [4]. In this study it was shown that a fraction of cytosolic glutaminyl-tRNA synthetase is imported into the mitochondrion where it aminoacylates the imported $tRNA^{Gln}$. These experiments suggest the absence of the transamidation pathway in yeast mitochondrion. The requirement of the cytosolic $tRNA^{Gln}$ for mitochondrial translation *in vivo* was shown by expressing a suppressor version of the cytosolic $tRNA^{Gln}$ which was able to rescue a cox2-114^{UAG} mutation. Surprisingly *in vitro* import of uncharged $tRNA^{Gln}$ did not depend on the addition of cytosolic factors suggesting that this tRNA is imported by a different import mechanism than the $tRNA^{lys}$(CUU). However cytosolic contamination of mitochondrial preparation cannot be excluded and additional experiments will be required to prove that there are indeed two distinct tRNA import mechanisms in yeast.

Aminoacylation or the involvement of aminoacyl-tRNA synthetases does not seem to be a prerequisite for tRNA import in general. In *Tetrahymena* only one of three $tRNA^{Gln}$ isoacceptors is imported [33]. In plants, *in vitro* tRNA import experiments

showed that aminoacylation is not required for import [34]. *In vivo* however absence of aminoacylation often correlates with absence of import. For example a non-acylated variant of $tRNA^{Ala}$ was not imported [25]. In addition, when misacylated with methionine, a mutant $tRNA^{Val}$ was retained in the cytosol of transgenic tobacco cells [23]. Nevertheless, while correct aminoacylation might be required for *in vivo* import, it is clearly not sufficient. In *Solanum tuberosum* three $tRNA^{Gly}$ isoacceptors are recognized by the same glycine-tRNA synthetase, but only two of them are imported [35]. In addition a mutant $tRNA^{Val}$ containing the D-domain of the cytosol specific $tRNA^{Met}$ is aminoacylated by valyl-tRNA synthetase but not imported [23]. More recently it was shown that the tobacco $tRNA^{Gly}$(UCC) containing the anticodon of the non imported $tRNA^{Gly}$(GCC) remains in the cytosol even if correctly aminoacylated [26]. In *Trypanosoma brucei* the aminoacylation is probably not necessary for *in vivo* import, since an unspliced mutant version of $tRNA^{Tyr}$ which cannot be aminoacylated is nevertheless imported albeit less efficiently than wild type [36]. In addition the $tRNA^{Met-i}$ and $tRNA^{Met-e}$ are aminoacylated by the same enzyme but only $tRNA^{Met-e}$ is imported, suggesting that the methionyl-tRNA synthetase is not involved in import. Finally no addition of cytosolic factors is required for *in vitro* import of tRNAs in trypanosomatids. In *Leishmania* aminoacylation did not influence the *in vitro* import efficiency [15]. As mentioned in part A.2.2. the determinant for import of trypanosomal $tRNA^{Met-e}$ is localized in the T-stem [16], and overlaps with the main determinants of $tRNA^{Met-i}$ preventing the binding to the elongation factor 1α (EF-1α) in vertebrates [37]. It is interesting to note that in *T. brucei* the only cytosol specific tRNAs are the $tRNA^{Met-i}$ and the $tRNA^{Sec}$, which are also the only tRNAs expected not to bind to EF-1α. This leads to the hypothesis that in *T. brucei* EF-1α might serve as a tRNA import factor. RNAi against EF-1α greatly decreased tRNA import efficiency of a newly synthesized tRNA (Bouzaidi-tiali *et al*, unpublished). However RNAi against eIF-2, which specifically binds to the $tRNA^{Met-i}$, did not affect import. The authors could show that the import defect was not a secondary effect of translational deficiency, because the tRNA import was affected before translation. Another evidence that EF-1α might be used as a tRNA import factor is provided by data recently obtained for the trypanosomal $tRNA^{Sec}$ (Aeby *et al*, unpublished). $tRNA^{Sec}$ does not depend on its binding to EF-1α for interaction with the ribosome. Instead it is recognized by a specific elongation factor called EFsec in eukaryotes [38]

and SelB in bacteria [39]. Expression of a $tRNA^{Sec}$ variant, where the two non Watson-crick base pairs supposed to act as antideterminant for EF-1α binding [40] were replaced, leads to import of a small fraction of the tRNA into the mitochondrion. Hence these results suggest that even if the trypanosomal *in vitro* tRNA import system does not require addition of cytosolic factors, *in vivo* import relies on soluble factors, which may act in binding of the tRNA to the mitochondrial surface.

A.3. Membrane translocation

A.3.1. Components

In yeast it was shown that an intact protein translocation machinery is required for import of the $tRNA^{Lys}$(CUU) [41]. It is thought that the $tRNA^{Lys}$ is cotranslocated with preMSK through the protein import channel. However unfolding of proteins is a prerequisite for import into mitochondria, which raises the question of how the unfolded preMSK could form a complex with the $tRNA^{Lys}$ during the import process. There is presently no data available about how the $tRNA^{Gln}$ crosses the yeast mitochondrial membranes, except that it is by a different mechanism.

In trypanosomatids tRNAs and proteins are translocated by two different pathways [42]. *In vitro* tRNA import studies showed that pretreatment of the mitochondria with proteinase inhibited tRNA import in *T. brucei* and two *Leishmania* species. This demonstrates the requirement of proteinaceous receptors on the surface of the mitochondria [43]. Moreover treatment of mitochondria with an antibody against a 15 kDa RNA binding protein associated with the outer membrane inhibited *in vitro* tRNA import in *Leishmania* [44]. However the identity of this protein is not known. The localization of this receptor revealed that it is both associated with mitochondria and, surprisingly, present throughout the cell [44]. Several results have been recently obtained about transfer through the mitochondrial inner membrane in *Leishmania*. First, a large multi-subunit complex of 640 kDa called RIC (RNA import complex) has been isolated from the inner membrane. When incorporated into liposomes this complex induced ATP- and proton motive force-dependent import activity [45]. In addition this complex contains a receptor for the type I tRNAs and another one for the

type II tRNAs. It was suggested that binding of type I tRNAs to their receptor induces a conformational change in the type II tRNA receptor which opens up or exposes its tRNA binding site. Then the attachment of type II tRNAs with their receptor would destabilize the type I complex. This model of allosteric inter-tRNA interactions is in agreement with the "ping-pong" model. Recently two components of the RIC were identified as the α-subunit of the F1 ATP synthase, termed RIC/F1α, and the homologue of the subunit 6b of ubiquinol cytochrome c reductase (respiratory complex III), termed RIC8A/UCR6b [46-48]. RIC/F1α interacts with and is activated by type I tRNAs and RIC8A/UCR6b is a type II tRNA receptor. In addition it was shown that both receptors interact cooperatively and antagonistically as predicted by the ping-pong model. Inducible antisense–mediated depletion of RIC/F1α affected *in vivo* import of type I and II tRNAs, and knock-down of RIC8A/UCR6b decreased import of type II tRNAs only. Thus in *Leishmania* it seems that the mitochondrial tRNA import machinery consists in part of bifunctional respiratory components.

A.3.2 Energetics

The extrusion of protons from the mitochondrial matrix generates a trans-membrane potential with a negative charge on the matrix side. This raises the question of how polyanionic tRNAs can cross the inner membrane against the electrostatic repulsion.
In yeast, this problem is probably solved by co-import with mitochondrial pre-proteins. In *Leishmania tropica*, as described below, the protons may act to neutralize the negative charges on the RNA phosphate groups [49].
In all systems studied so far, ATP is used as an energy source in tRNA import. In *Leishmania* [50] and *Trypanosoma* [9] ATP hydrolysis is required both in the matrix and outside of the mitochondrion. In the latter case the role of ATP is not clear: one hypothesis is that a helicase-like molecule would use ATP to unfold tRNA for subsequent transfer [15].
The role of the electrochemical proton gradient at the inner membrane has been investigated by using uncouplers which dissociate the proton flux toward the matrix from ATP synthesis. Protonophores affect tRNA import in yeast [41] and potato [34]. In trypanosomatids contradictory results were obtained. The *L. tropica* [45, 50] but not the *L. tarentolae* [51] system is sensitive to uncouplers. Moreover two different

results were obtained in two independent studies in *T. brucei* [9, 42]. The lack of consensus in these experiments might be explained by the fact that the precise final location of the tRNAs during the different import experiments was often not investigated. It is possible that the tRNAs can cross the outer but not the inner membrane in presence of an uncoupler. Crossing the outer membrane is sufficient for protection against RNAse treatment. A stepwise transfer of tRNA across the mitochondrial membranes of *Leishmania tropica* has been proposed, since the dissipation of the membrane potential and inhibition of the ATPase almost did not affect the translocation across the outer membrane but strongly decreased import through the inner membrane [50]. Interestingly all the *in vitro* import systems studied to date are sensitive to oligomycin, which inhibits the F1-F0 ATPase [15].

A.3.3 Model in *Leishmania*

The detailed study of bioenergetic properties of the reconstituted RIC-liposomes tRNA import system together with the recent identification of two molecular components of RIC greatly improved the comprehension of the tRNA import mechanism in *Leishmania tropica* [46-49]. The present section describes the main steps of tRNA import across the inner membrane of *Leishmania tropica* (fig. 1):

1) Type I tRNA binds to its specific receptor RIC/F1α, which induces the transport of ATP through the membrane via a channel similar or identical to a carboxyatractyloside-sensitive ADP/ATP translocator.

2) Binding of type I tRNA to RIC/F1α enables the binding of type II tRNAs to RIC8A/UCR6b, and activates ATP hydrolysis at the inner side of the membrane. This model includes the allosteric modulation of the type I and type II tRNA receptors, which is thought to regulate import of the tRNAs.

3) The energy produced by ATP hydrolysis is used to pump protons from inside to outside through an oligomycin sensitive channel, which generates a membrane potential inhibited by the protonophore uncoupler CCCP.

4) The proton gradient induces the opening of a still unknown tRNA import channel and subsequent translocation of tRNAs. Importantly it was shown that import of tRNA into RIC-liposomes still occured efficiently when ATP was replaced by low

external pH. In that case the tRNA import became insensitive to oligomycin, which makes sense since the proton pump is no more required in this situation.

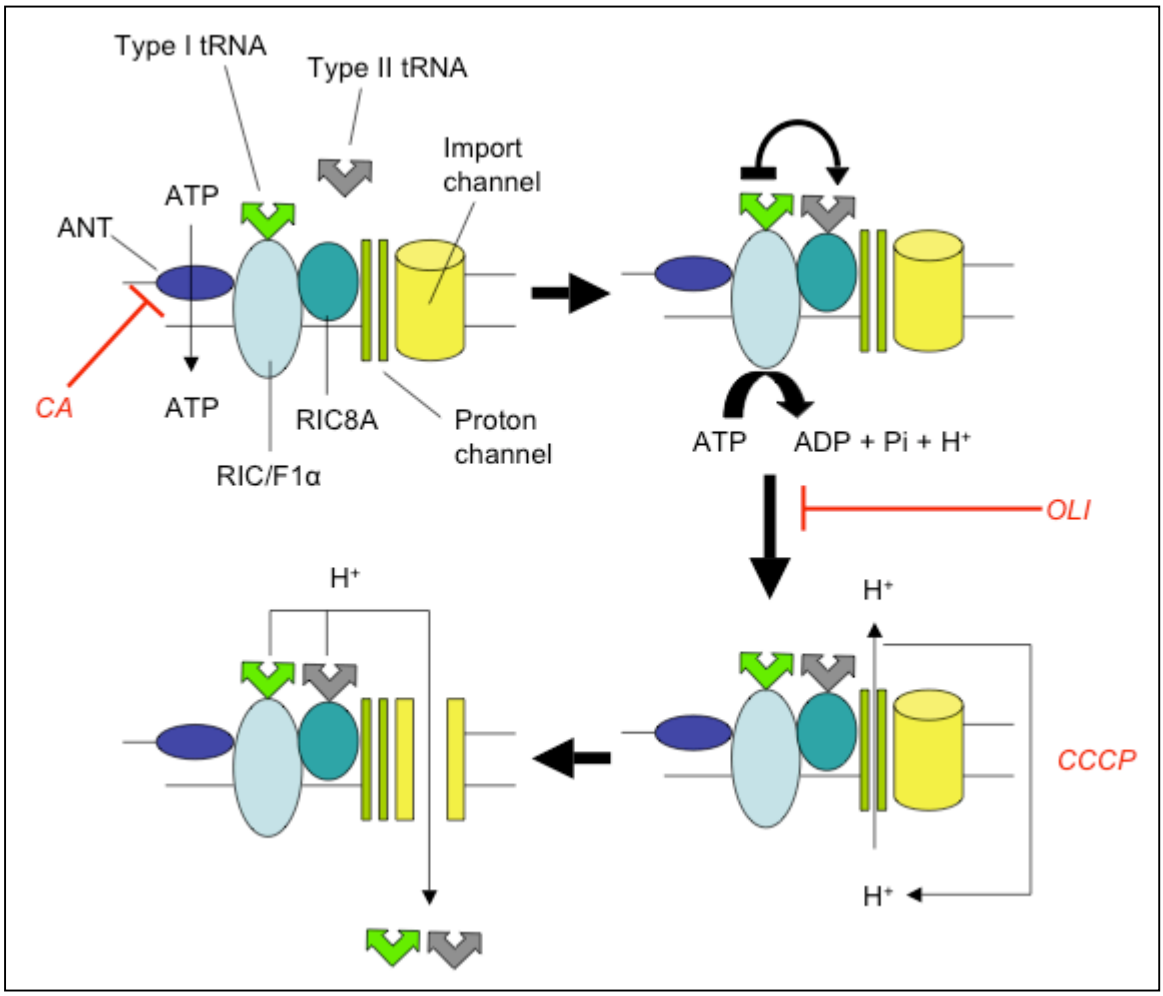

Fig. 1. Model for tRNA import through the inner membrane of *Leishmania* mitochondria (updated from [15]). For details see text. *CA*, carboxyatractyloside. *OLI*, oligomycin. *CCCP*, carbonylcyanide m-chlorophenylhydrazone (a protonophore).

In the future, the availability of efficient molecular tools will allow to study if, like in the *Leishmania* system, some ancient respiratory components are involved in mitochondrial tRNA import in the closely related species *Trypanosoma brucei.*

B. Consequences of mitochondrial tRNA import

An important feature of mitochondrial tRNA import is that the imported tRNAs are always of the eukaryotic-type. The mitochondrial translation system however, due to the evolutionary origin of the mitochondrion, is of bacterial-type and is expected to be incompatible with at least some eukaryotic-type tRNAs. Unique evolutionary adaptations of the mitochondrial translation system for proper recognition and use of eukaryotic-type tRNAs are therefore expected. Most of data presently available about the consequences of mitochondrial tRNA import have been obtained in *Trypanosoma brucei* and are reviewed in this chapter.

B.1. Translation initiation

B.1.1. $tRNA^{Met}$ in eukaryotic and bacterial translation systems

Protein synthesis is initiated with methionine in eukaryotes and archea and with formyl-methionine in bacteria and organelles. There are two types of $tRNA^{Met}$, namely the initiator $tRNA^{Met}$ ($tRNA^{Met-i}$), which is used for initiation of protein synthesis and the elongator $tRNA^{Met}$ ($tRNA^{Met-e}$), which functions in the insertion of methionine into the nascent polypeptidic chain [52, 53]. The elongator $tRNA^{Met}$ is similar in all organisms but the initiator $tRNA^{Met}$ can be sudivided into two classes, the eukaryotic and the bacterial-type initiator $tRNAs^{Met}$. Formylation of methionine on the charged $tRNA^{Met-i}$ is required in bacteria and organelles and is performed by an enzyme called methionyl-$tRNA^{Met}$ formyltransferase (MTF). This protein is present in bacteria and organelles, but not in the eukaryotic cytosol and in archea. The major recognition element for MTF is the C-A mismatch at position 1-72 which is conserved in bacterial $tRNA^{Met-i}$ [54]. The eukaryotic and archeal $tRNA^{Met-i}$ carry A-U instead of a mismatch at the same position. Interestingly in mitochondria there is often only a single $tRNA^{Met}$ which acts as an initiator in the formylated state and as an

elongator when non-formylated [55]. In these cases the $tRNA^{Met}$ resembles a $tRNA^{Met-i}$, but surprisingly contains a A1-U72 base pair, like the eukaryotic-type $tRNA^{Met-i}$.

At the beginning of the translation initiation process, the charged $tRNA^{Met-i}$ is bound to the initiation factor 2 (IF2), which promotes the GTP-dependent interaction of the complex with the ribosome [56]. In the cytosol the eukaryotic IF2 (eIF2) directly recognizes the eukaryotic-type methionyl-$tRNA^{Met-i}$ and promotes its binding to the ribosome. In bacteria and organelles however, the aminoacylated $tRNA^{Met-i}$ must be formylated before it can interact with the bacterial-type IF2.

B.1.2. Mitochondrial translation initiation in *T. brucei*

Unlike most trypanosomal tRNAs, the $tRNA^{Met-i}$ is exclusively localized in the cytosol. As a consequence, the only $tRNA^{Met}$ present in the mitochondrion of *T. brucei* is the imported eukaryotic $tRNA^{Met-e}$ [1]. It has been shown that trypanosomes adapt to this situation by formylating a fraction of the imported eukaryotic-type $tRNA^{Met-e}$ using an extraordinary large MTF with an unusual substrate specificity [2].

In the part A of the results we identified and characterized the mitochondrial initiation factor 2 (IF2) of *T. brucei* and we have shown that its carboxy-terminal domain binds the formylated, but not the unformylated, eukaryotic $tRNA^{Met-e}$.

B.2. Aminoacylation of tRNAs

In order to be used in translation, each tRNA needs to be charged with its cognate amino acid. This two-steps reaction is catalyzed by an aminoacyl-tRNA synthetase (aaRS) in presence of ATP. The amino acid is first activated by AMP and reacts then with the tRNA to produce the aminoacyl-tRNA [57]. Although there are some exceptions, there is generally a single aaRS for each amino acid. In a defined translation sytem all the tRNAs accepting the same amino acid are called isoacceptors and are aminoacylated by the same aaRS. One mechanism ensuring that a tRNA is charged with the correct amino acid is based on identity elements in certain positions

of the tRNA that are specifically recognized by the aaRS [58]. Usually the identity elements are found in the anticodon and / or the acceptor stem. For a few tRNAs, however, the major recognition elements are present in other regions of the tRNA molecule [59].

B.2.1. AaRSs in most eukaryotes

In most non plastid containing eukaryotes there are two sets of aaRSs: one group for aminoacylation in the cytosol and another one for charging of tRNAs in the mitochondria. The mitochondrial aaRSs are encoded in the nucleus and imported into the mitochondria [60]. Their evolutionary origin, like the one of the mitochondrial tRNAs, is nevertheless bacterial. Furthermore it is known that in most eukaryotes the cytosolic and mitochondrial sets of aaRSs overlap to some extent and that a few enzymes are dually targeted to both compartments [61]. For instance, a survey of the *Saccharomyces cerevisiae* genome database reveals annotated genes encoding 36 different aaRSs. They can be divided into 16 cytosol-specific ones, 14 mitochondrial enzymes and 4 which are known to be dually targeted (www.yeastgenome.org).

B.2.2. AaRSs in *Tetrahymena* and *T. brucei*

In organisms that import tRNAs we always find dual targeting of tRNAs. This means that the cytosolic and the mitochondrial fractions of an imported tRNA derive from the same nuclear gene. Therefore one can expect that both tRNA fractions are aminoacylated by the same aaRS. Analysis of the number of annotated aaRS genes for a given amino acid and the presence of a corresponding mitochondria-encoded tRNA gene allows a preliminary test of this hypothesis. Thus this analysis was performed with the genomes of *Tetrahymena thermophila* and *Trypanosoma brucei*. In *Tetrahymena thermophila* only 8 tRNA genes are encoded in the mitochondrial genome [62]. Therefore the missing tRNAs are probably imported from the cytosol. A genomic survey reveals that 83% of the aaRSs whose corresponding tRNAs are not mitochondria-encoded are represented by single genes (*Tetrahymena thermophila*

genome project, http://www.tigr.org/tdb/e2k1/ttg/) whereas for cytosol-specific tRNAs we find a single aaRS gene in 10% of the cases only (table 2).

Table 2: relationship between the number of predicted aaRS genes and the expected import of the corresponding tRNA in *Tetrahymena thermophila*.

Amino acid	AaRS annotated once	AaRS annotated twice	tRNA predicted to be imported [62]
Pro		x (3)	
Leu		x	
Asn	x		x
Trp		x	
Glu		x	
Tyr	x		
Gly	x		x
Phe		x (3)	
His		x	
Asp	x		x
Gln		x	x
Ile		x	x
Lys	x		x
Met		x	
Arg	x		x
Thr	x		x
Cys	x		x
Ala	x		x
Ser	x		x
Val	x		x

- Grey rows: only one synthetase is predicted to charge the cytosolic and mitochondrial fractions of the corresponding tRNA
- (3): annotated 3 times

In *T. brucei* all the mitochondrial tRNAs are partially imported from the cytosol [1] and are expected to be charged by the same set of enzymes in both compartments. This has been experimentally shown for $tRNA^{Glu}$ and $tRNA^{Gln}$ [63]. Furthermore, a genomic survey of the *T. brucei* genome database revealed that most (85%) aaRSs corresponding to imported tRNAs are represented by single genes (www.sanger.ac.uk/Projects/T_brucei/). However there are three aaRSs represented by two different genes, namely the lysyl-, aspartyl-, and tryptophanyl-tRNA synthetases (LysRS, AspRS and TrpRS). The reason why, in these three cases, there are two enzymes for the same substrate is not obvious. In order to address this question we decided to focus on the tryptophanyl-tRNA synthetases (TrpRS). In part

B of the results we show that the presence of two distinct TrpRSs in *T. brucei* is due to mitochondria-specific modifications of the $tRNA^{Trp}$.

B.2.3. Glutaminyl-tRNA formation

Although most organisms use 20 different aaRSs, one for each standard amino acid, many systems do not need the glutaminyl-tRNA synthetase (GlnRS). In these organisms the glutaminyl-$tRNA^{Gln}$ is indirectly synthesized by mischarging of the $tRNA^{Gln}$ with glutamate, a reaction achieved by a non-discriminating GluRS. The glutamyl group of the resulting glutamyl-$tRNA^{Gln}$ is then transformed into glutaminyl by an enzyme called Glu-$tRNA^{Gln}$ amidotransferase [64]. This process is called the transamidation pathway and is used by most bacteria (for exception see [65]) and archea but not by the eukaryotic cytosol which utilizes GlnRS [64, 66].
Since the mitochondria and chloroplasts have a bacterial origin, they are expected to use the transamidation pathway. Indeed it has been shown that most organelles lack the GlnRS activity and use the transamidation process for Gln-$tRNA^{Gln}$ formation [67]. However, some exceptions have been found: GlnRS activity has been detected in mitochondria of yeast [4], *Tetrahymena* [68] and trypanosomatids (see below) [63, 69].

B.2.3.1. Situation in *T. brucei*

It has been shown in this organism that the cytosol and mitochondrion contain the same eukaryotic-type GlnRS [63]. Furthermore the glutamyl-$tRNA^{Glu}$ synthesis in the cytosol and mitochondrion is catalyzed by a single eukaryotic-type discriminating GluRS. RNAi experiments demonstrated that these two enzymes are responsible for the entire GlnRS and GluRS activities that are detected in the cytosol and in the mitochondrion.
The evolutionary origin of mitochondria is bacterial. Thus, the mitochondrion of *T. brucei* originally contained mitochondrial tRNA genes. The absence of mitochondrial tRNA genes and the import of cytosolic nucleus-encoded tRNAs is therefore a derived trait [70]. It is possible that transamidation occured in the bacterial ancestor

but the former bacterial-type GluRS and Glu-tRNA^{Gln} amidotransferase could not recognize the eukaryotic-type tRNA^{Gln} during establishment of tRNA import. In that case the loss of the transamidation pathway and the subsequent appearance of direct glutaminyl-tRNA^{Gln} formation in the *T. brucei* mitochondrion would represent an adaptation to mitochondrial tRNA import.

C. Conclusions

The recent results obtained about identity of the RIC in *Leishmania* indicate that during evolution of mitochondrial tRNA import, ancient respiratory components acquired new molecular functions. It means that these proteins can assemble alternatively into two different complexes without causing disruption of either function. This differs from the yeast situation where the known tRNA import system consists of protein translocation components. Looking at the whole tRNA import process, differences between import systems are not only observed in the membrane translocation apparatus but also among the location of import signals and the cytosolic factors. Thus there is a great variability of the mitochondrial tRNA import process in different species. This suggests that mitochondrial tRNA import probably evolved multiple times independently in different species. This is in full agreement with the proposed polyphyletic evolutionary origin of tRNA import, based on the occurrence of tRNA import in some species and its absence in closely related ones [71].

The reason why some but not all mitochondria require imported eukaryotic-type tRNAs remains a matter of speculation. One possible explanation would be that the production of only one tRNA set for the whole cell (like in trypanosomatids) instead of two requires less energy and therefore would be an advantage. Alternatively, since generally the mutation rate is much higher in the mitochondrial genome than in the nucleus, the use of nucleus-encoded tRNAs would protect mitochondrial tRNAs from mutations.

Understanding mitochondrial tRNA import process is not only interesting for basic science, but also for biomedical research, since there are many important human pathogens which import tRNAs into their mitochondria:

- *Trypanosoma* species which cause sleeping sickness and chagas disease in human and Nagana in cattle.
- *Leishmania* species wich are spread by the bite of infected sandflies and responsible for leishmaniasis.
- *Toxoplasma gondii* which infects most mammals and is responsible for opportunistic infections associated with AIDS.
- *Plasmodium falciparum* which is the causing agent of malaria, the most important parasitic disease of humans.

Since the human or animal hosts of these parasites do not import any tRNA into their mitochondria, the import machinery would be an interesting drug target.

Understanding tRNA import process might also allow to develop strategies that potentially could cure mitochondrial diseases that are associated with mutations in mitochondria-encoded tRNAs, like MELAS (mitochondrial myopathy encephalopathy with acid lactosis and stroke-like episodes) and MERF (myoclonic epilepsy and ragged red fibres syndrome) [72]. In yeast it has been shown that an imported tRNA can suppress a mitochondrial mutation [73]. Isolated human mitochondria are able to import the yeast $tRNA^{Lys}$(CUU) in the presence of yeast soluble factors, suggesting that they contain a cryptic tRNA import pathway that is not used *in vivo*. Furthermore, expression of a derivative of the yeast $tRNA^{Lys}$ in human cells affected by the MERF mutation and subsequent internalization of this tRNA into the mitochondria suppressed the mitochondrial defects associated with this mutation [74].

Finally it was shown that an unspliced variant of $tRNA^{Tyr}$ can be used to import synthetic introns into the mitochondria of *Leishmania tarentolae* [75]. Since transformation of mitochondria is generally not possible, one could use the import of such synthetic introns to study mitochondrial gene function.

D. References

1. Tan TH, Pach R, Crausaz A, Ivens A, Schneider A: **tRNAs in Trypanosoma brucei: genomic organization, expression, and mitochondrial import**. *Mol Cell Biol* 2002, **22**(11):3707-3717.
2. Tan TH, Bochud-Allemann N, Horn EK, Schneider A: **Eukaryotic-type elongator tRNAMet of Trypanosoma brucei becomes formylated after import into mitochondria**. *Proc Natl Acad Sci U S A* 2002, **99**(3):1152-1157.
3. Tarassov IA, Martin RP: **Mechanisms of tRNA import into yeast mitochondria: an overview**. *Biochimie* 1996, **78**(6):502-510.
4. Rinehart J, Krett B, Rubio MA, Alfonzo JD, Soll D: **Saccharomyces cerevisiae imports the cytosolic pathway for Gln-tRNA synthesis into the mitochondrion**. *Genes Dev* 2005, **19**(5):583-592.
5. Esseiva AC, Naguleswaran A, Hemphill A, Schneider A: **Mitochondrial tRNA import in Toxoplasma gondii**. *J Biol Chem* 2004, **279**(41):42363-42368.
6. Shi X, Chen DH, Suyama Y: **A nuclear tRNA gene cluster in the protozoan Leishmania tarentolae and differential distribution of nuclear-encoded tRNAs between the cytosol and mitochondria**. *Mol Biochem Parasitol* 1994, **65**(1):23-37.
7. Hancock K, LeBlanc AJ, Donze D, Hajduk SL: **Identification of nuclear encoded precursor tRNAs within the mitochondrion of Trypanosoma brucei**. *J Biol Chem* 1992, **267**(33):23963-23971.
8. LeBlanc AJ, Yermovsky-Kammerer AE, Hajduk SL: **A nuclear encoded and mitochondrial imported dicistronic tRNA precursor in Trypanosoma brucei**. *J Biol Chem* 1999, **274**(30):21071-21077.
9. Yermovsky-Kammerer AE, Hajduk SL: **In vitro import of a nuclearly encoded tRNA into the mitochondrion of Trypanosoma brucei**. *Mol Cell Biol* 1999, **19**(9):6253-6259.
10. Sherrer RL, Yermovsky-Kammerer AE, Hajduk SL: **A sequence motif within trypanosome precursor tRNAs influences abundance and mitochondrial localization**. *Mol Cell Biol* 2003, **23**(24):9061-9072.
11. Hauser R, Schneider A: **tRNAs are imported into mitochondria of Trypanosoma brucei independently of their genomic context and genetic origin**. *Embo J* 1995, **14**(17):4212-4220.
12. Lima BD, Simpson L: **Sequence-dependent in vivo importation of tRNAs into the mitochondrion of Leishmania tarentolae**. *Rna* 1996, **2**(5):429-440.
13. Kapushoc ST, Alfonzo JD, Rubio MA, Simpson L: **End processing precedes mitochondrial importation and editing of tRNAs in Leishmania tarentolae**. *J Biol Chem* 2000, **275**(48):37907-37914.
14. Aphasizhev R, Karmarkar U, Simpson L: **Are tRNAs imported into the mitochondria of kinetoplastid protozoa as 5'-extended precursors?** *Mol Biochem Parasitol* 1998, **93**(1):73-80.
15. Bhattacharyya SN, Adhya S: **The complexity of mitochondrial tRNA import**. *RNA Biology* 2004, **1**(2):84-88.

16. Crausaz Esseiva A, Marechal-Drouard L, Cosset A, Schneider A: **The T-stem determines the cytosolic or mitochondrial localization of trypanosomal tRNAsMet**. *Mol Biol Cell* 2004, **15**(6):2750-2757.
17. Mahapatra S, Ghosh S, Bera SK, Ghosh T, Das A, Adhya S: **The D arm of tRNATyr is necessary and sufficient for import into Leishmania mitochondria in vitro**. *Nucleic Acids Res* 1998, **26**(9):2037-2041.
18. Bhattacharyya SN, Chatterjee S, Adhya S: **Mitochondrial RNA import in Leishmania tropica: aptamers homologous to multiple tRNA domains that interact cooperatively or antagonistically at the inner membrane**. *Mol Cell Biol* 2002, **22**(12):4372-4382.
19. Chen DH, Shi X, Suyama Y: **In vivo expression and mitochondrial import of normal and mutated tRNA(thr) in Leishmania**. *Mol Biochem Parasitol* 1994, **64**(1):121-133.
20. Kaneko T, Suzuki T, Kapushoc ST, Rubio MA, Ghazvini J, Watanabe K, Simpson L, Suzuki T: **Wobble modification differences and subcellular localization of tRNAs in Leishmania tarentolae: implication for tRNA sorting mechanism**. *Embo J* 2003, **22**(3):657-667.
21. Entelis NS, Kieffer S, Kolesnikova OA, Martin RP, Tarassov IA: **Structural requirements of tRNALys for its import into yeast mitochondria**. *Proc Natl Acad Sci U S A* 1998, **95**(6):2838-2843.
22. Rusconi CP, Cech TR: **The anticodon is the signal sequence for mitochondrial import of glutamine tRNA in Tetrahymena**. *Genes Dev* 1996, **10**(22):2870-2880.
23. Delage L, Duchene AM, Zaepfel M, Marechal-Drouard L: **The anticodon and the D-domain sequences are essential determinants for plant cytosolic tRNA(Val) import into mitochondria**. *Plant J* 2003, **34**(5):623-633.
24. Laforest MJ, Delage L, Marechal-Drouard L: **The T-domain of cytosolic tRNAVal, an essential determinant for mitochondrial import**. *FEBS Lett* 2005, **579**(5):1072-1078.
25. Dietrich A, Marechal-Drouard L, Carneiro V, Cosset A, Small I: **A single base change prevents import of cytosolic tRNA(Ala) into mitochondria in transgenic plants**. *Plant J* 1996, **10**(5):913-918.
26. Salinas T, Schaeffer C, Marechal-Drouard L, Duchene AM: **Sequence dependence of tRNA(Gly) import into tobacco mitochondria**. *Biochimie* 2005, **87**(9-10):863-872.
27. Crain PF, Alfonzo JD, Rozenski J, Kapushoc ST, McCloskey JA, Simpson L: **Modification of the universally unmodified uridine-33 in a mitochondria-imported edited tRNA and the role of the anticodon arm structure on editing efficiency**. *Rna* 2002, **8**(6):752-761.
28. Schneider A, McNally KP, Agabian N: **Nuclear-encoded mitochondrial tRNAs of Trypanosoma brucei have a modified cytidine in the anticodon loop**. *Nucleic Acids Res* 1994, **22**(18):3699-3705.
29. Goswami S, Chatterjee S, Bhattacharyya SN, Basu S, Adhya S: **Allosteric regulation of tRNA import: interactions between tRNA domains at the inner membrane of Leishmania mitochondria**. *Nucleic Acids Res* 2003, **31**(19):5552-5559.
30. Tarassov I, Entelis N, Martin RP: **Mitochondrial import of a cytoplasmic lysine-tRNA in yeast is mediated by cooperation of cytoplasmic and mitochondrial lysyl-tRNA synthetases**. *Embo J* 1995, **14**(14):3461-3471.

31. Entelis N, Brandina I, Kamenski P, Krasheninnikov IA, Martin RP, Tarassov I: **A glycolytic enzyme, enolase, is recruited as a cofactor of tRNA targeting toward mitochondria in Saccharomyces cerevisiae**. *Genes Dev* 2006, **20**(12):1609-1620.
32. Tarassov IA, Entelis NS: **Mitochondrially-imported cytoplasmic tRNA(Lys)(CUU) of Saccharomyces cerevisiae: in vivo and in vitro targetting systems**. *Nucleic Acids Res* 1992, **20**(6):1277-1281.
33. Rusconi CP, Cech TR: **Mitochondrial import of only one of three nuclear-encoded glutamine tRNAs in Tetrahymena thermophila**. *Embo J* 1996, **15**(13):3286-3295.
34. Delage L, Dietrich A, Cosset A, Marechal-Drouard L: **In vitro import of a nuclearly encoded tRNA into mitochondria of Solanum tuberosum**. *Mol Cell Biol* 2003, **23**(11):4000-4012.
35. Brubacher-Kauffmann S, Marechal-Drouard L, Cosset A, Dietrich A, Duchene AM: **Differential import of nuclear-encoded tRNAGly isoacceptors into solanum Tuberosum mitochondria**. *Nucleic Acids Res* 1999, **27**(9):2037-2042.
36. Schneider A, Martin J, Agabian N: **A nuclear encoded tRNA of Trypanosoma brucei is imported into mitochondria**. *Mol Cell Biol* 1994, **14**(4):2317-2322.
37. Drabkin HJ, Estrella M, Rajbhandary UL: **Initiator-elongator discrimination in vertebrate tRNAs for protein synthesis**. *Mol Cell Biol* 1998, **18**(3):1459-1466.
38. Hatfield DL, Gladyshev VN: **How selenium has altered our understanding of the genetic code**. *Mol Cell Biol* 2002, **22**(11):3565-3576.
39. Baron C, Böck A: **The selenocysteine-inserting tRNA species: structure and function.** *Transfer RNA: Structure, biosynthesis and function (Söll, D and RajBhandary, UL)* 1995:529-544.
40. Rudinger J, Hillenbrandt R, Sprinzl M, Giege R: **Antideterminants present in minihelix(Sec) hinder its recognition by prokaryotic elongation factor Tu**. *Embo J* 1996, **15**(3):650-657.
41. Tarassov I, Entelis N, Martin RP: **An intact protein translocating machinery is required for mitochondrial import of a yeast cytoplasmic tRNA**. *J Mol Biol* 1995, **245**(4):315-323.
42. Nabholz CE, Horn EK, Schneider A: **tRNAs and proteins are imported into mitochondria of Trypanosoma brucei by two distinct mechanisms**. *Mol Biol Cell* 1999, **10**(8):2547-2557.
43. Schneider A: **Unique aspects of mitochondrial biogenesis in trypanosomatids**. *Int J Parasitol* 2001, **31**(13):1403-1415.
44. Adhya S, Ghosh T, Das A, Bera SK, Mahapatra S: **Role of an RNA-binding protein in import of tRNA into Leishmania mitochondria**. *J Biol Chem* 1997, **272**(34):21396-21402.
45. Bhattacharyya SN, Chatterjee S, Goswami S, Tripathi G, Dey SN, Adhya S: **"Ping-pong" interactions between mitochondrial tRNA import receptors within a multiprotein complex**. *Mol Cell Biol* 2003, **23**(15):5217-5224.
46. Chatterjee S, Home P, Mukherjee S, Mahata B, Goswami S, Dhar G, Adhya S: **An RNA-binding respiratory component mediates import of type II tRNAs into Leishmania mitochondria**. *J Biol Chem* 2006.

47. Goswami S, Adhya S: **The alpha-subunit of Leishmania F1 ATP synthase hydrolyzes ATP in presence of tRNA**. *J Biol Chem* 2006, **281**(28):18914-18917.
48. Goswami S, Dhar G, Mukherjee S, Mahata B, Chatterjee S, Home P, Adhya S: **A bifunctional tRNA import receptor from Leishmania mitochondria**. *Proc Natl Acad Sci U S A* 2006, **103**(22):8354-8359.
49. Bhattacharyya SN, Adhya S: **tRNA-triggered ATP hydrolysis and generation of membrane potential by the leishmania mitochondrial tRNA import complex**. *J Biol Chem* 2004, **279**(12):11259-11263.
50. Mukherjee S, Bhattacharyya SN, Adhya S: **Stepwise transfer of tRNA through the double membrane of Leishmania mitochondria**. *J Biol Chem* 1999, **274**(44):31249-31255.
51. Rubio MA, Liu X, Yuzawa H, Alfonzo JD, Simpson L: **Selective importation of RNA into isolated mitochondria from Leishmania tarentolae**. *Rna* 2000, **6**(7):988-1003.
52. RajBhandary UL: **Initiator transfer RNAs**. *J Bacteriol* 1994, **176**(3):547-552.
53. Blanquet S, Mechulam Y, Schmitt E: **The many routes of bacterial transfer RNAs after aminoacylation**. *Curr Opin Struct Biol* 2000, **10**(1):95-101.
54. Lee CP, Seong BL, RajBhandary UL: **Structural and sequence elements important for recognition of Escherichia coli formylmethionine tRNA by methionyl-tRNA transformylase are clustered in the acceptor stem**. *J Biol Chem* 1991, **266**(27):18012-18017.
55. Takeuchi N, Vial L, Panvert M, Schmitt E, Watanabe K, Mechulam Y, Blanquet S: **Recognition of tRNAs by Methionyl-tRNA transformylase from mammalian mitochondria**. *J Biol Chem* 2001, **276**(23):20064-20068.
56. Boelens R, Gualerzi CO: **Structure and function of bacterial initiation factors**. *Curr Protein Pept Sci* 2002, **3**(1):107-119.
57. Voet D, Voet, J.G.: *Biochemistry* (Second edition).
58. Normanly J, Abelson J: **tRNA identity**. *Annu Rev Biochem* 1989, **58**:1029-1049.
59. Giege R, Sissler M, Florentz C: **Universal rules and idiosyncratic features in tRNA identity**. *Nucleic Acids Res* 1998, **26**(22):5017-5035.
60. Bullerwell CE, Gray MW: **Evolution of the mitochondrial genome: protist connections to animals, fungi and plants**. *Curr Opin Microbiol* 2004, **7**(5):528-534.
61. Small I, Wintz H, Akashi K, Mireau H: **Two birds with one stone: genes that encode products targeted to two or more compartments**. *Plant Mol Biol* 1998, **38**(1-2):265-277.
62. Brunk CF, Lee LC, Tran AB, Li J: **Complete sequence of the mitochondrial genome of Tetrahymena thermophila and comparative methods for identifying highly divergent genes**. *Nucleic Acids Res* 2003, **31**(6):1673-1682.
63. Rinehart J, Horn EK, Wei D, Soll D, Schneider A: **Non-canonical eukaryotic glutaminyl- and glutamyl-tRNA synthetases form mitochondrial aminoacyl-tRNA in Trypanosoma brucei**. *J Biol Chem* 2004, **279**(2):1161-1166.
64. Tumbula DL, Becker HD, Chang WZ, Soll D: **Domain-specific recruitment of amide amino acids for protein synthesis**. *Nature* 2000, **407**(6800):106-110.

65. Akochy PM, Bernard D, Roy PH, Lapointe J: **Direct glutaminyl-tRNA biosynthesis and indirect asparaginyl-tRNA biosynthesis in Pseudomonas aeruginosa PAO1**. *J Bacteriol* 2004, **186**(3):767-776.
66. Gagnon Y, Lacoste L, Champagne N, Lapointe J: **Widespread use of the glu-tRNAGln transamidation pathway among bacteria. A member of the alpha purple bacteria lacks glutaminyl-trna synthetase**. *J Biol Chem* 1996, **271**(25):14856-14863.
67. Schon A, Krupp G, Gough S, Berry-Lowe S, Kannangara CG, Soll D: **The RNA required in the first step of chlorophyll biosynthesis is a chloroplast glutamate tRNA**. *Nature* 1986, **322**(6076):281-284.
68. Suyama Y, Hamada J: *Genetics and biogenesis of chloroplasts and mitochondria* 1976:763-770.
69. Nabholz CE, Hauser R, Schneider A: **Leishmania tarentolae contains distinct cytosolic and mitochondrial glutaminyl-tRNA synthetase activities**. *Proc Natl Acad Sci U S A* 1997, **94**(15):7903-7908.
70. Schneider A: **Does the evolutionary history of aminoacyl-tRNA synthetases explain the loss of mitochondrial tRNA genes?** *Trends in Genetics* 2001, **17**(10):557-559.
71. Schneider A, Marechal-Drouard L: **Mitochondrial tRNA import: are there distinct mechanisms?** *Trends Cell Biol* 2000, **10**(12):509-513.
72. Howell N: **Human mitochondrial diseases: answering questions and questioning answers**. *Int Rev Cytol* 1999, **186**:49-116.
73. Kolesnikova OA, Entelis NS, Mireau H, Fox TD, Martin RP, Tarassov IA: **Suppression of mutations in mitochondrial DNA by tRNAs imported from the cytoplasm**. *Science* 2000, **289**(5486):1931-1933.
74. Kolesnikova OA, Entelis NS, Jacquin-Becker C, Goltzene F, Chrzanowska-Lightowlers ZM, Lightowlers RN, Martin RP, Tarassov I: **Nuclear DNA-encoded tRNAs targeted into mitochondria can rescue a mitochondrial DNA mutation associated with the MERRF syndrome in cultured human cells**. *Hum Mol Genet* 2004, **13**(20):2519-2534.
75. Sbicego S, Nabholz CE, Hauser R, Blum B, Schneider A: **In vivo import of unspliced tRNATyr containing synthetic introns of variable length into mitochondria of Leishmania tarentolae**. *Nucleic Acids Res* 1998, **26**(23):5251-5255.

II. Results

A

Mitochondrial Initiation Factor 2 of *Trypanosoma brucei* Binds Imported Formylated Elongator-type $tRNA^{Met}$

The Journal of Biological Chemistry
Vol. 280, No. 16, pp. 15659-15665, 2005

Fabien Charrière, Timothy H. P. Tan
and André Schneider

Department of Biology/Zoology, University of Fribourg, Chemin du Musée 10, CH-1700 Fribourg, Switzerland

THE JOURNAL OF BIOLOGICAL CHEMISTRY
Vol. 280, No. 16, Issue of April 22, pp. 15659–15665, 2005
Printed in U.S.A.

Mitochondrial Initiation Factor 2 of *Trypanosoma brucei* Binds Imported Formylated Elongator-type tRNA^{Met}*

Received for publication, October 12, 2004, and in revised form, February 23, 2005
Published, JBC Papers in Press, February 23, 2005, DOI 10.1074/jbc.M411581200

Fabien Charrière‡, Timothy H. P. Tan‡§, and André Schneider¶

From the Department of Biology/Zoology, University of Fribourg, Chemin du Musée 10, CH-1700 Fribourg, Switzerland

The mitochondrion of *Trypanosoma brucei* lacks tRNA genes. Its translation system therefore depends on the import of nucleus-encoded tRNAs. Thus, except for the cytosol-specific initiator tRNA^{Met}, all trypanosomal tRNAs function in both the cytosol and the mitochondrion. The only tRNA^{Met} present in *T. brucei* mitochondria is therefore the one which, in the cytosol, is involved in translation elongation. Mitochondrial translation initiation depends on an initiator tRNA^{Met} carrying a formylated methionine. This tRNA is then recognized by initiation factor 2, which brings it to the ribosome. To guarantee mitochondrial translation initiation, *T. brucei* has an unusual methionyl-tRNA formyltransferase that formylates elongator tRNA^{Met}. In the present study, we have identified initiation factor 2 of *T. brucei* and shown that its carboxyl-terminal domain specifically binds formylated trypanosomal elongator tRNA^{Met}. Furthermore, the protein also recognizes the structurally very different *Escherichia coli* initiator tRNA^{Met}, suggesting that the main determinant recognized is the formylated methionine. *In vivo* studies using stable RNA interference cell lines showed that knockdown of initiation factor 2, depending on which construct was used, causes slow growth or even growth arrest. Moreover, concomitantly with ablation of the protein, a loss of oxidative phosphorylation was observed. Finally, although ablation of the methionyl-tRNA formyltransferase on its own did not impair growth, a complete growth arrest was observed when it was combined with the initiation factor 2 RNA interference cell line showing the slow growth phenotype. Thus, these experiments illustrate the importance of mitochondrial translation initiation for growth of procyclic *T. brucei*.

All organisms have two distinct tRNAs^{Met}, one specialized for decoding the initiation codon (mainly AUG) and another one dedicated for the insertion of methionine into internal peptidic linkages (1, 2). The basic features of translation initiation, namely the binding of the initiator tRNA^{Met} (tRNA$^{Met\text{-}i}$)[1] to initiation factor 2 (IF2) and the subsequent GTP-dependent interaction of the complex with the ribosome are universally conserved (3). Thus, a general feature of IF2 from all organisms is that it must specifically bind tRNA$^{Met\text{-}i}$ and interact with the ribosome. However, a more detailed analysis reveals some interesting differences between the translation initiation process in bacteria and in the eukaryotic cytosol. In the latter, the aminoacylated eukaryotic tRNA$^{Met\text{-}i}$, carrying the diagnostic A1:U72 base pair, directly binds to eukaryotic IF2 and forms a GTP-dependent ternary complex that binds to the 40 S ribosome. In bacteria binding of aminoacylated bacterial-type tRNA$^{Met\text{-}i}$ (recognized by the C1:A72 mismatch) to bacterial IF2 requires prior formylation of the methionine on the charged tRNA$^{Met\text{-}i}$. This reaction is catalyzed by the methionyl-tRNA formyltransferase (MTF), which is not found in the eukaryotic cytosol (1, 3). Furthermore, bacterial ribosomes are smaller and in many ways qualitatively different from their eukaryotic counterparts. However, although bacterial and eukaryotic IF2 both bind tRNAs$^{Met\text{-}i}$, they are not (even though implied by their names) evolutionarily related. Instead, it is eIF5B that is the eukaryotic orthologue of bacterial IF2. eIF5B does not directly bind tRNA but, just as proposed for bacterial IF2, facilitates association of the two ribosomal subunits (4).

Mitochondria are of bacterial evolutionary origin, and their translation system is therefore of the bacterial type. Thus, the two key factors involved in bacterial translation initiation, MTF and IF2, are also found in mitochondria (5). MTF of yeast (6, 7) and bovine mitochondria (8) have been characterized and shown to formylate their respective mitochondria-encoded tRNA substrates. Interestingly, in mammalian mitochondria, only a single tRNA^{Met} is found, which is used as an initiator in the formylated state and as an elongator when carrying a non-derivatized methionine (5). In contrast to bacterial MTF, the yeast enzyme appears to be dispensable for mitochondrial translation, because a MTF disruption strain was still able to grow on non-fermentable carbon sources (6). Mitochondrial IF2 of yeast (9) and bovine (10, 11) have also been characterized. They are similar to the bacterial proteins, the highest homology being found in the GTP-binding domain. Less, but still recognizable, similarity is also detected in the carboxyl-terminal half of the protein, which binds the formylated tRNA$^{Met\text{-}i}$. The domain organization of the amino-terminal part of mitochondrial IF2s, however, is quite variable (5). In line with this, it has been shown in yeast that this domain is dispensible for IF2 function *in vivo* (12).

Mitochondrial translation in the parasitic protozoa *Trypanosoma brucei* is unusual, because (due to the complete absence of mitochondrial tRNA genes) it depends exclusively on the import of cytosolic, nucleus-encoded tRNAs. Thus, trypanosomal tRNAs all are of the eukaryotic type and function in both the

* This study was supported by Grant 31–067906.02 from the Swiss National Foundation. The costs of publication of this article were defrayed in part by the payment of page charges. This article must therefore be hereby marked "*advertisement*" in accordance with 18 U.S.C. Section 1734 solely to indicate this fact.

‡ Both authors contributed equally to this work.
§ Present address: Institute of Molecular and Cell Biology, Singapore 117609.
¶ To whom correspondence should be addressed: University of Fribourg, Chemin du Musée 10, CH-1700 Fribourg, Switzerland. Tel.: 41-26-3008877; Fax: 41-26-3009741; E-mail: andre.schneider@unifr.ch.

[1] The abbreviations used are: tRNA$^{Met\text{-}i}$, initiator transfer RNA^{Met}; IF2, initiation factor 2; MTF, methionyl-tRNA formyltransferase; GST, glutathione *S*-transferase; TLC, thin layer chromatography; RNAi, RNA interference; aa, amino acid(s); MOPS, 4-morpholinepropanesulfonic acid.

cytosol and the mitochondrion (13–15). The only exception is the eukaryotic-type $tRNA^{Met\text{-}i}$, which is found in the cytosol only (15). The elongator $tRNA^{Met}$, identical to all other elongator tRNAs, is in part imported into the mitochondrion and represents the only $tRNA^{Met}$ present in this compartment. A fraction of this tRNA becomes formylated after import (16). This results in the surprising situation in that, *T. brucei* mitochondria (a typical elongator $tRNA^{Met}$) functions in translation initiation, provided that it is formylated (17). In agreement with this, it has been shown that the trypanosomal MTF, unlike its counterpart in other organisms, selectively recognizes elongator $tRNA^{Met}$. The unusual nature of trypanosomal MTF is also confirmed by sequence comparisons, which show that the trypanosomal enzyme has twice the size of any of its homologues (16). The aim of the present study was to characterize mitochondrial IF2 of *T. brucei* to see whether, as predicted, it was able to interact with the formylated fraction of the imported elongator $tRNA^{Met}$.

EXPERIMENTAL PROCEDURES

Cells—Procyclic *T. brucei*, stock 427, was grown at 27 °C in SDM-79 medium supplemented with 5% fetal bovine serum. Cells were harvested at $3.5–4.5 \times 10^7$ cells/ml. Procyclic *T. brucei*, strain 29–13, on which the RNAi knockdown cell lines are based, was grown in SDM-79 supplemented with 15% fetal calf serum, 50 μg/ml hygromycin, and 15 μg/ml G-418 and was harvested at a density of $1–2 \times 10^7$ cells/ml.

Recombinant IF2—The carboxyl-terminal region of *T. brucei* IF2 (aa 412–721) (Gene DB annotation Tb07.28B13.850), or a variant thereof lacking the last 44 aa, were expressed as glutathione *S*-transferase (GST) fusion proteins. To do so, IF2 gene fragments were prepared by PCR using 5′-TAGGGATCCCCCGGGAAGACTACTTGCAG-3′ as a forward and 5′-TACTCGAGTCATATGGTGGTCTTCAC-3′ or 5′-TACTCGAGTCACACATCACGTGGCTCCTC-3′, for the variant lacking the carboxy terminus, as reverse primers and cloned into the BamHI- and XhoI-digested pGex-5x-3 plasmid (Amersham Biosciences). The resulting constructs were transfected into *Escherichia coli* BL21, and the cells were grown to mid-log phase. Induction was done by adding 0.1 mM of isopropyl-β-D-thiogalactoside for 2 h at 25–27 °C. Induced cells (250 ml) were washed in IF2 binding buffer (50 mM MOPS-NaOH, pH 7.5, 10 mM $MgCl_2$, 20 mM KCl, 1 mM dithiothreitol) and resuspended in ½₀ the volume of the same buffer. Lysis by sonication and batch mode purification of the recombinant protein by glutathione-Sepharose (Amersham Biosciences) were performed as described by the manufacturer, except that IF2 binding buffer was used. Binding was done overnight at 4 °C using 250 μl of a 50% slurry of glutathione-Sepharose and the clarified extract of a 250-ml culture. The yield was ~190 μg of recombinant protein/125 μl of bed volume of glutathione-Sepharose beads. The purity of the recombinant proteins was tested by SDS-PAGE. For the IF-2/tRNA binding assay described below, glutathione-Sepharose-bound recombinant proteins were used. To remove endogenous *E. coli* $tRNA^{Met\text{-}i}$, the glutathione-Sepharose-bound recombinant proteins had to be treated with micrococcus nuclease (20 units/250 μl slurry) for 15 min on ice. To do so, 1 mM of $CaCl_2$ had to be added. The reaction was stopped by washing the beads in 500 μl of IF2 binding buffer containing 3 mM EGTA. Subsequently, the beads were washed three times in 500 μl of IF2 binding buffer alone and, finally, resuspended in IF2 binding buffer to reach a 50% slurry.

Isolation of Total and Mitochondrial RNA—RNA from total cells and isolated mitochondrial fractions of *T. brucei*, as well as *E. coli* RNA, were purified by the acidic guanidinium isothiocyanate method (18). Isolated RNAs were resuspended in 10 mM Na-acetate, pH 4,0 to avoid deacylation during storage. Mitochondria were purified by the hypotonic lysis method as described previously (19). Mitochondrial fractions from the MTF-RNAi cell line (see Fig. 5) were obtained by digitonin extraction (15, 20).

IF2/tRNA Binding Assay—Mitochondrial or total RNA of *T. brucei* or total *E. coli* RNA (7 μg of each) was dissolved in 50 μl of IF2 binding buffer containing 20 units of SuperRNasin (Ambion). The binding reaction was initiated by the addition of 120 μl of a 50% slurry of IF2 binding buffer and glutathione-Sepharose beads containing ~90 μg each of IF2-GST fusion proteins or of GST alone. After incubation for 10 min at 23 °C, the reaction was spun at $500 \times g$, and 100 μl of the supernatant was removed and kept at 4 °C. The resulting pellet was washed twice in 100 μl of IF2 binding buffer, and the supernatant fractions from the washes were pooled with the first supernatant. The pellet (representing the bound RNAs) and the combined supernatants (representing the unbound RNA) were brought to 400 μl by adding H_2O. After the addition of 0.2 M Na-acetate, pH 4, the samples were extracted with H_2O-equilibrated phenol, and after the addition of 20 μg of glycogen, the samples were precipitated with 100% of ethanol. After a final wash with 75% of ethanol, each RNA pellet was processed for electrophoresis on a denaturing 8 M urea/10% polyacrylamide gel by resuspension in 10 μl of 90% formamide and 20 mM EDTA. Northern blots were done as described previously (14). The following 5′-end-labeled oligonucleotides were used as probes: 5′-GTGAGGCTCGAACTCACG-3′ (for the *T. brucei* elongator $tRNA^{Met}$), 5′-CCCACGCCTACGAATAGA-3′ (for the *T. brucei* $tRNA^{Leu}$), 5′-AGGCTGCTCCACCCCGCG-3′ (for the *E. coli* initiator $tRNA^{Met}$), and 5′-CCGCTCGGGAACCCCACC-3′ (for the *E. coli* $tRNA^{Tyr}$).

The ^{35}S-labeled mitochondrial RNA fraction used for the binding assay (shown in Fig. 2*B*) was prepared by *in organelle* aminoacylation using [^{35}S]methionine, as described previously (15). The labeled methionine species were released by deacylation in 0.1 N NaOH for 30 min at 37 °C. Analysis of the released [^{35}S]methionine species was done by thin layer chromatography (TLC) on a cellulose plate, which was developed in a 13:3:1 mixture of diethyl ether, acetic acid, and water (15).

RNAi—The RNAi constructs were prepared using the same previously described pLew 100-derived stem loop plasmid that carries convenient restriction sites for cloning (21). A 549-bp-long fragment, corresponding to position 156–704 of the IF2 coding sequence, was PCR-amplified using, as a forward primer, 5′-GCGGGATCCAAGCTTGAGTGATGACCCCCGATG-3′ and, as a reverse primer, 5′-GCGCTCGAGTCTAGATTGTGTGCAAGCTCAATC-3′. The resulting fragment was cloned into the plasmid in the sense direction using HindIII/XbaI sites and in the antisense direction using BamHI and XhoI sites. Two versions of the plasmid were prepared. In the first one (TbIF2-Tb), the sense and antisense sequences were separated by a fragment corresponding to 690 nucleotides of the trypanosomal spliced leader sequence (22), whereas in the second one (TbIF2-Mm), a 439-bp fragment, corresponding to positions 341–779 of the mouse Pex11b mRNA, was used as a spacer (23). Using the mouse sequence as a spacer yielded a more efficient down-regulation of the targeted mRNA than if the *T. brucei* sequence was used.[2] The plasmids were linearized with NotI and transfected into the procyclic *T. brucei* strain 29–13, which expresses T7 RNA polymerase and the tetracycline repressor. Selection with phleomycin, cloning, and induction with tetracycline were done as described previously (24). For the IF2/MTF double RNAi cell line (see Fig. 3*D*), we used the same plasmid that was used for the previously described MTF RNAi cell line (16), except that the phleomycin resistance gene was replaced by the puromycin resistance gene.

ATP Production Assay—ATP production assays using digitonin-purified mitochondria were done exactly as described previously (21, 25).

RESULTS

Primary Structure of IF2 of T. brucei—Searching the *T. brucei* genomic data base, we found an open reading frame of 721 aa predicted to encode the orthologue of bacterial IF2. The protein showed an overall identity of 33–35 and 30–32% to bacterial and mitochondrial IF2s, respectively. The predicted domain structure for mitochondrial IF2 (12) was retained (Fig. 1). A highly divergent amino-terminal domain (aa 1–135) was followed by the highly conserved GTP binding domain (aa 136–283). The carboxyl-terminal region (aa 284–721) was less conserved but contained the IF2 signature sequence (aa 628–650) as described in the PROSITE data base (Fig. 1*B*). Bioinformatic analysis did not predict an obvious mitochondrial targeting signal. However, in *T. brucei*, these signals were often difficult to identify, because they can be very short.

It has been shown, for bacterial IF2, that the carboxyl-terminal 110 aa are sufficient for binding of formylated $tRNA^{Met\text{-}i}$ (26). Fig. 1*B* shows a multiple sequence alignment of the carboxyl-terminal 310 aa of the *T. brucei* IF2 with the corresponding regions of two bacterial and two mitochondrial orthologues. The best characterized IF2 carboxyl-terminal domain is the one of *Bacillus stearothermophilus*, which has been subjected to

[2] E. Ullu, personal communication.

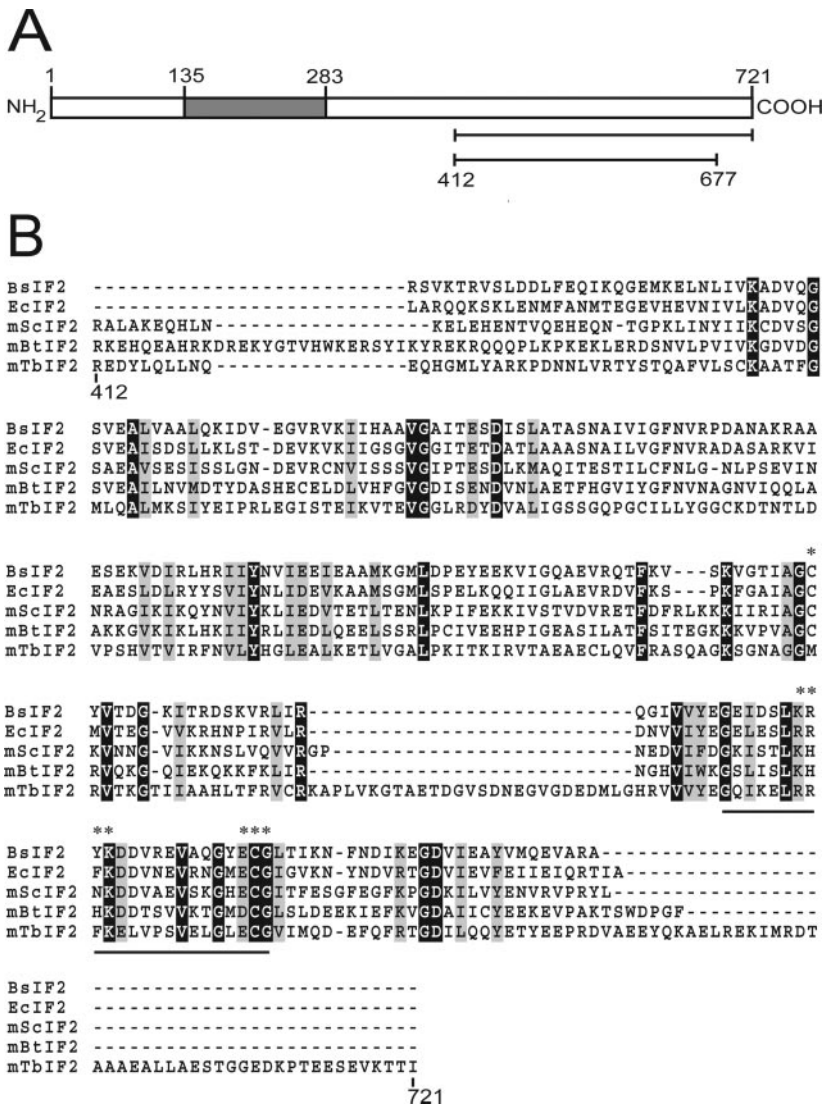

FIG. 1. **The *T. brucei* IF2 orthologue.** *A*, predicted domain structure of *T. brucei* IF2. The highly conserved GTP binding domain is shown in a *gray box*. The two regions of IF2 that were expressed as GST fusion proteins (Fig. 2) are indicated. *B*, multiple sequence alignment by ClustalW of the carboxyl-terminal 310 aa of the *T. brucei* IF2 (*Tb*) with the corresponding regions of two bacterial (*Bs*, *B. stearothermophilus*; *Ec*, *E. coli*) and two mitochondrial (*mSc*, *Saccharomyces cerevisiae*; *mBt*, *Bos taurus*) orthologues. Residues in the *B. stearothermophilus* protein identified as the main determinants for $tRNA^{Met\text{-}i}$ binding are indicated by *asterisks* (28). IF2 signature sequences (aa 628–650), as described in the PROSITE data base, are *underlined*.

extensive mutational analysis and which structure has recently been solved by NMR (26–28). These studies identified the Cys-668 and two short peptides, KRYK (aa 699–702) and ECG (aa 713–715), as the main determinants for $tRNA^{Met\text{-}i}$ binding (numbers refer to the position of amino acids in the *B. stearothermophilus* protein, Fig. 1*B*). Interestingly, except for three conservative replacements (C668M, K699R, Y701F), identical aa are found in the same relative position in the *T. brucei* protein (Fig. 1*B*, *asterisks*). Although bacterial IF2 interacts with $tRNA^{Met\text{-}i}$, the trypanosomal protein is predicted to bind an elongator-type $tRNA^{Met}$. Nevertheless, the elements, which in the bacterial IF2 are required for binding of the $tRNA^{Met\text{-}i}$, have been conserved in the trypanosomal protein.

However, there are also sequence elements that are unique for the trypanosomal IF2. These are an insertion of 27 aa and a carboxyl-terminal extension of 44 aa (Fig. 1*B*). Modeling of the trypanosomal sequence on the *B. stearothermophilus* structure (27) shows that the insertion localizes to a loop connecting two β sheets and thus will most likely not significantly disturb the structure. Interestingly, insertions at the same relative position are found in the IF2 orthologues of two other trypanosomatids (*Leishmania major* and *Trypanosoma cruzi*). However, although the length of these insertions (32 aa in *L. major* and 26 aa in *T. cruzi*) are very similar to the 27 aa observed in *T. brucei*, their sequences are not conserved. A similar situation is found for the carboxyl-terminal extensions. They are also present in *L. major (*length, 50 aa) and *T. cruzi* (length, 39); however, in contrast to the trypanosomatid-specific insertion, their sequences are highly similar.

The Carboxyl-terminal Domain of Trypanosomal IF2 Binds Formylated Elongator-type $tRNA^{Met}$—We wanted to test whether trypanosomal IF2, as predicted, binds imported formylated elongator $tRNA^{Met}$. Thus, we expressed the carboxyl-terminal 310 aa of the *T. brucei* IF2 (and a variant thereof lacking the carboxyl-terminal 44 aa) in *E. coli*. To simplify purification, the IF2 peptides were expressed as GST fusions. Affinity chromatography on glutathione-Sepharose beads yielded eluates consisting of single proteins of the expected molecular weights (data not shown). For the tRNA binding assay, the final elution step was omitted, and the beads containing the bound protein were directly incubated with isolated total or mitochondrial RNA fractions from *T. brucei*. Thus, our binding assay, comparable with the situation *in vivo*, was performed in a complex mixture of RNAs. It was important to isolate the RNAs under acidic conditions to keep the tRNAs in an aminoacylated state. After the binding step, the beads were recovered by centrifugation, and RNAs were isolated from the supernatant and, after a washing step, from the pellet. Both RNA fractions were separated by polyacrylamide gel electrophoresis and analyzed by Northern hybridizations. The results in Fig. 2*A* show that, when incubated with isolated mitochondrial RNAs, ~25% of the elongator $tRNA^{Met}$ present in this

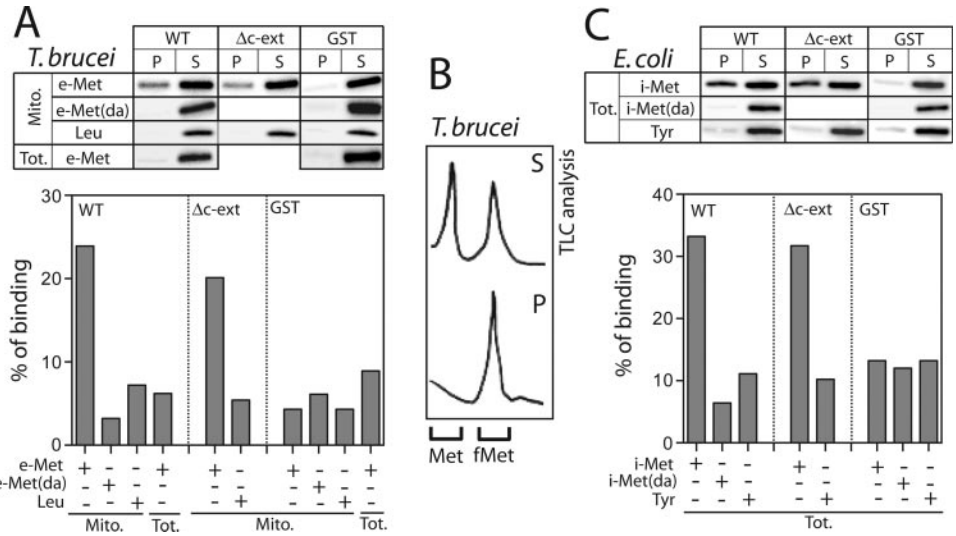

FIG. 2. **The carboxyl-terminal domain of *T. brucei* IF2 binds formylated tRNAs^{Met}.** *A*, IF2 binding assays using *T. brucei* RNA fractions as substrate. The carboxyl-terminal domain of wild-type (*WT*) trypanosomal IF2 (aa 412–721) or a variant thereof lacking the 44 last aa (Δ*c-ext*) were expressed as GST fusions. Glutathione-Sepharose beads saturated with the recombinant proteins or with GST alone were incubated with aminoacylated or deacylated (*da*) isolated mitochondrial RNA (*Mito.*), respectively. Identical experiments were also performed using isolated total RNA (*Tot.*). Northern blots containing bound (*P*) and unbound (*S*) RNA fractions were probed for elongator tRNA^{Met} (*e-Met*) or tRNA^{Leu} (*Leu*). The graph shows a quantification of the Northern blots signals as analyzed by a phosphorimaging device. The combined signals of the P and S fractions were set to 100%. *B*, IF2 binding assay using the *T. brucei* [^{35}S]methionine-labeled mitochondrial RNA fraction as substrate. Both supernatant (*S*) and pellet (*P*) fractions were deacylated, and the released [^{35}S]methionine species were analyzed by TLC. The graph shows the *tracings* of the [^{35}S]methionine signals from TLC as detected on the monitor of a multichannel analyzer of a gas flow Geiger Müller Counter (15). The positions of unlabeled methionine (*Met*) and formyl-methionine (*fMet*) separated under the same conditions as established in a parallel TLC lane are indicated. *C*, IF2 binding assays using total RNA isolated from *E. coli* as substrate. The same recombinant proteins as in *A* were tested for binding of aminoacylated or deacylated (*da*) *E. coli* tRNA^{Met-i} (*i-Met*) and tRNA^{Tyr}, respectively.

fraction is recovered in the pellet and thus is bound to the carboxyl-terminal 310 aa of *T. brucei* IF2. The observed binding was specific for elongator tRNA^{Met}, as another elongator-type tRNA, the tRNA^{Leu}, could not bind. Furthermore, interaction with IF2 required methionylated tRNA^{Met}, because it was prevented by prior deacylation of the RNA fraction. Interestingly, when incubated with isolated total RNA, consisting essentially of cytosolic RNAs, no binding of aminoacylated elongator tRNA^{Met} was observed. The only difference between cytosolic and imported mitochondrial elongator tRNA^{Met} is that 40–50% of the imported fraction is formylated (16), indicating that formylation is required for binding. As expected, GST alone did not significantly bind tRNA. In contrast, the variant of the IF2 peptide, which lacks the conserved trypanosomatid-specific carboxyl-terminal 44 aa, showed a binding activity that was comparable with the wild-type peptide.

To provide direct evidence that formylation is required for binding of the elongator tRNA^{Met}, we performed an IF2/tRNA binding assay using [^{35}S]methionine-labeled mitochondrial RNA as a substrate. The radioactive mitochondrial RNA fraction was prepared by *in organelle* aminoacylation. This procedure labels both the unformylated and formylated form of the imported elongator tRNAs^{Met} (15). After the binding reaction, the bound and unbound RNA fractions were deacylated, and the liberated [^{35}S]methionine and ^{35}S-formyl-methionine were analyzed by TLC. Fig. 2*B* shows that, as expected, it was mainly the ^{35}S-formyl-methionine that was recovered in the pellet fraction representing the bound RNA.

The same binding assays were also performed using isolated *E. coli* RNA as a substrate (Fig. 2*C*). Interestingly, ~35% of the *E. coli* tRNA^{Met-i} was able to bind to the trypanosomal IF2 peptide, provided that it was aminoacylated. Binding was specific, as an elongator tRNA^{Tyr} did not bind. Furthermore, as for the trypanosomal tRNA^{Met}, the very carboxyl terminus of IF2 (aa 678–721) was dispensable for binding.

In summary, these results show that the carboxyl-terminal domain of trypanosomal IF2 (aa 412–677) specifically binds elongator-type tRNA^{Met} of *T. brucei*, provided that the molecule is charged and formylated. Furthermore, when the IF2 peptide was assayed with *E. coli* RNAs, it specifically recognized the bacterial tRNA^{Met-i}.

In Vivo Depletion of IF2 by RNAi—Due to the availability of a tightly controlled tetracycline-inducible expression system (29), RNAi has become the method of choice to disrupt gene function in *T. brucei* (22, 23). Thus, to investigate the function of IF2 by RNAi, we prepared a construct that contained a defined sequence of the IF2 gene in the sense, as well as the antisense, direction. Both sequences were inserted downstream of a tetracycline-inducible promoter and were separated by a stuffer to simplify cloning. In the presence of tetracycline, the RNA was expressed and formed a stem loop that eventually led to the specific degradation of the IF2 mRNA. There have been two types of stuffer sequences used in stem loop constructs, one of trypanosomal origin as described previously (22) and another one of mouse origin (23). Surprisingly, it was shown that the efficiency of RNAi was generally higher when the mouse sequence was used.[2] The reason for this might be that the trypanosomal sequence still contains transcription signals that potentially interfere with the expression of the double-stranded RNA. We decided to take advantage of this situation and prepared RNAi strains that could be used for different purposes. Preparing the RNAi cell line using the construct containing the mouse stuffer sequence (TbIF2-Mm) resulted in the growth curve shown in Fig. 3*A*, which indicated, as expected, that IF2 is essential for growth of procyclic *T. brucei*. With the construct containing the trypanosomal stuffer (TbIF2-Tb), however, an RNAi cell line having a more moderate growth phenotype was obtained (Fig. 3*B*). Analysis of different clones from the two transfections show that the growth curves for the two plasmids, which are depicted in Fig. 3, *A* and *B*, are typical for the whole population. Thus, we think that the different growth phenotypes are caused by different efficiencies of RNAi due to the two stuffer sequences. However, because no antibodies against trypanosomal IF2 were avail-

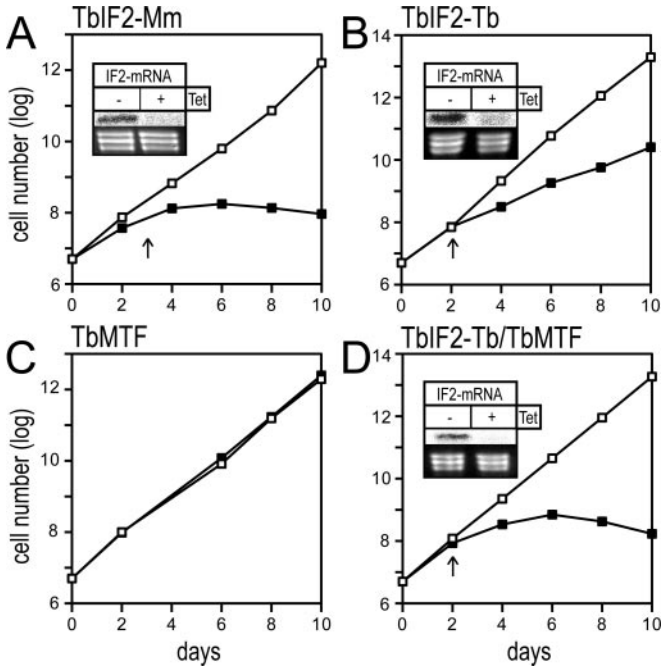

FIG. 3. **Mitochondrial translation initiation is essential for growth of procyclic *T. brucei*.** *A*, growth curve of a representative clonal *T. brucei* RNAi cell line ablated for IF2. The cell line was obtained using the stem loop construct containing the mouse stuffer sequence (TbIF2-Mm). *Open* and *filled squares* represent growth in the absence or presence of tetracycline (*Tet*), respectively. The *inset* shows a Northern blot for IF2 mRNA; time of sampling is indicated by the *arrow*. The rRNAs in the *lower panel* serve as loading controls. *B*, same as *A*, but the RNAi cell line was obtained using the stem loop construct containing the trypanosomal stuffer sequence (*TbIF2-Tb*). *C*, growth curve of a representative clonal *T. brucei* RNAi cell line ablated for MTF (*TbMTF*). Same results were obtained for the mouse and the trypanosomal stuffer sequence. MTF activity was measured by the assay described previously (16) and shown to be reduced to ~10–20% after three days of induction. *D*, growth curve for a representative clonal double RNAi cell line ablated for IF2 and MTF simultaneously. The cell line was obtained by transfecting TbIF2-Tb cells with the plasmid used to create the original MTF cell line (16), except that the resistance marker was changed. Down-regulation of IF2 mRNA and MTF activity was shown to be the same as in the corresponding single RNAi cell lines shown in *B* and *C*.

able, we could not verify this on the protein level.

Previous work from our laboratory has shown that, even though ablation of MTF resulted in an ~80–90% reduction of formylation activity (16), no growth phenotype was observed (Fig. 3*C*). Thus, the residual activity of MTF might still be sufficient to support growth, or MTF (as in yeast) might indeed not be required for normal growth (6, 7). The absence of a growth phenotype in MTF-ablated cells is surprising, because the enzyme is required for formylation of mitochondrial $tRNA^{Met}$, and the $tRNA^{Met}$ can only bind to IF2 in its formylated state (see Figs. 2 and 5). Both MTF and IF2 are therefore expected to be essential for the mitochondrial translation initiation pathway in *T. brucei*. Thus, to demonstrate the *in vivo* importance of trypanosomal MTF, we have used the clonal IF2 RNAi cell line (TbIF2-Tb) showing the moderate growth phenotype (Fig. 3*B*) and transfected it with the construct used to produce the original MTF-RNAi cell line (Fig. 3*C*) (16). Control experiments showed that, in induced cells of the resulting double RNAi knockdown cell line (TbIF2-Tb/TbMTF), IF2 mRNA is degraded, and MTF activity is reduced to the same level as in the two original cell lines (Fig. 3, *B* and *C*). Interestingly, the TbIF2-Tb/TbMTF-RNAi cell line shows a much stronger growth phenotype (Fig. 3*D*) than either the TbIF2-Tb-RNAi cell line (Fig. 3*B*) it is derived from or the TbMTF-RNAi cell line alone (Fig. 3*C*). These results show that, although reduced MTF activity does not affect growth of wild-type cells, it will stop growth of cells having reduced concentrations of IF2.

The growth phenotype observed in IF2 RNAi cells is expected to be due to the lack of mitochondrial protein synthesis. It is difficult to directly measure mitochondrial translation in trypanosomatids (30, 31). Thus, as an alternative, we decided to measure the consequences that ablation of IF2 has on mitochondrial ATP production (Fig. 4). We have recently established a sensitive luciferase-based assay to quantify ATP production in digitonin-isolated mitochondria of *T. brucei* in response to different substrates (21, 25). There are two fundamentally different ways by which mitochondria can produce ATP: (i) by oxidative phosphorylation using the electron transport chain or (ii) by substrate-level phosphorylation linked to the citric acid cycle. Our assay allows us to measure both ATP production pathways separately. To measure oxidative phosphorylation, mitochondria are incubated with ADP and the respiratory substrate succinate. This mode of ATP production is expected to be sensitive to antimycin, an inhibitor of the bc1 complex. To measure substrate-level phosphorylation, succinate is replaced by the citric acid cycle intermediate α-ketoglutarate. Substrate-level phosphorylation induced by α-ketoglutarate is antimycin-resistant. Thus, atractyloside, a specific inhibitor of the ADP/ATP translocator, is used as a control. Atractyloside blocks import of ADP and therefore will inhibit both substrate-level and oxidative phosphorylation. The results in Fig. 4 show that ablation of IF2 selectively knocks down oxidative phosphorylation but does not interfere with substrate-level phosphorylation. This is expected, because all mitochondria-encoded proteins in *T. brucei* are either components of the respiratory chain or the mitochondrial translation system. Thus, although oxidative phosphorylation depends on both imported, as well as mitochondria-encoded proteins, substrate-level phosphorylation will only require nucleus-encoded components.

Finally, we have used the MTF-RNAi cell line to verify that only formylated $tRNA^{Met}$ is able to bind to IF2. Mitochondrial RNA isolated from uninduced and induced cells was incubated with the glutathione-Sepharose-bound IF2/GST fusion protein. Fig. 5 shows that, although a fraction of the elongator $tRNA^{Met}$ present in mitochondrial RNA isolated from uninduced cells was recovered in the pellet, this amount was reduced to ~20% when the RNA was isolated from MTF-ablated cells. Thus, these results confirm the ones shown in Fig. 2, *A* and *B*, and provide independent evidence that formylation of the methionyl-$tRNA^{Met}$ is essential for *in vitro* binding of IF2.

DISCUSSION

The aim of the present study was to elucidate the role trypanosomal IF2 plays in the mitochondrial translation initiation pathway, in light of the fact that all tRNAs it can use are imported and of eukaryotic type. Interestingly, *T. brucei* and mammalian mitochondria each have only a single type of $tRNA^{Met}$. This tRNA is used as an elongator in the unformylated and as an initiator in the formylated states. However, although in mammalian mitochondria, the single $tRNA^{Met}$ is of the initiator-type, sharing features from both bacterial-type and eukaryotic-type $tRNA^{Met\text{-}i}$ (5), the one present in trypanosomal mitochondria is clearly an elongator (16). The main fraction of this tRNA actually resides in the cytosol and functions in cytosolic translation elongation (15). Thus, the question is how an elongator-type $tRNA^{Met}$ can be recruited to function in mitochondrial translation initiation. We have recently shown that, in *T. brucei*, this is achieved by an atypical MTF, which unlike its counterparts in other organisms, selec-

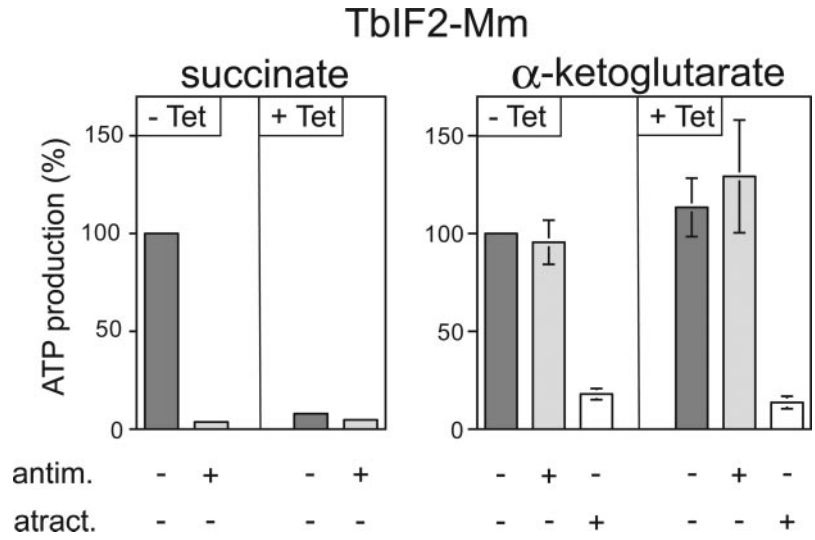

FIG. 4. **Succinate- and α-ketoglutarate-induced mitochondrial ATP production in the TbIF2-Mm RNAi cell line.** Uninduced cells (*−Tet*) are shown on the *left*, and induced cells (*+Tet*) on the *right* of each panel. The substrate tested is indicated at the *top* and additions of antimycin (*antim.*) and atractyloside (*atract.*) at the *bottom* of each panel. ATP productions in mitochondria isolated from uninduced cells tested without antimycin or atractyloside are set to 100%. The *bars* represent means expressed as percentages from three independent inductions. Standard errors are indicated.

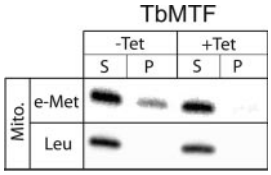

FIG. 5. **Mitochondrial tRNA^{Met} from the TbMTF RNAi cell line does not bind IF2.** IF2 binding assays using mitochondrial RNA (*Mito.*) isolated from uninduced (*−Tet*) and induced (*+Tet*) MTF-RNAi cells. Northern blots containing bound (*P*) and unbound (*S*) RNA fractions were probed for elongator tRNA^{Met} (*e-Met*) or tRNA^{Leu} (*Leu*). Quantifications of the signals for elongator tRNA^{Met} in the pellet fractions showed an ~5-fold reduction of binding in induced cells.

tively recognizes and formylates elongator tRNA^{Met} (16). In the present study, we were focusing on IF2, a component of the mitochondrial translation initiation pathway that acts after formylation of the tRNA^{Met}. IF2 promotes binding of the formylated tRNA^{Met} to mitochondrial ribosomes. Whether it does so by acting as a carrier or whether it interacts with the tRNA already bound to the small subunit of the ribosome is unknown. Using a homologous *in vitro* binding assay, we could show that, as predicted, the carboxyl-terminal domain of trypanosomal IF2 was able to specifically bind the elongator tRNA^{Met} when present in a mixture of total mitochondrial RNAs. The fact that only the elongator tRNA^{Met} in the mitochondrial RNA fraction was able to bind to IF2 (Fig. 2*A*), the relative enrichment of formyl-methionine in the bound RNA fraction (Fig. 2*B*), and the much reduced binding that is observed when mitochondrial RNA of the MTF-RNAi strain is used (Fig. 5) all strongly suggest that formylation of the methionyl-tRNA^{Met} is a prerequisite for binding to IF2. Furthermore, we showed that, when incubated with *E. coli* RNA, trypanosomal IF2 selectively recognized the heterologous tRNA$^{Met\text{-}i}$ (Fig. 2*C*). Trypanosomal elongator tRNA^{Met} (16) and *E. coli* tRNA$^{Met\text{-}i}$ (1) have very different structures; however, both of them are at least in part formylated, suggesting that the formylated methionine is the main recognition determinant for the trypanosomal protein.

Similar to the situation in bacteria, formylated tRNA$^{Met\text{-}i}$ has long been known to be the preferred ligand for mitochondrial IF2s. However, there is evidence that, to a limited extent, unformylated tRNA$^{Met\text{-}i}$ may be able to bind as well. The extent to which this can occur depends on the organism. Thus, whereas in an *in vitro* binding assay, bovine mitochondrial IF2 showed a strong preference (20–50-fold) for formylated tRNA$^{Met\text{-}i}$ (11), much less specificity (4-fold) is seen when yeast IF2 is used (9). Furthermore, the fact that a yeast strain deleted for MTF did not show a growth phenotype on non-fermentable carbon sources (6, 7) shows that *in vivo* mitochondrial translation initiation can also, in principle, occur without formylated tRNA$^{Met\text{-}i}$. Thus, it appears that the bovine IF2 shows a much stronger preference for formylated tRNA$^{Met\text{-}i}$ than the yeast protein. This makes sense when one considers that yeast mitochondria have distinct genes for the elongator and tRNA$^{Met\text{-}i}$, whereas mammalian mitochondria have only a single one. For mammals, the formyl group is therefore the only distinguishing feature between the elongator and the initiator tRNA^{Met}. However, it should be mentioned that a recent study has shown that the bovine IF2 could replace yeast IF2 in a MTF deletion strain, indicating that, at least *in vivo*, it is must bind unformylated tRNA$^{Met\text{-}i}$ (12).

RNAi-mediated ablation of trypanosomal IF2 causes a growth arrest (Fig. 3*A*) and a concomitant loss of oxidative phosphorylation (Fig. 4). This is expected as oxidative phosphorylation requires mitochondria-encoded protein and is known to be essential for procyclic *T. brucei*. Surprisingly, however, even though MTF and IF2 are known to act in the same pathway, growth of a trypanosomal MTF-RNAi knockdown cell line was not affected (16). How can this be explained? Do we have the same situation as in yeast, where IF2, under most growth conditions, can efficiently use unformylated tRNA^{Met} (6, 7)? We think this is unlikely, because in the *in vitro* assay, trypanosomal IF2 showed a strong preference for formylated tRNA^{Met}. In fact, for unformylated tRNA^{Met}, only a background level of binding was observed (Fig. 2*A*). However, RNAi-mediated ablation is known to not completely remove the ablated gene product. After induction of RNAi in the MTF-RNAi strain, ~10–20% of the MTF activity was retained (16). We therefore think that the residual amount of formylated tRNA^{Met} is sufficient to support normal growth. If, on the other hand, MTF activity was ablated in a cell line that already had limited amounts of IF2 (using the IF2-RNAi cell with the slow growth phenotype shown in Fig. 3*B*), a growth arrest was observed. This indicates that, under these conditions, both components of the translation initiation pathway, IF2 and MTF, are essential.

Initiation of protein synthesis in *E. coli* depends strictly on formylated tRNA$^{Met\text{-}i}$ (32), whereas *Pseudomonas aeruginosa* is able to use unformylated tRNA (33). Elegant experiments have shown that translation initiation in *E. coli* can be rendered formylation-independent by complementing an *E. coli* IF2 mutant with the *P. aeruginosa* IF2 (34). Furthermore, a single amino acid substitution (H774K) in the IF2 of *P. aeruginosa*, which introduces the corresponding amino acid found in the *E. coli* protein, resulted in a formylation-dependent protein. Structural modeling suggests that the mutation increases the

positive charge in the aa binding cleft of *P. aeruginosa* IF2. Surprisingly, in the *T. brucei* IF2, the aa corresponding to the His-774 of the *P. aeruginosa* protein is an uncharged alanine and thus reduces the positive charge potential. The *T. brucei* protein nevertheless shows great specificity for formylated methionine *in vitro*, indicating that this position is not the sole determinant involved in binding specificity.

We have previously shown that, using an elongator-type $tRNA^{Met}$ in translation initiation, *T. brucei* mitochondria requires a MTF with a unique substrate specificity (16). In this study, we showed that, once formylated, the elongator $tRNA^{Met}$ can bind to a rather conventional trypanosomal IF2 that is also able to selectively recognize *E. coli* $tRNA^{Met\text{-}i}$.

Acknowledgments—We thank Drs. G. Cross, P. Englund, and E. Ullu for providing us with plasmids and cell lines. *T. brucei* sequence data was obtained from the Sanger Institute website at www.sanger.ac.uk/Projects/T brucei/. Sequencing of the *T. brucei* genome was accomplished by the sequencing centers the Sanger Centre and The Institute of Genomic Research (TIGR).

REFERENCES

1. RajBhandary, U. L. (1994) *J. Bacteriol.* **176,** 547–552
2. Blanquet, S., Mechulam, Y., and Schmitt, E. (2000) *Curr. Opin. Struct. Biol.* **10,** 95–101
3. Boelens, R., and Gualerzi, C. O. (2002) *Curr. Protein Pept. Sci.* **3,** 107–119
4. Kapp, L. D., and Lorsch, J. R. (2004) *Annu. Rev. Biochem.* **73,** 657–704
5. Spremulli, L. L., Coursey, A., Navratil, T., and Hunter, S. E. (2004) *Prog. Nucleic Acid Res. Mol. Biol.* **77,** 211–261
6. Li, Y., Holmes, W. B., Appling, D. R., and RajBhandary, U. L. (2000) *J. Bacteriol.* **182,** 2886–2892
7. Vial, L., Gomez, P., Panvert, M., Schmitt, E., Blanquet, S., and Mechulam, Y. (2003) *Biochem. J.* **42,** 932–939
8. Takeuchi, N., Vial, L., Panvert, M., Schmitt, E., Watanabe, K., Mechulam, Y., and Blanquet, S. (2001) *J. Biol. Chem.* **276,** 20064–20068
9. Garofalo, C., Trinko, R., Kramer, G., Appling, D. R., and Hardesty, B. (2003) *Arch. Biochem. Biophys.* **413,** 243–252
10. Liao, H. X., and Spremulli, L. L. (1990) *J. Biol. Chem.* **265,** 13618–13622
11. Liao, H. X., and Spremulli, L. L. (1991) *J. Biol. Chem.* **266,** 20714–20719
12. Tibbetts, A. S., Oesterlin, L., Chan, S. Y., Kramer, G., Hardesty, B., and Appling, D. R. (2003) *J. Biol. Chem.* **278,** 31774–31780
13. Hancock, K., and Hajduk, S. L. (1990) *J. Biol. Chem.* **265,** 19208–19215
14. Simpson, A. M., Suyama, Y., Dewes, H., Campbell, D. A., and Simpson, L. (1989) *Nucleic Acids Res.* **17,** 5427–5445
15. Tan, T. H. P., Pach, R., Crausaz, A., Ivens, A., and Schneider, A. (2002) *Mol. Cell. Biol.* **22,** 3707–3717
16. Tan, T. H. P., Bochud-Allemannn, N., Horn, E. K., and Schneider, A. (2002) *Proc. Natl. Acad. Sci. U. S. A.* **99,** 1152–1157
17. Martin, N. C. (2002) *Proc. Natl. Acad. Sci. U. S. A.* **99,** 1110–1112
18. Chomczyinski, P., and Sacchi, N. (1987) *Anal. Biochem.* **162,** 156–159
19. Harris, M. E., Moore, D. R., and Hajduk, S. L. (1990) *J. Biol. Chem.* **265,** 11368–11376
20. Crausaz-Esseiva, A., Marechal-Drouard, L., Cosset, A., and Schneider, A. (2004) *Mol. Biol. Cell* **15,** 2750–2757
21. Bochud-Allemann, N., and Schneider, A. (2002) *J. Biol. Chem.* **277,** 32849–32854
22. Shi, H., Djikeng, A., Mark, T., Wirtz, E., Tschudi, C., and Ullu, E. (2000) *RNA* **6,** 1069–1076
23. Wang, Z., Morris, J. C., Drew, M. E., and Englund, P. T. (2000) *J. Biol. Chem.* **275,** 40174–40179
24. Beverley, S. M., and Clayton, C. E. (1993) *Methods Mol. Biol.* **21,** 333–348
25. Allemann, N., and Schneider, A. (2000) *Mol. Biochem. Parasitol.* **111,** 87–94
26. Spurio, R., Brandi, L., Caserta, E., Pon, C. L., Gualerzi, C. O., Misselwitz, R., Krafft, C., Welfle, K., and Welfle, H. (2000) *J. Biol. Chem.* **275,** 2447–2454
27. Meunier, S., Spurio, R., Czisch, M., Wechselberger, R., Guenneugues, M., Gualerzi, C. O., and Boelens, R. (2000) *EMBO J.* **19,** 1918–1926
28. Guenneugues, M., Caserta, E., Brandi, L., Spurio, R., Meunier, S., Pon, C. L., Boelens, R., and Gualerzi, C. O. (2000) *EMBO J.* **19,** 5233–5240
29. Wirtz, E., and Clayton, C. (1995) *Science* **268,** 1179–1183
30. Horvath, A., Berry, E. A., and Maslov, D. A. (2000) *Science* **287,** 1639–1640
31. Horvath, A., Kingan, T. G., and Maslov, D. A. (2000) *J. Biol. Chem.* **275,** 17160–17165
32. Guillon, J. M., Mechulam, Y., Schmitter, J. M., Blanquet, S., and Fayat, G. *J. Bacteriol.* **174,** 4294–4301
33. Newton, D. T., Creuzenet, C., and Mangroo, D. (1999) *J. Biol. Chem.* **274,** 22143–22146
34. Steiner-Mosonyi, M., Creuzenet, C., Keates, R. A., Strub, B. R., and Mangroo, D. (2004) *J. Biol. Chem.* **279,** 52262–52269

B

Dual Targeting of a Single $tRNA^{Trp}$ Requires Two Different Tryptophanyl-tRNA Synthetases in *Trypanosoma brucei*

Proc. Natl. Acad. Sci. USA
Vol. 103, No. 18, pp. 6847-6852, 2006

Fabien Charrière[1], Sunna Helgadóttir[2], Elke K. Horn[1], Dieter Söll[2] and André Schneider[1]

1- Department of Biology/Zoology, University of Fribourg, Chemin du Musée 10, CH-1700 Fribourg, Switzerland
2- Departments of Molecular Biophysics and Biochemistry and Chemistry, Yale University, New Haven, CT 06520-8114

Dual targeting of a single tRNA^{Trp} requires two different tryptophanyl-tRNA synthetases in *Trypanosoma brucei*

Fabien Charrière*, Sunna Helgadóttir†, Elke K. Horn*, Dieter Söll†‡§, and André Schneider*§

*Department of Biology/Cell and Developmental Biology, University of Fribourg, Chemin du Musée 10, CH-1700 Fribourg, Switzerland; and Departments of †Molecular Biophysics and Biochemistry and ‡Chemistry, Yale University, New Haven, CT 06520-8114

Contributed by Dieter Söll, March 22, 2006

The mitochondrion of *Trypanosoma brucei* does not encode any tRNAs. This deficiency is compensated for by the import of a small fraction of nearly all of its cytosolic tRNAs. Most trypanosomal aminoacyl-tRNA synthetases are encoded by single-copy genes, suggesting the use of the same enzyme in the cytosol and mitochondrion. However, the *T. brucei* genome contains two distinct genes for eukaryotic tryptophanyl-tRNA synthetase (TrpRS). RNA interference analysis established that both TrpRS1 and TrpRS2 are essential for growth and required for cytosolic and mitochondrial tryptophanyl-tRNA formation, respectively. Decoding the mitochondrial tryptophan codon UGA requires mitochondria-specific C→U RNA editing in the anticodon of the imported tRNA^{Trp}. *In vitro* charging assays with recombinant TrpRS enzymes demonstrated that the edited anticodon and the mitochondria-specific thiolation of U33 in the imported tRNA^{Trp} act as antideterminants for the cytosolic TrpRS1. The existence of two TrpRS enzymes, therefore, can be explained by the need for a mitochondrial synthetase with extended substrate specificity to achieve aminoacylation of the imported thiolated and edited tRNA^{Trp}. Thus, the notion that, in an organism, all nuclear-encoded tRNAs assigned to a given amino acid are charged by a single aminoacyl-tRNA synthetase, is not universally valid.

genetic code | mitochondria | RNA editing | aminoacyl-tRNA synthetase

In animal and most fungal mitochondria, the total set of tRNAs required for translation is encoded in the mitochondrial genome and, therefore, of bacterial evolutionary origin. The aminoacyl-tRNA synthetases (aaRSs) responsible for charging of mitochondrial tRNAs always are nuclear-encoded and, therefore, need to be imported into mitochondria (1). However, their evolutionary origin, just as the one of their substrate tRNAs, is in most cases bacterial. Thus eukaryotes, if we exclude all plastid-containing organisms, generally have two sets of aaRSs, one for cytosolic and a second one for mitochondrial aminoacyl-tRNA synthesis. In most eukaryotes, however, there are a few aaRSs that are targeted to both the cytosol and the mitochondria, indicating that the two sets of enzymes overlap to a limited extent (2).

Most mitochondrial genetic systems show deviations from the universal genetic code. The most common one is a reassignment of the termination codon UGA to tryptophan (3). Thus, to decode the UGA tryptophan codon, mitochondria require a nonstandard tRNA^{Trp} carrying a UCA instead of CCA anticodon. Cytosolic tRNA$^{Trp}_{CCA}$ is aminoacylated by a eukaryotic tryptophanyl-tRNA synthetase (TrpRS) (4), whereas the mitochondrial-encoded tRNA$^{Trp}_{UCA}$ is charged by a bacterial-type TrpRS (5). The CCA anticodon is a known identity element for both enzymes (6–8). It is clear, however, that the bacterial-type enzyme in mitochondria must be able to tolerate an UCA anticodon (5).

In contrast to animals and most fungi, mitochondria from protozoa and plants generally lack a variable number of mitochondrial tRNA genes. In these cases, the missing tRNAs are replaced by import of a small fraction of the corresponding nuclear-encoded cytosolic tRNAs (9). As a consequence, the imported tRNAs are always of a eukaryotic evolutionary origin. An intriguing situation is found in trypanosomatids, e.g., *Trypanosoma brucei* and *Leishmania* spp., which have lost all mitochondrial tRNA genes (10–12). Their mitochondrial translation system therefore must function exclusively with imported eukaryotic-type tRNAs.

Trypanosomatid mitochondria use UGA as tryptophan codon. However, the only tRNA^{Trp} gene in *T. brucei* is nuclear and carries the standard tryptophan anticodon CCA. Recent work in *Leishmania* revealed that trypanosomatids use RNA editing to convert the CCA anticodon of ≈40% of the imported tRNA^{Trp} to UCA; the resulting tRNA now is able to recognize UGA codons (13). Besides RNA editing, the imported tRNA^{Trp} is subjected to additional mitochondria-specific modifications; most importantly, the thiolation of U33, the "universally unmodified" uridine in all known tRNAs (14). tRNA editing is not required for thiolation of U33 but it is possible that the modification is needed for editing. In any case, the close proximity of the thiolated U33 to the anticodon suggests that it influences decoding.

Cytosolic and mitochondrial tRNAs of trypanosomatids originate from the same set of nuclear genes. Therefore, it is reasonable to assume that the same aaRSs are used in the cytosol and in mitochondria. This assumption is supported by the fact that in *T. brucei*, most aaRSs are represented by single genes only (15). Furthermore a dual localization in the cytosol and in mitochondria has been shown for *T. brucei* glutaminyl-tRNA synthetase and the glutamyl-tRNA synthetase (16). The imported trypanosomal tRNA^{Trp}, however, represents a special case, because its anticodon loop, due to the editing event and the thiolation of U33, differs from its cytosolic counterpart (14). This situation raises the question of how cytosolic and mitochondrial tryptophanyl-tRNA species are formed in *T. brucei*? Here we show that unlike most other trypanosomal tRNAs, because of the mitochondrial use of UGA as tryptophan codon, cytosolic and mitochondrial aminoacylation of tRNA^{Trp} requires two distinct eukaryotic-type TrpRSs.

Results

The *T. brucei* Genome Encodes Two Eukaryotic TrpRSs. In the genome of *Saccharomyces cerevisiae*, probably the best characterized eukaryote, we find annotated genes for 36 different aaRSs (www.yeastgenome.org). These enzymes can be divided into 16 cytosol-specific ones, 14 of which are specific for mitochondria, and four are known to be doubly targeted to the cytosol and the mitochondria (these numbers are still, in part, based on predictions and, therefore, represent approximations). It is striking to compare yeast with *T.*

Conflict of interest statement: No conflicts declared.

Abbreviations: aaRS, aminoacyl-tRNA synthetase; OXPHOS, oxidative phosphorylation; RNAi, RNA interference; TrpRS, tryptophanyl-tRNA synthetase.

§To whom correspondence may be addressed. E-mail: dieter.soll@yale.edu or andre.schneider@unifr.ch.

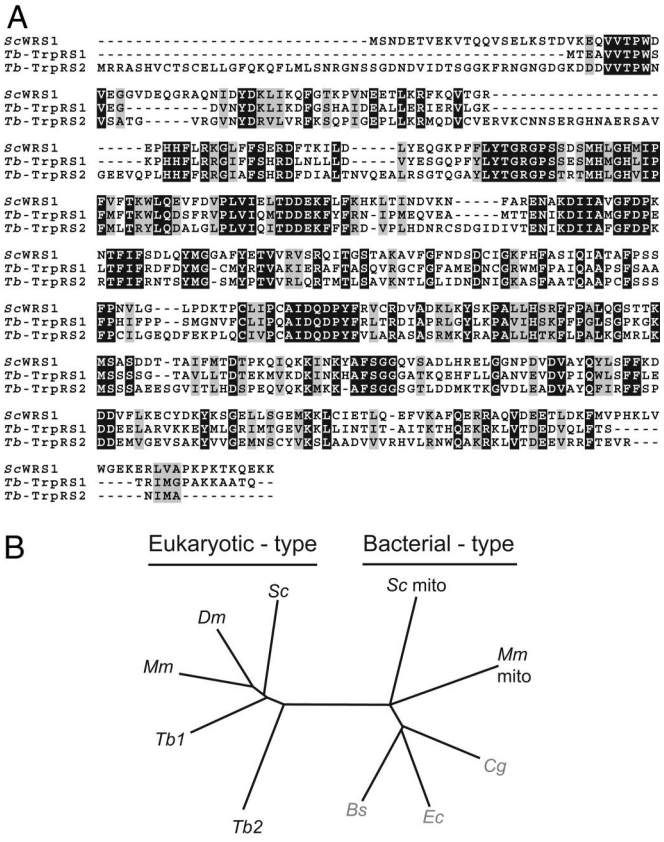

Fig. 1. *T. brucei* contains two eukaryotic TrpRSs. (*A*) Multiple sequence alignment of the cytosolic TrpRS from *S. cerevisiae* (*Sc*WRS1) and the two *T. brucei* orthologues (*Tb*-TrpRS1 and *Tb*-TrpRS2). The sequences were aligned by using the CLUSTAL W program with default parameters. Strictly conserved residues and conservative replacements are shown in black and gray boxes, respectively. (*B*) Position of the two trypanosomal enzymes *Tb*-TrpRS1 (*Tb1*) and *Tb*-TrpRS2 (*Tb2*) in a phylogenetic tree based on a multiple sequence alignment of the cytosolic TrpRS from mouse [*Mus musculus* (*Mm*)], *Drosophila melanogaster* (*Dm*), and yeast [*S. cerevisiae* (*Sc*)]; the mitochondrial enzyme of yeast (*Sc* mito) and mouse (*Mm* mito); and, indicated by gray letters, the TrpRS from the bacteria *Corynebacterium glutamicum* (*Cg*), *Bacillus subtilis* (*Bs*), and *E. coli* (*Ec*). The tree was constructed by using TREEVIEW, which is available on http://taxonomy.zoology.gla.ac.uk/rod/treeview.html.

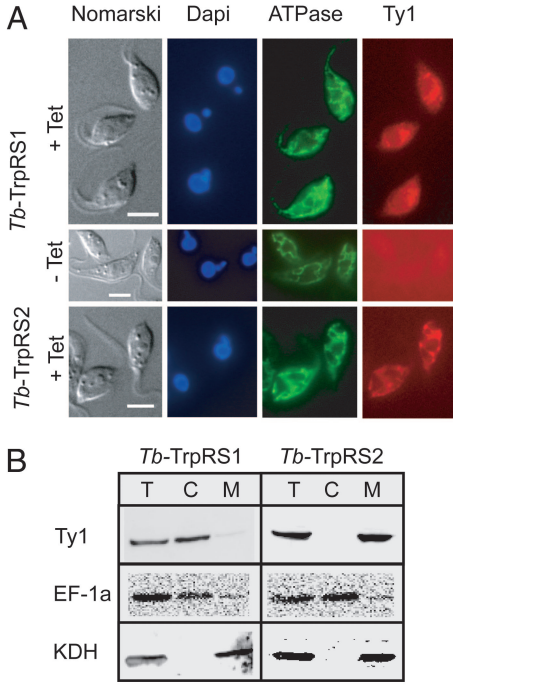

Fig. 2. Localization of trypanosomal TrpRSs. (*A Top and Center*) Double immunofluorescence analysis of a *T. brucei* cell line expressing *Tb*-TrpRS1 carrying the Ty1 tag at its carboxyl terminus under the control of the tetracycline-inducible (+Tet and −Tet) procyclin promoter. The cells were stained for DNA by using DAPI, for a subunit of the ATPase, serving as a mitochondrial marker and with a monoclonal antibody recognizing the Ty1-Tag. (*A Bottom*) Same as *Top* and *Center*, but a cell line expressing carboxyl-terminally Ty1-tagged *Tb*-TrpRS2 was analyzed. (Scale bars: 10 μm.) (*B*) Immunoblot analysis of total cellular (T), crude cytosolic (C), and crude mitochondrial extracts (M) for the presence of the Ty1-tagged *Tb*-TrpRS1 and *Tb*-TrpRS2, respectively. Elongation factor 1a (EF-1a) served as a cytosolic and α-ketoglutarate dehydrogenase (KDH) as a mitochondrial marker.

brucei, whose genome encodes only 23 annotated aaRSs (15). This low number makes sense because the tRNAs in the cytosol and mitochondria derive from the same nuclear genes (10); it therefore can be expected that the same aaRSs are used in both compartments. Nevertheless, two distinct genes are found for aspartyl-tRNA synthetase, lysyl-tRNA synthetase, and TrpRS. Furthermore, in each case, one of the two proteins is predicted to have a mitochondrial targeting sequence. It is not obvious why *T. brucei* should have two aspartyl- or lysyl-tRNA synthetases, because the corresponding cytosolic and mitochondrial substrate tRNAs derived from the same nuclear genes. However, the need for two distinct TrpRSs might be explained by the fact that because of editing in the mitochondrion, cytosolic and mitochondrial $tRNA^{Trp}$ differ in an anticodon nucleotide (13). In this study, we focus on the functional analysis of *Tb*-TrpRS1 and *Tb*-TrpRS2, the two trypanosomal TrpRS homologues. The two proteins are 41% identical, phylogenetic analysis shows that both are of the eukaryotic type, and *Tb*-TrpRS2 contains a predicted 50-aa mitochondrial presequence (Fig. 1). *Tb*-TrpRS1 shares 48–53% sequence identity to eukaryotic TrpRSs, whereas *Tb*-TrpRS2 is more diverged, showing an identity to other eukaryotic TrpRSs of only 39–41%. Interestingly, essentially the same situation is found in *Leishmania* (17). The two leishmanial proteins *Lm*-TrpRS1 and *Lm*-TrpRS2 are 76% and 59% identical to their trypanosomal counterparts.

Intracellular Localization of *Tb*-TrpRS1 and *Tb*-TrpRS2. *Tb*-TrpRS2 is predicted to have a mitochondrial targeting signal. However, in *T. brucei*, such predictions are difficult because mitochondrial presequences can be very short (18). Thus, to determine the localization of the two enzymes, we prepared transgenic cell lines, allowing inducible expression of *Tb*-TrpRS1 and *Tb*-TrpRS2 versions carrying the 10-aa-long Ty1-peptide as epitope tags at their carboxyl termini (19). Immunofluorescence analysis by using an anti Ty1-antibody showed a tetracycline-inducible diffuse staining of the tagged *Tb*-TrpRS1, consistent with a cytosolic localization (Fig. 2*A Top* and *Center*). For tagged *Tb*-TrpRS2, on the other hand, a staining identical to the one seen with the mitochondrial marker was obtained (Fig. 2*A Bottom*). Furthermore, the two transgenic cell lines were subjected to a biochemical analysis that showed that the tagged *Tb*-TrpRS1 copurifies with the cytosolic marker, whereas the tagged *Tb*-TrpRS2 together with the mitochondrial marker is recovered in the pellet (Fig. 2*B*). These results are consistent with the immunofluorescence analysis and show that the two TrpRSs have a nonoverlapping intracellular distribution: *Tb*-TrpRS1 is exclusively cytosolic and *Tb*-TrpRS2 is exclusively mitochondrially localized.

RNA Interference (RNAi)-Mediated Ablation of *Tb*-TrpRS1 and *Tb*-TrpRS2. To determine the function of *Tb*-TrpRS1 and *Tb*-TrpRS2, we established two stable transgenic cell lines, which allow tetra-

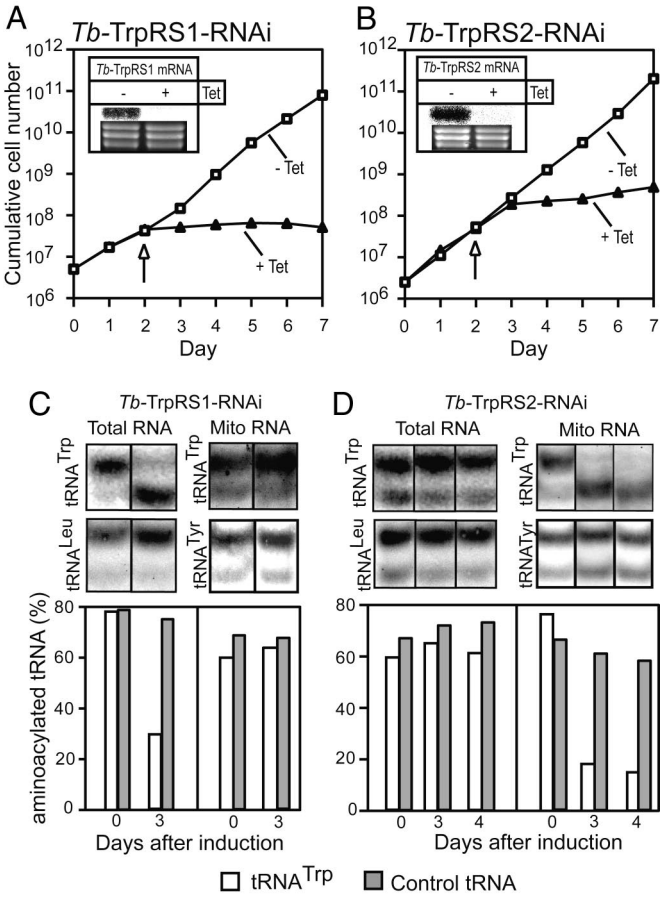

Fig. 3. *Tb*-TrpRS1 and *Tb*-TrpRS2 are essential for the growth of procyclic *T. brucei* and are responsible for formation of tryptophanyl-tRNA in the cytosol and the mitochondria, respectively (*A*) Growth curve in the presence and absence of tetracycline (+Tet and −Tet) of a representative clonal *T. brucei* RNAi cell line ablated for *Tb*-TrpRS1. (*A Inset*) A Northern blot for *Tb*-TrpRS1 mRNA. The time of sampling is indicated by the arrow. The rRNAs in the lower panel serve as loading controls. (*B*) Same as *A* for an RNAi cell line ablated for *Tb*-TrpRS2. (*C*) Northern blot analysis of total and mitochondrial RNA isolated under acidic conditions from the *Tb*-TrpRS1 RNAi cell line. The total RNA fraction only contains ≈5% of mitochondrial RNA and, thus, essentially represents cytosolic RNA. Days of induction (0 and 3) by tetracycline are indicated at the bottom. The blots were probed for the *T. brucei* $tRNA^{Trp}$ as well as $tRNA^{Leu}$ and $tRNA^{Tyr}$, which serve as controls not affected by the RNAi. The RNA fractions were resolved on long acid urea gels, which allow separation of aminoacylated from deacylated tRNAs. The bar graph shows the quantification of the results. Relative amounts of aminoacylated tRNAs are indicated for the $tRNA^{Trp}$ and the controls ($tRNA^{Leu}$ and $tRNA^{Tyr}$), respectively. For each lane, the sum of aminoacylated and deacylated tRNA was set to 100%. (*D*) Same as *C*, but analysis was done for the *Tb*-TrpRS2 RNAi cell line.

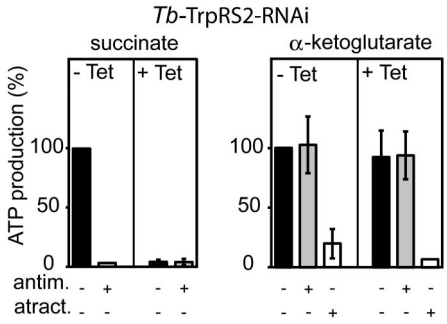

Fig. 4. Ablation of *Tb*-TrpRS2 selectively abolishes OXPHOS. Succinate and α-ketoglutarate mitochondrial ATP production in crude mitochondrial fractions of the *Tb*-TrpRS2 RNAi cell line. Uninduced cells (−Tet) are shown on the left, and induced cells (+Tet) are shown on the right of the graphs. The substrate tested is indicated at the top, and additions of antimycin (antim.) and atractyloside (atract.) are indicated at the bottom. ATP productions in mitochondria isolated from uninduced cells tested without antimycin or atractyloside are set to 100%. The bars represent means expressed as percentages from three or more independent inductions. SEs are indicated.

cycline-inducible ablation of each of the two enzymes. The Northern blot insets in Fig. 3 *A* and *B* show that induction of RNAi in these two cell lines leads to specific degradation of the corresponding *Tb*-TrpRS mRNAs. Most importantly, concomitant with the depletion of the mRNAs, a growth arrest is observed 2 (for *Tb*-TrpRS1) and 3 days (for *Tb*-TrpRS2) after the addition of tetracycline (Fig. 3 *A* and *B*). Thus, *Tb*-TrpRS1 and *Tb*-TrpRS2 are both essential for growth of insect stage *T. brucei*.

To determine the biochemical phenotype of the two RNAi cell lines, we isolated total and mitochondrial RNA from untreated cells and from cells grown in the presence of tetracycline. Subsequently, the RNAs were resolved on long acid urea polyacrylamide gels (20), followed by Northern blot analysis, to determine the ratio of uncharged $tRNA^{Trp}$ to tryptophanyl-$tRNAs^{Trp}$ (Fig. 3 *C* and *D*). The results in Fig. 3*C Left* show that ablation of *Tb*-TrpRS1 results in the accumulation of uncharged cytosolic $tRNA^{Trp}$. Interestingly, in measurements of the levels of tryptophanyl-$tRNA^{Trp}$ in the induced *Tb*-TrpRS2 cell line, the converse result was obtained, and a selective accumulation of deacylated mitochondrial $tRNA^{Trp}$ was observed (Fig. 3*D Right*). As expected, ablation of either TrpRS had no influence on the aminoacylation levels of cytosolic $tRNA^{Leu}$ or mitochondrial $tRNA^{Tyr}$. These results show that, in agreement with its exclusive cytosolic localization, *Tb*-TrpRS1 is responsible for aminoacylation of the cytosolic $tRNA^{Trp}$. On the other hand *Tb*-TrpRS2, in line with its mitochondrial localization, is required for charging of imported mitochondrial $tRNA^{Trp}$.

Ablation of *Tb*-TrpRS2 abolishes mitochondrial protein synthesis and, consequently, is expected to interfere with oxidative phosphorylation (OXPHOS). Mitochondria produce ATP, by OXPHOS and by substrate level phosphorylation linked to the citric acid cycle. We recently established an assay that allows quantitation of both modes of ATP production in isolated *T. brucei* mitochondria (21, 22). To measure antimycin-sensitive OXPHOS, mitochondria are incubated with ADP and succinate. α-ketoglutarate is used in the determination of the antimycin-resistant substrate level phosphorylation, whereas atractyloside treatment that prevents mitochondrial import of the added ADP is the control. The results in Fig. 4 show that ablation of *Tb*-TrpRS2 selectively knocks down OXPHOS that, in part, depends on mitochondrial-encoded proteins but does not interfere with substrate level phosphorylation, which depends solely on nuclear encoded proteins.

Substrate Specificities of *Tb*-TrpRS1 and *Tb*-TrpRS2. Recent work in *Leishmania* (14) showed that the imported $tRNA^{Trp}$ is present in two main forms: (*i*) the $tRNA^{Trp}_{CCA}$ carrying a mitochondria-specific methylation on the C34 and (*ii*) the $tRNA^{Trp}_{UCA}$ in which the methylated C34 has been edited to a methylated U and which also contains a mitochondria-specific thiolated U33. Furthermore, it was shown that both $tRNA^{Trp}$ forms contain a mitochondria-specific methylation on the Ψ32 (Fig. 5*A*). Fig. 5*B* shows that in *T. brucei* ≈85% of the imported $tRNA^{Trp}$ is thiolated. Furthermore, RT-PCR analysis by using cytosolic and mitochondrial RNA as substrates demonstrates that ≈40% of mitochondrial $tRNA^{Trp}$ is edited (Fig. 5*C*). Thus, in contrast to *Leishmania*, where all thiolated $tRNA^{Trp}$ is edited (14), there is a population of *T. brucei* $tRNA^{Trp}$, which is thiolated but not edited.

To test their substrate specificities, recombinant proteins of

BIOCHEMISTRY

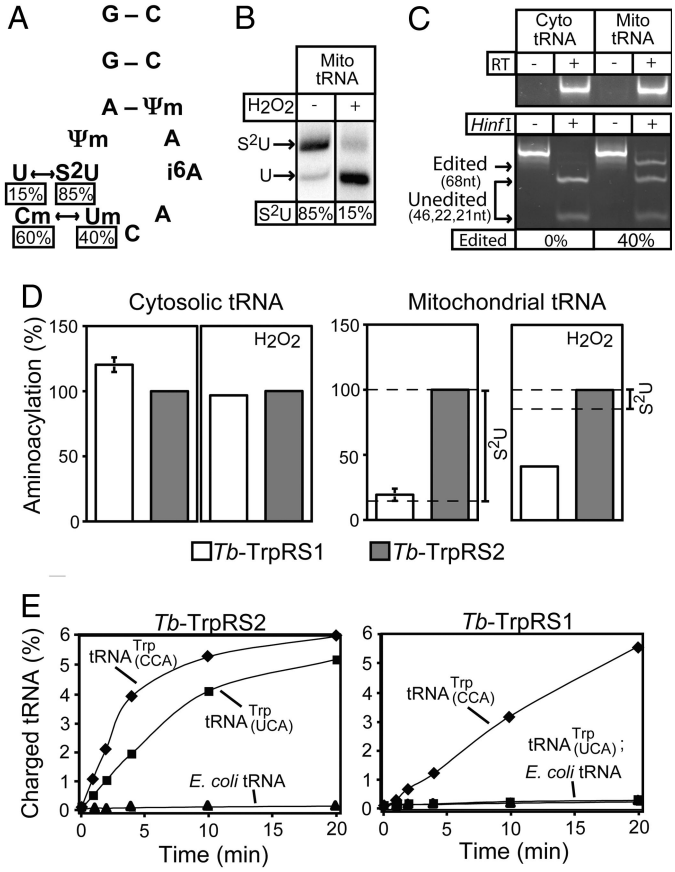

Fig. 5. *Tb*-TrpRS1 and *Tb*-TrpRS2 have distinct substrate specificities. (*A*) Mitochondrial editing and modification events of the anticodon loop of the $tRNA^{Trp}$ as described for *Leishmania* (14). The percentages of the thiolated U (s^2U) and the C→U editing as determined for *T. brucei* $tRNA^{Trp}$ are indicated. (*B Left*) The percentage of thiomodified mitochondrial $tRNA^{Trp}$ of *T. brucei* was measured by *N*-acryloylaminophenylmercuric chloride gel electrophoresis (33) and Northern blot hybridization. The shifted band represents thiolated $tRNA^{Trp}(S^2U)$. (*B Right*) The fraction of thiolated mitochondrial $tRNA^{Trp}$ that remains thiolated after H_2O_2 treatment was determined as in the left lane. (*C*) Quantitative RT-PCR assay for edited $tRNA^{Trp}$. (*C Upper*) The cytosolic and mitochondrial tRNA fractions that were used as templates are free of DNA. (*C Lower*) The blot shows that RNA editing can be analyzed by a restriction digest because it destroys a HinfI site that is present in the cDNA derived from the unedited $tRNA^{Trp}$ (14). Introduction of a synthetic HinfI plus 20 flanking nucleotides at the 5′ end of the 5′ RT-PCR primer provides an internal control for the HinfI digestion, allowing the quantitative determination of RNA editing. cDNA amplified from unedited $tRNA^{Trp}$ contains two HinfI sites and, thus, will be digested into three fragments (46, 22, and 21 nt; unedited). The cDNA derived from edited $tRNA^{Trp}$ contains the synthetic HinfI site only and will be digested into two fragments (68 and 21 nt; edited). Measuring the intensities of the diagnostic bands for nonedited (46 nt) and edited (68 nt) $tRNA^{Trp}$ allows, after correcting for their different molecular mass, determination of the fraction of edited $tRNA^{Trp}$ in *T. brucei* mitochondria. (*D*) *In vitro* aminoacylation assays by using [^{3}H]tryptophan and recombinant *Tb*-TrpRS1 as well as *Tb*-TrpRS2 as enzymes. (*Left* and *Center Left*) Untreated and H_2O_2-treated cytosolic tRNA were charged. (*Right* and *Center Right*) Same as *Left* and *Center Left* but with untreated and H_2O_2-treated mitochondrial tRNAs. For each graph, the tRNA charged by the *Tb*-TrpRS2 was set to 100%. The percentage of mitochondrial $tRNA^{Trp}$ that is thiolated in the untreated and treated fractions is indicated on the right. The means and SE for three independent experiments are shown for aminoacylation of untreated tRNAs. For experiments using H_2O_2-treated tRNAs, the mean of two experiments is shown. The two values each for cytosolic and mitochondrial tRNAs varied by 20% and 10%, respectively. (*E*) Aminoacylation of *T. brucei* $tRNA^{Trp}$ overexpressed in *E. coli* by using 200 nM enzyme and 0.25 $\mu g/\mu l$ tRNA. (*Right*) *Tb*-TrpRS1 charging of total *E. coli* tRNA with *T. brucei* $tRNA^{Trp}_{UCA}$ overexpressed (■), total *E. coli* tRNA with *T. brucei* $tRNA^{Trp}_{CCA}$ overexpressed (◆), and total *E. coli* tRNA (▲). (*Left*) *Tb*-TrpRS2 charging of total *E. coli* tRNA with *T. brucei* $tRNA^{Trp}_{UCA}$ overexpressed (■), total *E. coli* tRNA with *T. brucei* $tRNA^{Trp}_{CCA}$ overexpressed (◆), and total *E. coli* tRNA (▲).

Tb-TrpRS1 and *Tb*-TrpRS2 were overexpressed in *Escherichia coli* and purified to >95% homogeneity. *In vitro* charging assays showed that although neither enzyme was able to recognize *in vitro* transcripts corresponding to unedited or edited $tRNA^{Trp}$ (data not shown), both efficiently aminoacylated isolated *T. brucei* cytosolic tRNA (Fig. 5*D Left*). Thus, the cytosolic unedited $tRNA^{Trp}_{CCA}$ can be charged with very similar efficiencies by both the cytosolic and the mitochondrial enzyme. Interestingly, however, when using isolated mitochondrial tRNAs as a substrate, the level of aminoacylation achieved by the cytosolic *Tb*-TrpRS1 dropped to 19% of that obtained with the mitochondrial enzyme (Fig. 5*D Center Right*). This fraction correlates with the level of nonthiolated mitochondrial $tRNA^{Trp}$ (Fig. 5*B*), suggesting that, in contrast to mitochondrial *Tb*-TrpRS2, *Tb*-TrpRS1 is not able to charge thiolated $tRNA^{Trp}$. Fig. 5*B* shows that hydrogen peroxide treatment produces a mitochondrial $tRNA^{Trp}$ population in which only 15% (instead of 85%) of the molecules contain thiolated U33. Interestingly, the H_2O_2-treated mitochondrial tRNA fraction can be charged by cytosolic *Tb*-TrpRS1 to a level that corresponds to ≈40% of the one observed with the mitochondrial enzyme (Fig. 5*D Right*). However, the reactivity of either enzyme did not change when tested with H_2O_2-treated cytosolic tRNAs, which do not contain thiolated $tRNA^{Trp}$ (Fig. 5*D Center Left*). Thus, removing the thio group converts a population of mitochondrial $tRNA^{Trp}$ into a substrate for the cytosolic *Tb*-TrpRS1. Interestingly, even in the absence of thiolated U33, ≈60% of the mitochondrial $tRNA^{Trp}$ remained refractory to aminoacylation by the cytosolic enzyme. The uncharged fraction represents ≈50% of the thiolated U33 lacking $tRNA^{Trp}$ population and, thus, is similar to the ≈40% observed for the edited population. Therefore, the most parsimonious explanation of these results is that the edited U34, just as the thiolated U33, both act as independent antideterminants for cytosolic *Tb*-TrpRS1. To confirm the charging results presented above, we expressed the *T. brucei* $tRNA^{Trp}_{UCA}$ and $tRNA^{Trp}_{CCA}$ genes in *E. coli* and isolated total tRNA. Aminoacylation of these tRNA samples with the two TrpRSs demonstrated (Fig. 5*E*) that the mitochondrial *Tb*-TrpRS2 enzyme charged both $tRNA^{Trp}$ isoacceptors, whereas the cytosolic *Tb*-TrpRS1 acylated only $tRNA^{Trp}_{CCA}$. Neither enzyme charged *E. coli* tRNA. Thus, *Tb*-TrpRS2 efficiently aminoacylates the unedited and edited fraction of mitochondrial $tRNA^{Trp}$. Furthermore, the *in vivo* aminoacylation level of total mitochondrial $tRNA^{Trp}$ was shown to be close to 80% (Fig. 3*D*). These results suggest that both isoacceptors are used in mitochondrial protein synthesis, the unedited $tRNA^{Trp}$ being restricted to decode the standard UGG tryptophan codons.

Our current understanding of the structure of eukaryotic TrpRS does not allow a prediction of the anticodon binding sites that might explain the different tRNA recognition properties. Based on structural modeling of human TrpRS (D. Kennedy and W. Yin, unpublished data), the putative anticodon-binding domain of *Tb*-TrpRS1 extends from G270-F373. The sequences of the two *Tb*-TrpRSs are quite different in this region; they share only 30% amino acid identity.

Discussion

One of the few generalizations about mitochondrial tRNA import states that only a small fraction of a given nuclear encoded tRNA is imported and that the remainder functions in cytosolic translation (9). Thus, in all organisms, imported tRNAs are always of the eukaryotic type. Mitochondrial translation, however, is of a bacterial evolutionary origin. tRNA import, therefore, can be considered as a horizontal gene product transfer between the eukaryotic and bacterial domains. There are some fundamental differences between eukaryotic and bacterial-type translation systems that, for some tRNAs, are expected to prevent the dual use in the cytosol and in mitochondria. One such difference is necessitated by mitochondrial variants of the genetic code. The most frequent code deviation

is the reassignment of the stop codon UGA to tryptophan (3). Reading this reassigned codon requires a $tRNA^{Trp}$ with a UCA anticodon. Simultaneous use of this tRNA in the cytosol and in mitochondria, however, is not possible because it would act as a nonsense suppressor in the cytosol. In line with this constraint, it was recently shown that in most organisms that import tRNAs the mitochondrial $tRNA^{Trp}$ gene has been retained (23). Thus, it is unexpected that trypanosomatids import the $tRNA^{Trp}$. The way *Leishmania* mitochondria accommodate the change in the genetic code is by mitochondria-specific C→U editing of the first anticodon position of the imported $tRNA^{Trp}$ (13). In the present work, we have analyzed the situation in the closely related *T. brucei* and shown that although editing of the imported $tRNA^{Trp}$ is necessary, it is not sufficient to allow decoding of the mitochondrial UGA codons. The problem that arises is that the mitochondrially localized $tRNA^{Trp}$ cannot be aminoacylated by the standard eukaryotic-type TrpRS (*Tb*-TrpRS1). In contrast to most other trypanosomal aaRSs, which have dual location and are used to charge cytosolic and imported tRNAs (16), *Tb*-TrpRS1 is exclusively found in the cytosol. A survey of the genome showed that *T. brucei* has a second TrpRS (*Tb*-TrpRS2) that is related to the cytosolic *Tb*-TrpRS1 but is localized exclusively in mitochondria. This enzyme has an extended substrate specificity and aminoacylates *in vitro* both cytosolic and mitochondrial $tRNA^{Trp}$. Further studies showed that both the thio-modified U33 and the C→U editing of the first nucleotide in the anticodon prevent mitochondrial $tRNA^{Trp}$ to be recognized by the cytosolic *Tb*-TrpRS1. The function of the thiolated U33 in mitochondrial $tRNA^{Trp}$ of trypanosomatids is unknown (14). However, the fact that it is localized immediately 5′ of the first position of the anticodon suggests that it influences the decoding properties of the $tRNA^{Trp}$ or that it even may be required for tRNA editing. In most systems, the reassignment of the UGA codon is accommodated by a single mutation in the mitochondrial $tRNA^{Trp}$ gene, which probably requires an adaptation of the mitochondrial TrpRS (3). The situation is different for mitochondria of trypanosomatids because they need (*i*) a mitochondria-specific tRNA editing enzyme that produces the $tRNA^{Trp}_{UCA}$ (13) and (*ii*) a separate TrpRS (*Tb*-TrpRS2) with an extended substrate specificity. The need for a record TrpRS is due to the fact that the C→U editing not only changes the decoding properties of the $tRNA^{Trp}$ but also its identity toward the classic TrpRS (*Tb*-TrpRS1). Thus, recoding of UGA to tryptophan appears to be more costly for trypanosomatids than for other organisms.

Doubly targeted aaRSs, which are able to aminoacylate both nuclear-encoded tRNAs in the cytosol and the corresponding mitochondrial encoded tRNAs, are found in most, if not all, eukaryotes (2). In this study, we describe the converse situation in that tRNAs derived from the same nuclear gene require two distinct aaRSs for proper function. Thus, the presence of a single modification, be it the thio group on the U33 or the C→U editing of the anticodon, is sufficient to prevent aminoacylation by *Tb*-TrpRS1. Our results show that the notion that in an organism all nuclear-encoded tRNA isoacceptors for a given amino acid are charged by a single aaRS (4) is not universally valid.

The anticodon and the discriminator nucleotide are the major identity elements for TrpRS (6, 7). Whereas the anticodon is a phylogenetically shared identity element, the discriminator nucleotide differs between bacteria and eukaryotes (6), which explains why the two TrpRSs cannot efficiently cross-aminoacylate the corresponding $tRNA^{Trp}$ species (24, 25). Most mitochondria decode UGA as tryptophan, thus it is clear that the bacterial-type mitochondrial TrpRS has evolved to tolerate an UCA anticodon (3, 5). Interestingly, the same applies for the eukaryotic mitochondria-localized *Tb*-TrpRS2 in *T. brucei* because, unlike the cytosolic *Tb*-TrpRS1, it is able to charge eukaryotic $tRNA^{Trp}$ carrying an UCA anticodon. Thus, the existence of both bacterial and eukaryotic TrpRSs that are able to charge mitochondrial $tRNA^{Trp}$ carrying the nonstandard UCA anticodon is a result of convergent evolution. Whether bacterial or eukaryotic TrpRS is used inside mitochondria might be determined to a great extent by the discriminator nucleotide on the corresponding $tRNA^{Trp}$ and, therefore, depends on whether the $tRNA^{Trp}$ is encoded in the mitochondrial DNA or imported from the cytosol.

Thus *Tb*-TrpRS2 represents an adaptation to the fact that the trypanosomal mitochondrial translation system has to function with eukaryotic-type tRNAs. Another adaptation of the same kind is the unusual *T. brucei* methionyl-$tRNA^{Met}$ formyltransferase (MTF), which because of the absence of a bacterial-type initiator $tRNA^{Met}$, has to formylate the only $tRNA^{Met}$ present in mitochondria, which is the imported elongator $tRNA^{Met}$ (26, 27). To perform their function, the trypanosomal MTF and the *Tb*-TrpRS2 had to develop a substrate specificity that is distinct from their orthologues. Trypanosomal MTF completely switched its specificity and exclusively formylates elongator $tRNA^{Met}$, unlike all other MTFs, which only recognize bacterial-type initiator $tRNAs^{Met}$. In the case of *Tb*-TrpRS2, the enzyme still recognizes the standard substrate for eukaryotic TrpRS, the $tRNA^{Trp}_{CCA}$, but has extended its substrate specificity to $tRNAs^{Trp}$ carrying a thiolated U33 and an UCA anticodon.

Studies of the adaptations of mitochondrial translation factors that interact directly with tRNAs (e.g., aaRSs, initiation factor 2 (28), or elongation factor Tu) to imported eukaryotic tRNAs should yield additional surprises and reveal more fundamental requirements of translation.

Materials and Methods

Cells. Procyclic *T. brucei*, strain 29-13 (29) was grown in SDM-79, supplemented with 15% FCS/25 μg/ml hygromycin/15 μg/ml G-418 at 27°C, and harvested at 1.5–3.5 × 10^7 cells per ml.

Production of Transgenic Cell Lines. As a tag to localize *Tb*-TrpRS1 (accession no. *Tb*927.3.5580) and *Tb*-TrpRS2 (accession no. *Tb*927.8.2240), we used a 10-aa epitope of the major structural protein of yeast Ty1, which is recognized by the monoclonal antibody BB2 (19). The sequences corresponding to the carboxyl-terminal Ty1-tagged *Tb*-TrpRS1 and *Tb*-TrpRS2 were cloned into a derivative of pLew-100 to allow tetracycline-inducible expression of the tagged proteins (29).

RNAi of *Tb*-TrpRS1 and *Tb*-TrpRS2 was performed by using stem loop constructs containing the puromycin resistance gene (22). As inserts, we used a 537-bp fragment (nucleotides 4–540) of the *Tb*-TrpRS1 gene and a 537-bp fragment (nucleotides 4–540) of the *Tb*-TrpRS2 gene.

Transfection of *T. brucei* and selection with antibiotics, cloning, and induction with tetracycline were done as described in ref. 30.

Cell Fractionation by Digitonin. Fractionation of Ty1 epitope-tagged *Tb*-TrpRS1- and *Tb*-TrpRS2-expressing cells was done by digitonin extraction. Washed *T. brucei* cells (10^8 cells) were resuspended in 0.5 ml of SoTE (0.6 M sorbitol/20 mM Tris·HCl, pH 8/2 mM EDTA). After the addition of 0.5 ml of SoTE containing 0.03% (wt/vol) of digitonin, the samples were mixed by pipetting and incubated on ice for 5 min. The suspensions were centrifuged at 6,800 × *g* for 5 min at 4°C, resulting in a pellet that corresponds to a crude mitochondrial fraction and a supernatant faction. The latter was cleared by centrifugation (10 min at 21,000 × *g* at 4°C), yielding a crude cytosolic fraction. Finally, 0.3 × 10^7 cell equivalents each of total protein extract, crude cytosolic, and crude mitochondrial fractions were separated by SDS-gel electrophoresis and analyzed by immunoblotting.

Analysis of *in Vivo* Aminoacylation. Mitochondria from uninduced and induced *Tb*-TrpRS1 and *Tb*-TrpRS2 RNAi cell lines were

BIOCHEMISTRY

isolated by digitonin extraction and subsequent RNase treatment as described to yield a crude mitochondrial fraction that is essentially free of cytosolic RNAs (10). RNA was isolated from the crude mitochondrial fractions as well as uninduced and induced total cells by using the acid guanidinium isothiocyanate procedure (31), which allows isolation of charged tRNA. Then charged tRNA was separated from free tRNA on acid urea polyacrylamide gels as described in ref. 20 and visualized by Northern blot hybridization with labeled oligonucleotides ($tRNA^{Trp}$, TGAGGACTGCAGGGATTG; $tRNA^{Leu}_{CAG}$, CCTCCGGAGAGATGACGA; $tRNA^{Tyr}_{GUA}$, TGGTCCTTCCGGCCGGAATCGAA).

Cloning, Overexpression, and Purification of *Tb*-TrpRS1 and *Tb*-TrpRS2. The gene sequences were PCR-amplified by using the Expand High Fidelity PCR System (Roche Applied Science). *Tb*-TrpRS1 was cloned into NcoI/XhoI in pET20b (Novagen) with a C-terminal His tag. For *Tb*-TrpRS2, the N-terminal 21 amino acids (mitochondrial leader sequence) were omitted, and the sequence was cloned into the NdeI/XhoI in pET15b (Novagen). After sequence verification, the resulting plasmids were transformed into *E. coli* Bl-21-CodonPlus(DE3)-RIL cells (Stratagene).

Cells were grown at 37°C in LB medium supplemented with ampicillin (100 μg/ml) and chloramphenicol (34 μg/ml), and protein expression was autoinduced by using the Overnight Express Autoinduction System (Novagen) according to the manufacturer's instructions. After harvest, the cells were sonicated, and the proteins were purified by Ni-NTA chromatography (Qiagen, Valencia, CA). The desired fractions were pooled, dialyzed against 50 mM Na_2HPO_4, pH 8.0/5 mM 2-mercaptoethanol/50% glycerol, and stored at −20°.

In Vitro* Aminoacylation Assays.** ***(i) Using native tRNA. Mitochondria were prepared by hypotonic lysis and Percoll gradient centrifugation as described in ref. 32. The supernatant obtained after the initial lysis was used to isolate cytosolic RNAs by repeated phenol extractions and ethanol precipitations. Mitochondrial RNA was isolated from gradient purified mitoplasts by the acid guanidinium isothiocyanate procedure (31). A cumulative 25-liter *T. brucei* culture yielded 6 mg of mitochondrial RNA. Total and mitochondrial RNA were deacylated in 0.3 M Tris·HCl (pH 9.0) at 30°C for 1 h. Finally, tRNAs were isolated from both fractions by using Qiagen-Tip columns as described in ref. 16. The percentage yield of tRNAs from deacylated total and mitochondrial RNAs was ≈5%. H_2O_2 treatment of mitochondrial and total tRNA was done at 0.2 mg/ml by using 0.21% (wt/vol) of H_2O_2 in 10 mM Tris·HCl (pH 7.5) for 20 h at 20°C. The reaction was stopped by adding 2-mercaptoethanol to 50 mM, and tRNAs were purified by ethanol precipitation. The presence and absence of thiolated U33 was monitored by using 8 M urea/10% polyacrylamide gels containing a 25 mM concentration of *N*-acryloylaminophenylmercuric chloride (33).

In vitro aminoacylation assay were performed in 50 mM Hepes, pH 7.0/10 mM Mg-acetate/2 mM ATP/4 mM DTT/0.05% (wt/vol) BSA, and a mixture of 38 μM cold and 2 μM [^{3}H]tryptophan (32 Ci/mmol; 1 Ci = 37 GBq). The enzyme and tRNA concentrations used were as follows: 400 nM recombinant *Tb*-TrpRS1 or *Tb*-TrpRS2 and 1 mg/ml isolated total or mitochondrial tRNA as substrates. Incubation was for 10 min at 37°C, and Trp-tRNA was determined as described in ref. 34.

(ii) Using* E. coli *tRNA in which* T. brucei *$tRNA^{Trp}_{UCA}$ and $tRNA^{Trp}_{CCA}$ were overexpressed. Reactions were carried out as described above with the following modifications: 75.5 μM cold and 4.5 μM [^{3}H]tryptophan (32 Ci/mmol)/200 nM TrpRS/0.25 mg/ml tRNA.

Miscellaneous. Northern blots of tRNAs and ATP production assays were done as described in refs. 10 and 22. For the RT-PCR to amplify cDNA of cytosolic and mitochondrial $tRNA^{Trp}$, the oligonucleotides used were as follows: forward primer (AGAGAGAGCGAGGAAGGCGAGATTCTCAGTGGTAGAGCATTGG, containing a synthetic HinfI site) and reverse primer (TGGTGAGGACTGCAGGGATTG).

We thank G. Cross (The Rockefeller University, New York) and D. Speijer (University of Amsterdam, Amsterdam) for cell lines, plasmids, and antisera and J. Rinehart for encouragement. This work was supported by Swiss National Foundation Grant 3100-067906 (to A.S.), a Fellowship of the Roche Research Foundation (to F.C.), and grants from the National Institute of General Medical Sciences (to D.S.).

1. Bullerwell, C. E. & Gray, M. W. (2004) *Curr. Opin. Microbiol.* **7,** 528–534.
2. Small, I., Wintz, H., Akashi, K. & Mireau, H. (1998) *Plant Mol. Biol.* **38,** 265–277.
3. Knight, R. D., Freeland, S. J. & Landweber, L. F. (2001) *Nat. Rev. Genet.* **2,** 49–58.
4. Woese, C. R., Olsen, G. J., Ibba, M. & Söll, D. (2000) *Microbiol. Mol. Biol. Rev.* **64,** 202–236.
5. Jorgensen, R., Sogaard, T. M. M., Rossing, A. B., Martensen, P. M. & Justesen, J. (2000) *J. Biol. Chem.* **275,** 16820–16826.
6. Xue, H., Shen, W., Giege, R. & Wong, J. T.-F. (1993) *J. Biol. Chem.* **268,** 9316–9322.
7. Ulmasov, B., Topin, A., Chen, Z., He, S. H. & Folk, W. R. (1998) *Nucleic Acids Res.* **26,** 5139–5141.
8. Yesland, K. D., Nelson, A. W., Feathers, D. M. S. & Johnson, J. D. (1993) *J. Biol. Chem.* **268,** 217–220.
9. Schneider, A. & Marechal-Drouard, L. (2000) *Trends Cell Biol.* **10,** 509–513.
10. Tan, T. H. P., Pach, R., Crausaz, A., Ivens, A. & Schneider, A. (2002) *Mol. Cell. Biol.* **22,** 3707–3717.
11. Hancock, K. & Hajduk, S. L. (1990) *J. Biol. Chem.* **265,** 19208–19215.
12. Simpson, A. M., Suyama, Y., Dewes, H., Campbell, D. A. & Simpson, L. (1989) *Nucleic Acids Res.* **17,** 5427–5445.
13. Alfonzo, J. D., Blanc, V., Estevez, A. M., Rubio, M. A. T. & Simpson, L. (1999) *EMBO J.* **18,** 7056–7062.
14. Crain, P. F., Alfonzo, J. D., Rozenski, J., Kapushoc, S. T., McCloskey, J. A. & Simpson, L. (2002) *RNA* **8,** 752–761.
15. Berriman, M., Ghedin, E., Hertz-Fowler, C., Blandin, G., Renauld, H., Bartholomeu, D. C., Lennard, N. J., Caler, E., Hamlin, N. E., Haas, B., *et al.* (2005) *Science* **309,** 416–422.
16. Rinehart, J., Horn, E. K., Wei, D., Söll, D. & Schneider, A. (2004) *J. Biol. Chem.* **279,** 1161–1166.
17. Ivens, A. C., Peacock, C. S., Worthey, E. A., Murphy, L., Aggarwal, G., Berriman, M., Sisk, E., Rajandream, M. A., Adlem, E., Aert, R., *et al.* (2005) *Science* **309,** 436–442.
18. Häusler, T., Stierhof, Y.-D., Blattner, J. & Clayton, C. (1997) *Eur. J. Cell Biol.* **73,** 240–251.
19. Bastin, P., Bagherzadeh, A., Matthews, K. R. & Gull, K. (1996) *Mol. Biochem. Parasitol.* **77,** 235–239.
20. Varshney, U., Lee, C.-P. & RajBhandary, U. L. (1991) *J. Biol. Chem.* **266,** 24712–24718.
21. Schneider, A., Bouzaidi-Tiali, N., Chanez, A.-L. & Bulliard, L. (2006) *Methods Mol. Biol.*, in press.
22. Bochud-Allemann, N. & Schneider, A. (2002) *J. Biol. Chem.* **277,** 32849–32854.
23. Schneider, A. (2001) *Trends Genet.* **17,** 557–558.
24. Xu, F., Chen, X., Xin, L., Chen, L., Jin, Y. & Wang, D. (2001) *Nucleic Acids Res.* **29,** 4125–4133.
25. Guo, Q., Gong, Q., Tong, K. L., Vestergaard, B., Costa, A., Desgres, J., Wong, M., Grosjean, H., Zhu, G., Wong, J. T., *et al.* (2002) *J. Biol. Chem.* **277,** 14343–14349.
26. Tan, T. H. P., Bochud-Allemannn, N., Horn, E. K. & Schneider, A. (2002) *Proc. Natl. Acad. Sci. USA* **99,** 1152–1157.
27. Martin, N. C. (2002) *Proc. Natl. Acad. Sci. USA* **99,** 1110–1112.
28. Charrière, F., Tan, T. H. P. & Schneider, A. (2005) *J. Biol. Chem.* **280,** 15659–15665.
29. Wirtz, E., Leal, S., Ochatt, C. & Cross, G. A. (1999) *Mol. Biochem. Parasitol.* **99,** 89–101.
30. McCulloch, R., Vassella, E., Burton, P., Boshart, M. & Barry, J. D. (2004) *Methods Mol. Biol.* **262,** 53–86.
31. Chomczyinski, P. & Sacchi, N. (1987) *Anal. Biochem.* **162,** 156–159.
32. Schneider, A., Charrière, F., Pusnik, M. & Horn, E. K. (2006) *Methods Mol. Biol.*, in press.
33. Igloi, G. L. (1992) *Anal. Biochem.* **206,** 363–368.
34. Nabholz, C. E., Hauser, R. & Schneider, A. (1997) *Proc. Natl. Acad. Sci. USA* **94,** 7903–7908.

C

Trypanosoma Seryl-tRNA Synthetase Is a Metazoan-like Enzyme with High Affinity for $tRNA^{Sec}$

Submitted

Renaud Geslain[2], Eric Aeby[3], Tanit Guitart[2], Thomas E. Jones[2], Manuel Castro de Moura[2], Fabien Charrière[3], André Schneider[3] and Lluís Ribas de Pouplana[1, 2]

1- Institutió Catalana de Recerca i Estudis Avançats (ICREA)
2- Barcelona Institute for Biomedical Research, Barcelona Science Park C/ Samitier 1-5, Barcelona 08015, Catalonia, Spain
3- Department of Biology/Zoology, University of Fribourg, Chemin du Musée 10, CH-1700 Fribourg, Switzerland

Trypanosoma seryl-tRNA synthetase is a metazoan-like enzyme with high affinity for $tRNA^{Sec}$

Renaud Geslain[#•], Eric Aeby[§•], Tanit Guitart[#], Thomas E. Jones[#], Manuel Castro de Moura[#], Fabien Charrière[§], André Schneider[§], and Lluís Ribas de Pouplana[|#*]

[|] Institució Catalana de Recerca i Estudis Avançats (ICREA) and

[#] Barcelona Institute for Biomedical Research, Barcelona Science Park

C/ Samitier 1-5, Barcelona 08015, Catalonia, Spain.

[§] Department of Biology/Cell & Developmental Biology, University of Fribourg,

Chemin du Musée 10, 1700 Fribourg, Switzerland

* corresponding author. Email: lluisribas@pcb.ub.es Tel.(+34)934034868, Fax.(+34)934034870

• These authors contributed equally to this work.

Trypanosomatids are important human pathogens that form a basal branch of eukaryotes. Their evolutionary history is still unclear, as are many aspects of their molecular biology. Here we characterize essential components required for the incorporation of serine and selenocysteine into the proteome of *Trypanosoma*. First, the biological function of a putative *Trypanosoma* seryl-tRNA synthetase is characterized *in vivo*. Secondly, the molecular recognition by *Trypanosoma* seryl-tRNA synthetase of its cognate tRNAs is dissected *in vitro*. The cellular distribution of $tRNA^{Sec}$ is studied, and the catalytic constants of its aminoacylation are determined. These are found to be markedly different from those reported in other organisms, indicating that this reaction is particularly efficient in trypanosomatids. Our functional data are analyzed in the context of a new phylogenetic analysis of eukaryotic seryl-tRNA synthetases that includes *Trypanosoma* and *Leishmania* sequences. Our results show that trypanosomatid seryl-tRNA synthetases are functionally and evolutionarily more closely related to their metazoan homologous enzymes than to other eukaryotic enzymes. This conclusion is supported by sequence synapomorphies that clearly connect metazoan and trypanosomatid seryl-tRNA synthetases.

The formation of aminoacyl-tRNA, catalyzed by aminoacyl-tRNA synthetases (ARS), is a crucial step in maintaining the fidelity of protein biosynthesis. In order to avoid misacylation of non-cognate tRNAs, each synthetase recognizes identity elements idiosyncratic to their cognate substrates. tRNA identity elements can be unique and universally distributed, as in the case of the G3:U70 base pair presented by all $tRNA^{Ala}$ (1,2). On the other hand, the evolutionary constraints imposed by the necessity of translation fidelity are not rigid, and the set of recognition elements for many tRNAs have changed during evolution (1,3). Thus, the comparison between sets of tRNA recognition elements in extant species could be used to estimate their evolutionary or biological relatedness.

Here we study the evolution of the serylation reaction of $tRNA^{Ser}$ and $tRNA^{Sec}$ by characterizing this activity in trypanosomatids, a group of protozoa normally considered to form a basal group within eukaryal (4). Intriguingly, the analysis of the evolutionary history of *Trypanosoma* SerRS, and the determination of the identity elements used by this enzyme to recognize $tRNA^{Ser}$, show that *Trypanosoma* SerRSs are closer relatives of metazoan SerRSs than plant, fungi, or other protozoan enzymes.

Seryl-tRNA synthetases (SerRSs) are class II ARS that contain the characteristic active site domain of this family of enzymes (5,6). In addition to this domain, the structures of most SerRSs include a coiled-coil domain at the amino end of their sequence and, in the case of eukaryotic enzymes, a C-terminal extension that plays a modest role on protein stability and amino acid recognition (7,8). The N-terminal coiled-coil domain is essential for the recognition of the elbow and, especially, the long variable loop of $tRNA^{Ser}$ (9,10).

Studies of the recognition modes between SerRS and $tRNA^{Ser}$ from different kingdoms of life have shown that some, but not all, $tRNA^{Ser}$ identity determinants have been conserved during evolution (for a review see (11)), and that different recognition modes exist. Thus, in bacteria and *Saccharomyces cerevisiae* the specific charging of $tRNA^{Ser}$ depends on the recognition of some base pairs in the acceptor

stem, but not of the discriminator base at position 73 (12-14). In these cases the sequence of the variable loop is also crucial. The crystallographic structures of *T. thermophilus* SerRS complexed with $tRNA^{Ser}$, confirm these observations (15,16).

A second type of recognition mode, seen in archaeal and human SerRS, is characterized by the crucial role of the discriminator base (17-19). In these cases the sequence of the variable loop is not important, but its size and orientation is fundamental for the interaction with the enzyme (20,21). The main common features between the bacterial and eukaryotic recognition strategies are the importance of the variable loop and the dispensable character of the anticodon stem-loop.

Finally, a third type of $tRNA^{Ser}$ recognition is seen in the SerRSs of methanogenic archaea, which use a idiosyncratic N-terminal domain to recognize the acceptor stem and the variable loop of their tRNA substrates (22). These unusual enzymes are also sensitive to the discriminator base position of their cognate tRNAs (23).

SerRS also aminoacylates $tRNA^{Sec}$ with serine, as the first step for the incorporation of selenocysteine into proteins. Components of the selenocysteine insertion machinery have been identified by computational methods in species of the three branches of the tree of life. Recently some of these components have also been identified in trypanosomatids, and the existence of a $tRNA^{Sec}$ in these organisms has been verified (24).

The serylation reaction of $tRNA^{Sec}$ has been characterized in detail in *E. coli* and *Homo sapiens* (25,26), but the system has not been characterized in protozoans or other basal eukaryotes. In *H. sapiens* and *E. coli,* $tRNA^{Sec}$ transcripts have been described as being, respectively, 10 and 100 fold less efficient substrates for SerRS than $tRNA^{Ser}$. It has been proposed that this difference is caused by the unique structure of $tRNA^{Sec}$ (26).

Here we report the first characterization of the serylation of $tRNA^{Sec}$ in trypanosomatids. We confirm the expression of $tRNA^{Sec}$ in *Trypanosoma brucei* and show that, unlike most trypanosomal tRNAs, it is exclusively localized in the cytosol. Furthermore we characterize its aminoacylation with serine by *Trypanosoma cruzi* SerRS. We show that the aminoacylation constants of $tRNA^{Sec}$ in *Trypanosoma* differ substantially from those reported in other organisms, suggesting that kinetic differences in the serylation activity of $tRNA^{Sec}$ may be species-specific, and that regulatory strategies may exist based on the efficiency of serine-$tRNA^{Sec}$ synthesis.

EXPERIMENTAL PROCEDURES

Materials - Oligonucleotides were synthesized by Sigma-Genosys. L-[^{3}H] serine and HisTrap nickel columns were from Amersham Biosciences. Restriction enzymes were from New England Biolabs, Pfu Ultra DNA polymerase was from Stratagene and vector pQE-70 from Quiagen. Novablue cells were from Novagen. *T. cruzi* genomic DNA was a gift from Dr. P. Bonay (Universidad Autónoma de Madrid, Spain).

RNAi-mediated ablation of SerRS - RNAi-mediated ablation of the *T. brucei* SerRS was performed using stem loop constructs containing the puromycine resistance gene as described (27). As an insert we used a 498 bp fragment (nucleotides 1 to 498) of the *T. brucei* SerRS gene. Transfection of *T. brucei* (strain 29-13), selection with antibiotics, cloning and induction with tetracycline were done as described (28). To analyze the in vivo charging levels of the $tRNA^{Ser}$ and the $tRNA^{Sec}$ we isolated total RNA from uninduced and induced cells by using the acid guanidinium isothiocyanate procedure (29). The tRNAs remain aminoacylated during this procedure due to the low pH employed by the method. Subsequently, the RNA samples were analyzed on 50 cm long acid urea polyacrylamide gels as described (30), which can resolve aminoacylated from deacylated tRNAs. The gels were analyzed by Northern hybridization (31). The following [^{32}P] 5'-end labeled oligonucleotides were used as probes: 5'TGGCGTCACCAGCAGGATTC3' (for the $tRNA^{Ser}_{CGA}$) and 5'ACCAGCTGAGCTCATCGTGGC3' (for $tRNA^{Sec}$).

tRNA localization studies - To determine the intracellular localization of $tRNA^{Sec}$ we prepared mitochondria free of cytosolic RNAs by digitonin extraction and subsequent RNase A digestion from procyclic *T. brucei* as described (31). RNAs from total cells or isolated mitochondria were purified as indicated above (29). To test whether $tRNA^{Sec}$ concentrations were different in different life stages of *T. brucei*, total RNA of procyclic (strain 427) and bloodstream (strain AnTat1.1, a gift from Dr.

Seebeck, University of Bern, Switzerland) stages of *T. brucei* was purified. To test whether expression of $tRNA^{Sec}$ is induced in medium containing selenium, or under oxidative stress, total RNA was isolated from procyclic *T. brucei* grown in the absence (0) or the presence of 0.005 and 0.5 μg/ml of added Na_2SeO_3, or in the absence or presence of 10 and 25 μMol of added H_2O_2 (data not shown). For all RNA fractions the relative expression level of the $tRNA^{Sec}$ was analyzed by Northern hybridization using the $tRNA^{Sec}$-specific oligonucleotide indicated above. The $tRNA^{Ile}$ was detected using the oligonucleotide 5'TGCTCCCGGCGGGTTCGAA3'.

tRNA preparation - Constructions containing a T7 promoter followed by the gene encoding wild type or mutated tRNAs were assembled using six DNA oligonucleotides that were first annealed, and then ligated, between HindIII and BamHI restriction sites of plasmid pUC19. *In vitro* transcription using T7 RNA polymerase was performed according to standard protocols (32). Transcripts were separated on denaturing PAGE, full-length tRNAs were eluted from gel using an electroelution apparatus (Schleicher & Schüll) and refolded (2 min at 90 ºC followed by a gradual reduction of temperature in presence of 2.5 mM $MgCl_2$).

Enzyme cloning and purification - The 1.4-kbp intron-less gene coding for *T. cruzi* SerRS (Tc00.1047053511163.10) was amplified by PCR from genomic DNA (strain MC) using Pfu Ultra DNA polymerase and cloned in the vector pQE-70 for bacterial expression of a C-terminal His_6-tagged protein. The correct sequence of the gene was checked by sequencing it entirely. Novablue *E. coli* cells (Novagen) transformed with this construction were grown at 21 ºC up to A_{700nm}=0.3. Protein expression was then induced with 0.1 mM IPTG during 12 hours. Purification on nickel affinity columns was performed using standard procedures.

Aminoacylation assays - Aminoacylation was performed at 37 ºC in 50 mM Tris-HCl, pH 7.6, 15 mM $MgCl_2$, 4 mM DTT, 5 mM ATP, 10 mM NaCl, 100 μM L-[^{3}H] serine (300 Ci/mol) and varying concentrations of tRNA transcripts (1-80 μM). Reaction was initiated by addition of pure enzyme and samples of 20 μl were spotted onto Whatman 3MM discs at varying time intervals (usually 2 min). Radioactivity was measured by liquid scintillation. Enzyme concentration was experimentally determined for each tRNA in order to obtain linear velocities. Kinetic constants were obtained from Lineweaver-Burk plots using a minimum of two independent measurements and five tRNA concentrations.

Phylogenetic and sequence analyses - The sequences of seryl-tRNA synthetases used were pulled from GENBANK, either directly or by BLAST searches of available genomic sequences (33). The total set of sequences was aligned with CLUSTALX (34). All sequences were initially included in our analysis, but were later culled to focus our analysis on the eukaryotic clade that contains the *Trypanosoma* sequences. Coiled-coil predictions were done using the programs PAIRCOIL (35), COILS (36) and MULTICOIL (37). Phylogenetic distributions were calculated by parsimony, distance and maximum likelihood methods using PHYLIP 3.63 package (38). Maximum parsimony analysis (MP) was done using PROTPARS. The neighbour-joining method was applied using the programs NEIGHBOR and PROTDIST, with the Dayhoff 120 substitution matrix. Maximum likelihood (ML) phylogenies were calculated with the program PROML (38) using the JTT substitution matrix. The programs SEQBOOT and CONSENSE (38) were used to estimate the confidence limits of branching points from 1000 bootstrap replicates in the parsimony and distance calculations, while 100 bootstrap replicates were used for the maximum likelihood trees. Several combinations of sequences were used in our analyses to test the robustness of the trees obtained. All the groups of sequences used produced exactly the same tree topology reported here.

RESULTS

RNAi-mediated ablation of the trypanosomal SerRS.

To confirm that the putative *T. brucei* SerRS gene encodes the functional enzyme in charge of serylation of $tRNA^{Ser}$ and $tRNA^{Sec}$ we established a stable transgenic cell line, that allows tetracycline-inducible RNAi-mediated ablation of the protein. This cell line stops growing after induction of RNAi, confirming that the putative SerRS is essential for normal growth of the parasite (Fig. 1A). To determine the biochemical phenotype of the RNAi cell line we isolated total RNA from untreated cells and from cells grown in the presence of tetracycline. Subsequently, the RNAs were resolved on long acid urea polyacrylamide gels (30) which in

combination with Northern analysis allow to determine the ratio of charged to uncharged $tRNA^{Ser}$ and $tRNA^{Sec}$, respectively. The results in Fig. 1B and 1C show that ablation of the putative SerRS results in selective accumulation of both uncharged $tRNA^{Ser}$ and uncharged $tRNA^{Sec}$, indicating that the SerRS identified in our study is the enzyme responsible for *in vivo* serylation of both of these tRNAs.

Localization of the $tRNA^{Sec}$.

Unlike in other eukaryotes most tRNAs in trypanosomatids have a dual localization: Approx. 95% are found in the cytosol and function in cytosolic translation, however a small fraction (approx. 5%) are imported into the mitochondrion and function in organelar protein synthesis (31). Consequently, trypanosomal tRNAs are always encoded in nucleus and never on the mitochondrial DNA. *T. brucei* encodes a single *selC* gene, coding for the $tRNA^{Sec}$ (24). In order to confirm the expression of this tRNA and to determine its intracellular localization we carried out Northern blot analyses using total and mitochondrial RNA fractions from procyclic *T. brucei*. The result in Figure 2A shows that the $tRNA^{Sec}$ is only detected in the cytosol but not in the mitochondrion. Exclusive cytosolic localization is exceptional in trypanosomatids, the only cytosol-specific tRNA known to date being the initiator $tRNA^{Met}$ (31).

$tRNA^{Sec}$ expression is not influenced by the life cycle stage, selenium or H_2O_2.

In a next series of Northern blots, we tested whether the relative amount of $tRNA^{Sec}$ when compared to other tRNAs was dependent on the life cycle stage, or sensitive to the concentration of selenium or H_2O_2 in the culture media. Figure 2B shows that trypanosomal $tRNA^{Sec}$ is expressed to very similar levels in both the procyclic and bloodstream forms of *T. brucei*. This suggests that selenocysteine-containing proteins play a role throughout the life cycle of *T .brucei*. In contrast to reports in vertebrates (39), the expression of the $tRNA^{Sec}$ in procyclic *T. brucei* is not affected by the addition of selenium to the growth medium (Fig. 2C). A similar result was obtained when the parasites were grown in the presence of H_2O_2 (data not shown).

Characterization of the serylation reaction of $tRNA^{Ser}$ and $tRNA^{Sec}$ by T. cruzi SerRS .

The cloning of SerRS gene was performed directly from genomic DNA. The 54 kDa protein was expressed in *E. coli*, and purified to homogeneity by affinity chromatography. Gel filtration experiments with the purified enzyme confirmed its ability to form dimers (data not shown), suggesting that *T. cruzi* SerRS is a classical class II aminoacyl-tRNA synthetase (5).

Transcripts of *Trypanosoma* $tRNA^{Ser}$ and $tRNA^{Sec}$ were used in aminoacylation assays and both were shown to be efficiently aminoacylated by SerRS (Fig. 3A). The kinetic constants for the serylation of both tRNAs by SerRS were then determined (Fig. 3B). The K_m for $tRNA^{Ser}$ of *T. cruzi* SerRS was calculated at 3,2 μM, a value comparable to those found in other systems but eight fold higher than that calculated for $tRNA^{Sec}$ with the same enzyme. On the other hand, the K_{cat} was essentially identical to that calculated for $tRNA^{Sec}$. As a result, the K_{cat}/K_m value for *Trypanosoma* $tRNA^{Ser}$ is seven fold lower than that of *T. cruzi* $tRNA^{Sec}$. Interestingly, these values are markedly different from those reported in other species. Thus, in the human system (25), the serylation of $tRNA^{Sec}$ is 10 fold less efficient than that for $tRNA^{Ser}$, and this difference grows to a 100 fold in favour of $tRNA^{Ser}$ in *E. coli* (26) (Fig. 3C).

Identity determinants in the acceptor stem of $tRNA^{Ser}$.

To understand how *T. cruzi* SerRS recognizes its cognate tRNAs, mutants of $tRNA^{Ser}_{CGA}$ were produced and their ability to be charged with serine was measured *in vitro* in presence of purified SerRS. Fourteen tRNA variants were generated, covering nearly 80 % of the primary structure. The design of the mutations was dictated both by the sequence conservation among *T. cruzi* $tRNA^{Ser}$ and $tRNA^{Sec}$ sequences (Fig. 4A), and by the distribution of identity elements in homologous $tRNA^{Ser}$ sets. A set of modifications targeted individual nucleotides or base pairs in the acceptor stem (variants 1 to 9) (Fig. 4B), whereas a second set of changes introduced large deletions or sequence swaps of discrete tRNA domains (variants 10 to 14) (Fig. 4C).

The change of the discriminator base G73 for pyrimidines had a dramatic effect on the charging of $tRNA^{Ser}$ (mutants 1 and 2) (Table 1), indicating that the enzyme strongly recognizes this position of the acceptor stem. This sensitivity to the discriminator base sequence is reminiscent of the recognition mechanisms

described for *H. sapiens* and archaeal SerRSs (17-19).

The first base pair (1:72) was found to be the most sensitive position in the acceptor stem of $tRNA^{Ser}$. Indeed, the simple inversion of the G1:C72 base pair (mutant 4) completely abolished the aminoacylation of this substrate by the enzyme. The introduction of a G1:U72 base pair in the $tRNA^{Ser}$ scaffold had no effect on the ability of this tRNA to be charged by SerRS (mutant 5), indicating that G1 may be contributing important contacts to the recognition by SerRS (Table 1). It should be noted that both the discriminator base G73 and the G1 base found to be essential for recognition of $tRNA^{Ser}$ by *Trypanosoma* SerRS are conserved in the sequences of $tRNA^{Sec}$ of the same species.

Additional mutations in other regions of the acceptor stem had no significant effect on the overall recognition of $tRNA^{Ser}$ by *T. cruzi* SerRS (mutant 6 to 9). Overall, our acceptor stem mutations affect mostly K_{cat} values, suggesting a defect in the reactive positioning of the acceptor extremity rather than a loss in binding energy.

Identity determinants beyond the acceptor stem of $tRNA^{Ser}$.

Next, we wanted to investigate the importance of the pseudoknot (D arm, T arm and variable loop) and anticodon domains of *T. cruzi* $tRNA^{Ser}$ for its recognition by SerRS. The three domains of the tRNA that form the pseudoknot were individually flipped (mutants 11 to 13) in order to vary their sequences without modifying the local secondary structure or the strength of their internal base pairs (Fig. 4C). None of the three corresponding mutants showed any catalytic defect, suggesting that the recognition mechanism for the elbow of the tRNA is based exclusively on interactions with the sugar-phosphate backbone (Table 1).

To further test this hypothesis the entire variable loop was excised, and replaced by the most commonly found class I variable loop (mutant 14) (Fig. 4C). This replacement had a dramatic effect on aminoacylation, causing a >8000 fold drop in K_{cat}/K_m. This mutation affected both catalytic and affinity constants. Our combined data indicates that this domain is recognized in a sequence-unspecific manner, provides binding energy, and acts as a guide for the reactive positioning of the tRNA (Table 1).

Finally, the entire anticodon loop was deleted and replaced by a stretch of four uridines (mutant 10) (Fig. 4C). This linker was used because it is the least likely to stabilize unanticipated structures in this region of the tRNA (13). This deletion mutant had only a modest effect on the velocity of the aminoacylation reaction. This is in agreement with other studies that have shown that the anticodon domain of eukaryotic $tRNA^{Ser}$ contributes poorly to the serine identity (for a review see (11)) (Table 1).

Phylogeny of Trypanosoma SerRS.

The known genomes of *Trypanosoma* code for only one SerRS gene. The corresponding protein is likely used both in the cytoplasm and the mitochondria, but no conventional targeting sequence can be identified in their sequences. The protein is 477 amino acids long, and it contains an N-terminal domain predicted to form a coiled coil domain (36), as seen in the available structural data for homologous enzymes (16, 40).

Multiple sequence alignments readily show the presence of a large synapomorphy that clusters trypanosomatid SerRSs with the rest of metazoan sequences (Fig. 5A). This synapomorphy is an insertion of twenty amino acids located at the center of the N-terminal coiled-coil motif of this group of SerRSs (Fig. 5B). Coiled-coil prediction of this group of sequences suggest that in metazoans and trypanosomatids this region may extend beyond the length seen in the structures solved so far (data not shown).

Our phylogenetic analysis of SerRS sequences is the first one of this enzyme to include kinetoplastid sequences. When sequences from all life domains were used, our results consistently agreed with previous analyses (41-44), supporting the conclusion that the overall evolution of this enzyme conforms to the canonical phylogenetic tree derived from ribosomal RNA sequences (Fig. 6A) (41,43). Although we were unable to obtain significant bootstrap support for the central branching points of the general tree, the trypanosomatid sequences strongly associated with metazoan sequences with strong bootstrap support, both in general trees and those limited to the major eukaryotic lineages (Fig. 6A and 6B). It should be stressed here that the region corresponding to the synapomorphy that also links *Trypanosoma* sequences with metazoan ones was not used in our phylogenetic analyses.

DISCUSSION

The constraints acting over tRNA recognition are strictly intra-specific and, for each species constitute a complex set of recognition and rejection elements that ensures faithful translation (45). Possibly this complex set of positive and negative identity elements contributes to the stability of the genetic code and limits its size, because the incorporation of new amino acids would require an increase in complexity of the recognition problem which may be impossible to assume without increasing the rate of aminoacylation errors (3).

In order to study the evolution of these sets of recognition elements we decided to characterize the recognition of $tRNA^{Ser}$ and $tRNA^{Sec}$ by *Trypanosoma* SerRS. In doing so we were expecting to extract information about the evolution of this recognition mechanism in the basal part of the eukaryotic phylogenetic tree. For convenience we chose *Trypanosoma brucei* as a model for the *in vivo* studies, while the *in vitro* studies were performed with *Trypanosoma cruzi* proteins and tRNAs. The overall identity between *T. cruzi* and *T. brucei* SerRSs is 80 %, and the sequences of their $tRNA^{Ser}$ are essentially identical.

We have shown that *Trypanosoma* SerRS recognizes its cognate tRNAs using a combination of structural signals in the variable loop and the sequence information of the discriminator base and the first base pair of the acceptor stem. The discriminator base G73 and the G1 base are essential for recognition by *Trypanosoma* SerRS. These bases are conserved among all serine tRNA isoacceptors in *Trypanosoma*, and strongly influence the velocity of the serylation reaction.

Previous studies on $tRNA^{Ser}$ recognition in the three kingdoms of life show that acceptor stem recognition by SerRS fluctuates between the first four base pairs and the discriminator base of the acceptor stem (17, 46, 47). In the case of *Trypanosoma*, this recognition has shifted towards the CCA end of the molecule, and the discriminator base and the first base pair constitute the region recognized by SerRS.

We have established that the presence of a long variable loop is a pre-requisite to $tRNA^{Ser}$ recognition, but that this mechanism is not sequence specific. Moreover, the complete deletion of $tRNA^{Ser}$ anticodon domain does not affect its serylation by SerRS, confirming that the entire stem and anticodon loop is ignored by the enzyme during the recognition process. This feature is common to all serine systems studied so far with the only exception of *M. barkeri* SerRS, which displays a strong interaction with the G30:C40 base pair in the anticodon stem (46).

In summary, our data suggest that the tRNA specificity of *Trypanosoma* SerRS relies on a two-pronged mechanism based on interactions with the G73 discriminator base and the G1 base on one side, and the sequence-independent recognition of the variable loop on the other. Interestingly, this recognition mechanism functionally associates trypanosomatid SerRSs with their metazoan homologs, and separates them from other eukaryotic enzymes such as *S. cerevisiae* SerRS. This functional relationships are in agreement with the phylogenetic connections that we report here, and the presence of clear sequence synapomorphies that link these enzymes evolutionarily.

A possible explanation to this functional convergence would be a lateral gene transfer event between trypanosomatids and metazoans that could be favored by the parasitic nature of the former. A second possibility, more in agreement with polyphiletic views of eukaryote evolution (4), would be that the recognition solution displayed by metazoans and trypanosomatids is ancient, having persisted in these two groups of organisms since their radiation at the base of the eukaryotic evolutionary tree. Our phylogenetic studies do not allow us to discard either possibility.

Another interesting feature of trypanosomatid SerRSs is their apparently high affinity for $tRNA^{Sec}$. Indeed, the K_{cat}/K_m value for the aminoacylation of *Trypanosoma* $tRNA^{Ser}$ (which are comparable to values established for other species) is seven fold lower than that found for *T. cruzi* $tRNA^{Sec}$, a result that is in direct contrast with the values reported for the human system (25) (where the $tRNA^{Ser}$ is 10 fold more efficiently charged than $tRNA^{Sec}$) or in *Escherichia coli* (26) (100 fold difference in favour of $tRNA^{Ser}$) (Fig. 3B).

It should be noted here that all the studies where these values are reported (including this one) were performed with transcript tRNAs, thus excluding the potential effect of base modifications in either substrate. However, there seems to be a clear difference between the relative aminoacylation of $tRNA^{Sec}$ and $tRNA^{Ser}$ between trypanosomatids and other species. This may be explained by a high requirement for

selenoprotein synthesis in these species. Our attempts to increase the levels of $tRNA^{Sec}$ in *T. brucei* by the presence of oxidative stress or different growth conditions were unsuccessful, but these results are not necessarily contradictory with a high level of selenocysteine use by these organisms.

From our studies it is clear that $tRNA^{Sec}$ is not imported into the mitochondria of *T. brucei*. Some of us have recently shown that tRNA localization signals in this species are confined to two nucleotide pairs in the T-stem (48). In the cytosol-specific initiator $tRNA^{Met}$ these positions include the anti-determinants that, based on experiments with vertebrate initiator $tRNA^{Met}$ (49), are predicted to prevent interaction with translation elongation factor 1a (eEF-1a). The T-stem sequence of the cytosolic $tRNA^{Sec}$ is different to all other *T. brucei* tRNAs including the cytosolic initiator $tRNA^{Met}$. However, a feature that is shared between the two cytosol-specific tRNAs in *T. brucei* is that neither interacts with eEF-1a. Instead, the initiator $tRNA^{Met}$ interacts with initiation factor 2, and the $tRNA^{Sec}$ with the specialized elongation factor SelB/EFsec.

Thus, while the structural determinants that prevent interaction with EF-1a are different for both tRNAs, the mechanism for cytosolic localization might in both cases be achieved by exclusion of EF-1a binding. In other words, all tRNAs that interact with eEF-1a might be imported into mitochondria, and the ones which do not remain in the cytosol.

REFERENCES

1. Hou, Y.M. and P. Schimmel. (1989). *Biochemistry* 28, 6800-6804.
2. Gabriel, K., J. Schneider, and W.H. McClain. (1996). *Science* 271, 195-197.
3. Ribas de Pouplana, L. (2005). *Life* 57, 523-524.
4. Baldauf, S.L., A.J. Roger, I. Wenk-Siefert, and W.F. Doolittle. (2000). *Science.* 290, 972-977.
5. Eriani, G., M. Delarue, O. Poch, J. Gangloff, and D. Moras. (1990). *Nature* 347, 203-206.
6. Ribas de Pouplana, L. and P. Schimmel. (2001). *Cell* 104, 191-193.
7. Weygand-Durasevic, I., B. Lenhard, S. Filipic, and D. Söll. (1996). *J. Biol. Chem.* 271, 2455-2461.
8. Lenhard, B., S. Filipic, I. Landeka, I. Skrtic, D. Söll, and I. Weygand-Durasevic. (1997). *J. Biol. Chem.* 272, 1136-1141.
9. Borel, F., C. Vincent, R. Leberman, and M. Härtlein. (1994). *Nucleic Acids Res.* 22, 2963-2969.
10. Lenhard, B., M. Praetorius-Ibba, S. Filipic, D. Soll, and I. Weygand-Durasevic. (1998). *FEBS Lett.* 439, 235-240.
11. Lenhard, B., O. Orellana, M. Ibba, and I. Weygand-Durasevic. (1999). *Nucleic Acids Res.* 27, 721-729.
12. Himeno, H., S. Yoshida, A. Soma, and K. Nishikawa. (1997). *J. Mol. Biol* .268, 704-711.
13. Sampson, J.R. and M.E. Saks. (1993). *Nucleic Acids Research* 21, 4467-4475.
14. Normanly, J., T. Ollick, and J. Abelson. (1992). *Proc. Natl. Acad. Sci. USA* 89, 5680-5684.
15. Cusack, S., A. Yaremchuk, and M. Tukalo. (1996). *EMBO J.* 15, 2834-2842.
16. Biou, V., M. Yoremchuk, M. Tukalo, and S. Cusack. (1994). *Science* 263, 1404-1410.
17. Metzger, A.U., M. Heckl, D. Willbold, K. Breitschopf, U.L. RajBhandary, P. Rosch, and H.J. Gross. (1997). *Nucleic. Acids. Res.* 25, 4551-4556.
18. Breitschopf, K. and H.J. Gross. (1996). *Nucleic Acids Res* 24, 405-410.
19. Achsel, T. and H.J. Gross. (1993). *EMBO J.* 12, 3333-3338.
20. Wu, X.Q. and H.J. Gross. (1993). *Nucleic Acids Research* 21, 5589-5594.
21. Heckl, M., K. Busch, and H.J. Gross. (1998). *FEBS Lett.* 427, 315-319.
22. Bilokapic, S., T. Maier, D. Ahel, I. Gruic-Sovulj, D. Soll, I. Weygand-Durasevic, and N. Ban. (2006). *Embo J* 4, 4.
23. Bilokapic, S., D. Korencic, D. Soll, and I. Weygand-Durasevic. (2004). *Eur. J. Biochem.* 271, 694-702.
24. Cassago, A., E.M. Rodrigues, E.L. Prieto, K.W. Gaston, J.D. Alfonzo, M.P. Iribar, M.J. Berry, A.K. Cruz, and O.H. Thiemann. (2006). *Mol. Biochem. Parasitol.* 23, 23.
25. Amberg, R., T. Mizutani, X.Q. Wu, and H.J. Gross. (1996). *J. Mol. Biol.* 263, 8-19.
26. Baron, C. and A. Böck. (1991). *Journal of Biological Chemistry* 266, 20375-20379.

27. Bochud-Allemann, N. and A. Schneider. (2002). *J. Biol. Chem.* 277, 32849-32854. Epub 32002 Jul 32842.
28. McCulloch, R., E. Vassella, P. Burton, M. Boshart, and J.D. Barry. (2004). *Methods Mol. Biol.* 262, 53-86.
29. Chomczynski, P. and N. Sacchi. (1987). *Anal Biochem.* 162, 156-159.
30. Varshney, U., C.P. Lee, and U.L. RajBhandary. (1991). *J. Biol. Chem.* 266, 24712-24718.
31. Tan, T.H., R. Pach, A. Crausaz, A. Ivens, and A. Schneider. (2002). *Mol. Cell. Biol.* 22, 3707-3717.
32. Sampson, J.R. and O.C. Uhlenbeck. (1988). *Proc. Natl. Acad. Sci. USA* 85, 1033-1037.
33. Benson, D.A., I. Karsch-Mizrachi, D.J. Lipman, J. Ostell, and D.L. Wheeler. (2005). *Nucleic Acids Res.* 33, D34-38.
34. Thompson, J.D., T.J. Gibson, F. Plewniak, F. Jeanmougin, and D.G. Higgins. (1997). *Nucleic Acids Res.* 25, 4876-4882.
35. Berger, B., D.B. Wilson, E. Wolf, T. Tonchev, M. Milla, and P.S. Kim. (1995). *Proc Natl Acad Sci U S A.* 92, 8259-8263.
36. Lupas, A., M. Van Dyke, and J. Stock. (1991). *Science.* 252, 1162-1164.
37. Wolf, E., P.S. Kim, and B. Berger. (1997). *Protein Sci.* 6, 1179-1189.
38. Felsenstein, J. (1988). *Annu Rev Genet.* 22, 521-565.
39. Choi, I.S., A.M. Diamond, P.F. Crain, J.D. Kolker, J.A. McCloskey, and D.L. Hatfield. (1994). *Biochemistry.* 33, 601-605.
40. Chimnaronk, S., M. Gravers Jeppesen, T. Suzuki, J. Nyborg, and K. Watanabe. (2005). *Embo J* 15, 15.
41. Taupin, C.M. and R. Leberman. (1999). *J Mol Evol.* 48, 408-420.
42. Kim, H.S., U.C. Vothknecht, R. Hedderich, I. Celic, and D. Soll. (1998). *J Bacteriol* 180, 6446-6449.
43. Wolf, Y.I., L. Aravind, N.V. Grishin, and E.V. Koonin. (1999). *Genome Res.* 9, 689-710.
44. Woese, C.R., G.J. Olsen, M. Ibba, and D. Söll. (2000). *Microbiol Mol Biol Rev* 64, 202-236.
45. Giegé, R., M. Sissler, and C. Florentz. (1998). *Nucleic Acids Res.* 26, 5017-5035.
46. Korencic, D., C. Polycarpo, I. Weygand-Durasevic, and D. Soll. (2004). *J. Biol. Chem.* 279, 48780-48786.
47. Saks, M.E. and J.R. Sampson. (1996). *EMBO J.* 15, 2843-2849.
48. Crausaz Esseiva, A., L. Marechal-Drouard, A. Cosset, and A. Schneider. (2004). *Mol Biol Cell.* 15, 2750-2757. Epub 2004 Apr 2752.
49. Drabkin, H.J., M. Estrella, and U.L. Rajbhandary. (1998). *Mol Cell Biol.* 18, 1459-1466.

FOOTNOTES

This work was supported by grants BIO2003-02611 from the Spanish Ministry of Science and Education, and 3100-067906 of the Swiss National Foundation (A. S.), a Marie Curie International Reintegration Fellowship (L.R.P.), and a Fellowship of the Novartis Foundation (F. C.). We are grateful to Dr. Bonay (Hospital de la Princesa) for the gift of *T. cruzi* genomic DNA and to Dr. Seebeck (University of Bern) for bloodstream stage *T. brucei* cells. We thank Drs. Guigó and Chappel (Pompeu Fabra University), Dr. Gladyshev (University of Nebraska), Dr. Eriani (CNRS, Strasbourg), and Dr. Roy (Ohio State University) for useful discussions.

FIGURE LEGENDS

Fig. 1. SerRS is essential for growth of procyclic *T. brucei* and is responsible for the serylation of both $tRNA^{Ser}$ and $tRNA^{Sec}$. (A) Growth curve in the presence and absence of tetracycline (+, -Tet) of a representative clonal *T. brucei* RNAi cell line ablated for the trypanosomal SerRS homologue. (B) Northern blot analysis of total RNA isolated under acidic conditions from the SerRS RNAi cell line. Hours of induction by tetracycline are indicated at the top. The blots were probed for the *T. brucei* $tRNA^{Ser}$ and $tRNA^{Ile}$. The latter serves as controls that is not affected by the RNAi. The RNA fractions were resolved on long acid urea gels that allow to separate aminoacylated (aa) from deacylated (dea) tRNAs. The relative amounts of deacylated $tRNA^{Ser}$ and $tRNA^{Ile}$ are indicated at the bottom. For each lane the sum of aminoacylated and deacylated tRNA was set to 100% percent. (C)

Same as (B) but analysis was done for the $tRNA^{Sec}$. The x refers to an unidentified band probably corresponding to phosphoserine.

Fig. 2. Expression of $tRNA^{Sec}$ in *T. brucei*. (A) $tRNA^{Sec}$ is not imported into the mitochondrion. Left panel: 0.1 x 10^8 cell equivalents of total (Tot.) and 2 x 10^8 cell equivalents of mitochondrial (Mito.) RNA, isolated by digitonin extraction from procyclic *T. brucei*, were separated on a 10% polyacrylamide/8 M urea gel and stained with ethidium bromide. Right panel: the gel was processed for Northern hybridization and probed for $tRNA^{Sec}$ and imported $tRNA^{Ile}$. (B) $tRNA^{Sec}$ is expressed in both life cycle stages. Total RNA, 5 and 7 µg each, of procyclic (Proc.) and bloodstream stage *T. brucei* was analyzed by Northern hybridization as in (A). The relative expression levels (set to be 1 for procyclic RNA) of the $tRNA^{Sec}$ when compared to the expression of tRNAIle are indicated at the bottom. (C) Expression of $tRNA^{Sec}$ is not induced in medium containing selenium. Five µg of total RNA isolated from procyclic *T. brucei* grown in the absence (0) or the presence of 0.005 and 0.5 µg/ml of added Na_2SeO_3 were analyzed by Northern hybridization as in (A) and (B). The relative expression levels are indicated.

Fig. 3. Comparison of charging efficiency of $tRNA^{Sec}$ and $tRNA^{Ser}$ from various origins. (A) Aminoacylation plot of trypanosomal $tRNA^{Ser}$ (■) and $tRNA^{Sec}$ (♦) in the presence of purified seryl-tRNA synthetase and [^{3}H] serine. Three independent measures have shown only minimal variations of the charging activity, ranging from 1 to 15% (data not shown on the graph for visual clarity). (B) Comparison of the kinetic values for the *in vitro* serylation of trypanosomal, human and *E. coli* transcribed $tRNA^{Ser}$ and $tRNA^{Sec}$ (25, 26, this work). N.D., not determined (C) Histogram showing the efficiency of aminoacylation of $tRNA^{Sec}$ with respect to $tRNA^{Ser}$ for *T. cruz*i, *H. sapiens*, and *E. coli*. The level of aminoacylation efficiency of $tRNA^{Ser}$ is indicated by a dashed line. The gray columns represents the level of aminoacylation efficiency of $tRNA^{Sec}$. *T. cruzi* $tRNA^{Sec}$ is 7 fold more efficiently aminoacylated than *T. cruzi* $tRNA^{Ser}$. * The data concerning *E. coli* $tRNA^{Ser}$ and $tRNA^{Sec}$ were reported from experiments using total protein extract as the source of SerRS (26).

Fig. 4. Secondary structure of $tRNA^{Ser}_{CGA}$ and its mutants. (A) The cloverleaf structure of $tRNA^{Ser}_{CGA}$ is presented. The circles denote nucleotides conserved among the four *T. cruzi* $tRNA^{Ser}$ isoacceptors. The squares denote nucleotides conserved both in $tRNA^{Ser}$ and $tRNA^{Sec}$. (B) Detail of the mutations performed on the acceptor stem of $tRNA^{Ser}_{CGA}$. Each mutant is labeled in parenthesis. (C) Detail of the mutation performed beyond the acceptor stem. Curved arrows and dashed lines are used to denote the flipping, and the deletion of sequences, respectively.

Fig. 5. Sequence alignment of the region of SerRS sequences that contains the synapomorphy that links metazoan and trypanosomatid enzymes. (A) The alignment was performed using CLUSTAL X (34). *T. cruzi* and *T. brucei* SerRS sequences are in bold. Helix 1 and helix 2 indicate the long helices that form the coiled-coil arm found in *T. thermophilus* SerRS. The insertion that is present in metazoan and trypanosomatid sequences is boxed and labeled accordingly. (B) Crystallographic structure of one monomer of *T. thermophilus* SerRS (16). The coiled-coil arm important for the stabilization of the $tRNA^{Ser}$ pseudoknot is highlighted in green. The apparent insertion point of the metazoan and trypanosomatid synapomorphy is marked by an arrow and labeled accordingly.

Fig. 6. Phylogenetic analysis of trypanosomal SerRS.
(A) Maximum likelihood tree of archaeal, bacterial, and eukaryotic seryl-tRNA synthetase sequences. The overall architecture of this tree was obtained with all methods used, but bootstrap support was weak (not shown). (B) Consensus tree of eukaryotic seryl-tRNA synthetase sequences. The association between trypanosomatid and metazoan SerRSs is highlighted. Numbers correspond to percentages of bootstrap support for each node from the parsimony, distance, and ML analyses.

Table 1. Serylation parameters of tRNASec, $tRNA^{Ser}$ and its variants in presence of SerRS. The rate of aminoacylation of the wild type $tRNA^{Ser}$ is 9.56 s^{-1}. For better readability the *kcat* of each mutant is expressed as a percentage of the *kcat* value of the wild type $tRNA^{Ser}$ (i.e. a rate of 9.56 s^{-1} corresponds to a *kcat* of 100%). The overall efficiency of serylation has been determined as the ratio between the *Km* and the *kcat*. To enhance the readability the efficiency of the wild type $tRNA^{Ser}$ have been set at 1.

Values higher than 1 denote tRNA variants that are less efficiently aminoacylated and *vice versa*. Numbers in parentheses refers to the mutations detailed on figure 4B and 4C.
[a]ND, not determined

Figure 1

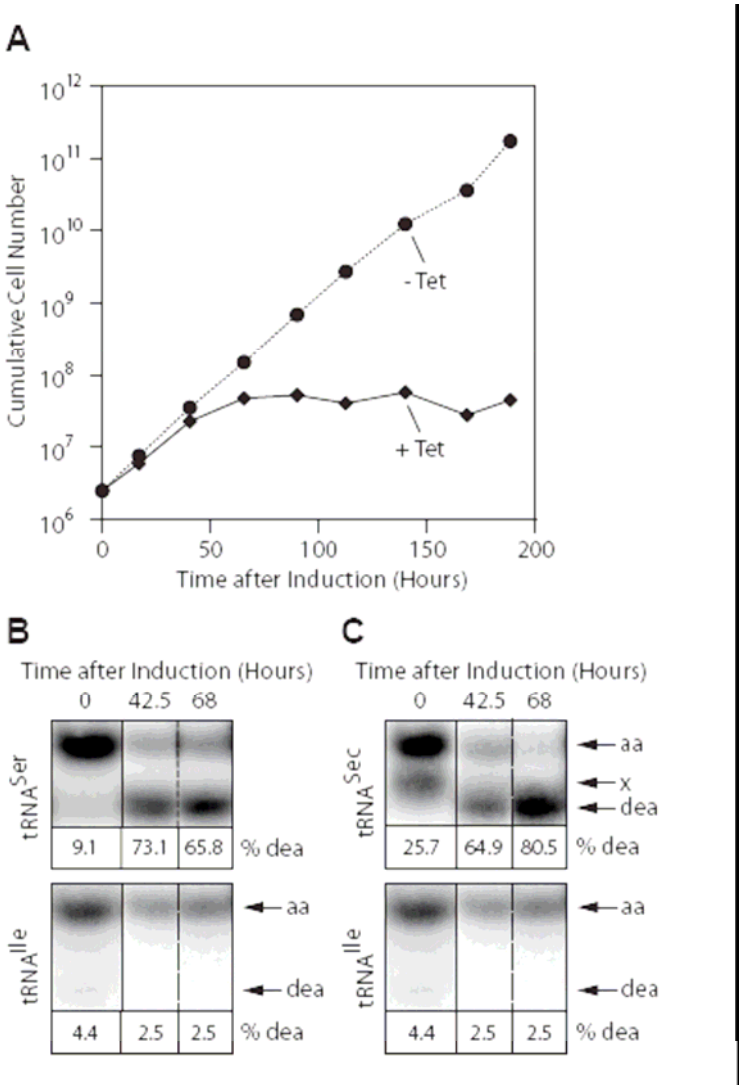
A
Cumulative Cell Number
10^{12}
10^{11}
10^{10}
10^{9}
10^{8}
10^{7}
10^{6}
- Tet
+ Tet
0
50
100
150
200
Time after Induction (Hours)
B
Time after Induction (Hours)
0
42.5
68
$tRNA^{Ser}$
9.1
73.1
65.8
% dea
$tRNA^{Ile}$
aa
dea
4.4
2.5
2.5
% dea
C
Time after Induction (Hours)
0
42.5
68
$tRNA^{Sec}$
aa
x
dea
25.7
64.9
80.5
% dea
$tRNA^{Ile}$
aa
dea
4.4
2.5
2.5
% dea

Figure 2

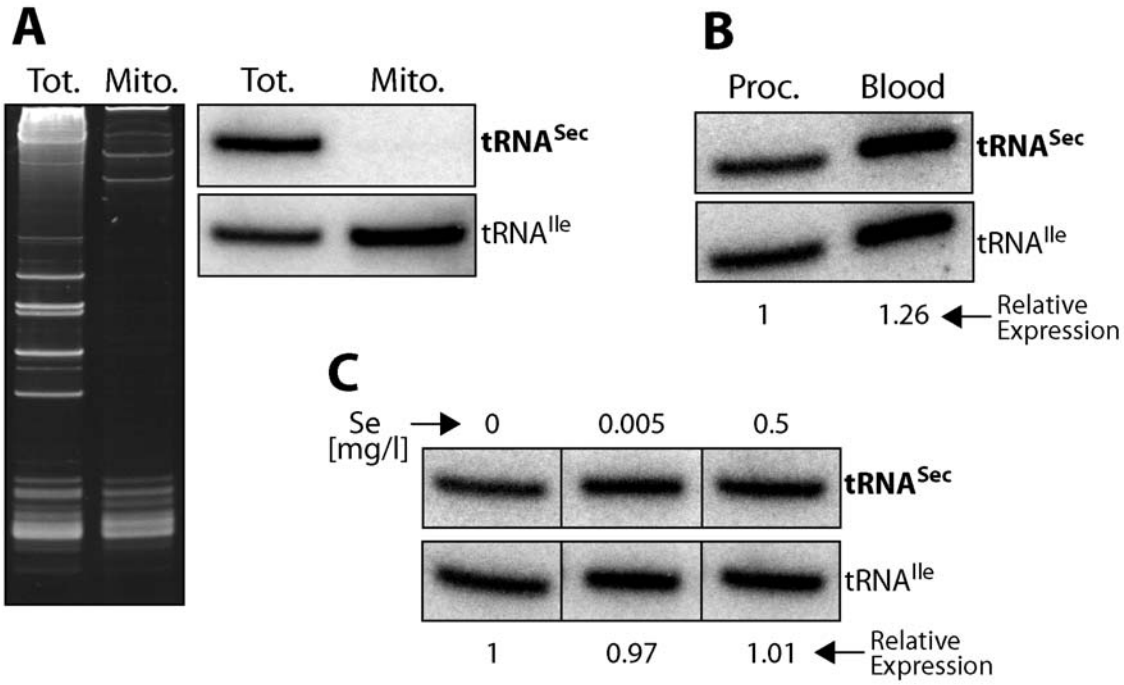
A
Tot.
Mito.
Tot.
Mito.
tRNA^Sec
tRNA^Ile
B
Proc.
Blood
tRNA^Sec
tRNA^Ile
1
1.26
Relative Expression
C
Se [mg/l]
0
0.005
0.5
tRNA^Sec
tRNA^Ile
1
0.97
1.01
Relative Expression

Figure 3

A

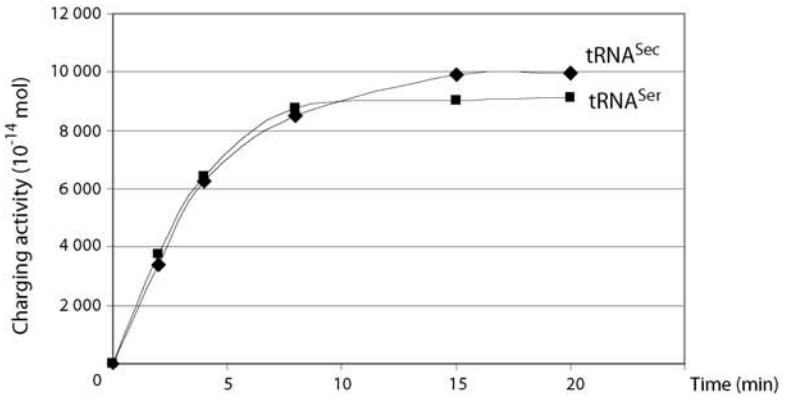

B

Species	Transcript	Kcat (s^{-1})	Km (µM)	Ref.
Trypanosoma cruzi	tRNA$^{Ser}_{CGA}$	9.56	3.2	(this work)
	tRNA$^{Sec}_{UCA}$	8.69	0.4	
Homo sapiens	tRNA$^{Ser}_{UGA}$	0.11	1.2	(25)
	tRNA$^{Sec}_{UCA}$	0.01	11.2	
Escherichia coli	tRNA$^{Ser}_{UGA}$	n.d.	0.2	(26)
	tRNA$^{Sec}_{UCA}$	n.d.	1.3	

C

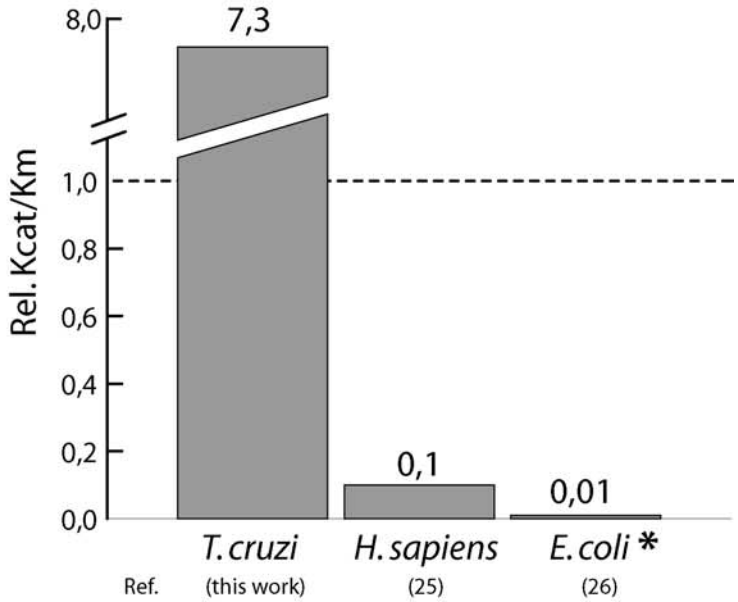

Figure 4

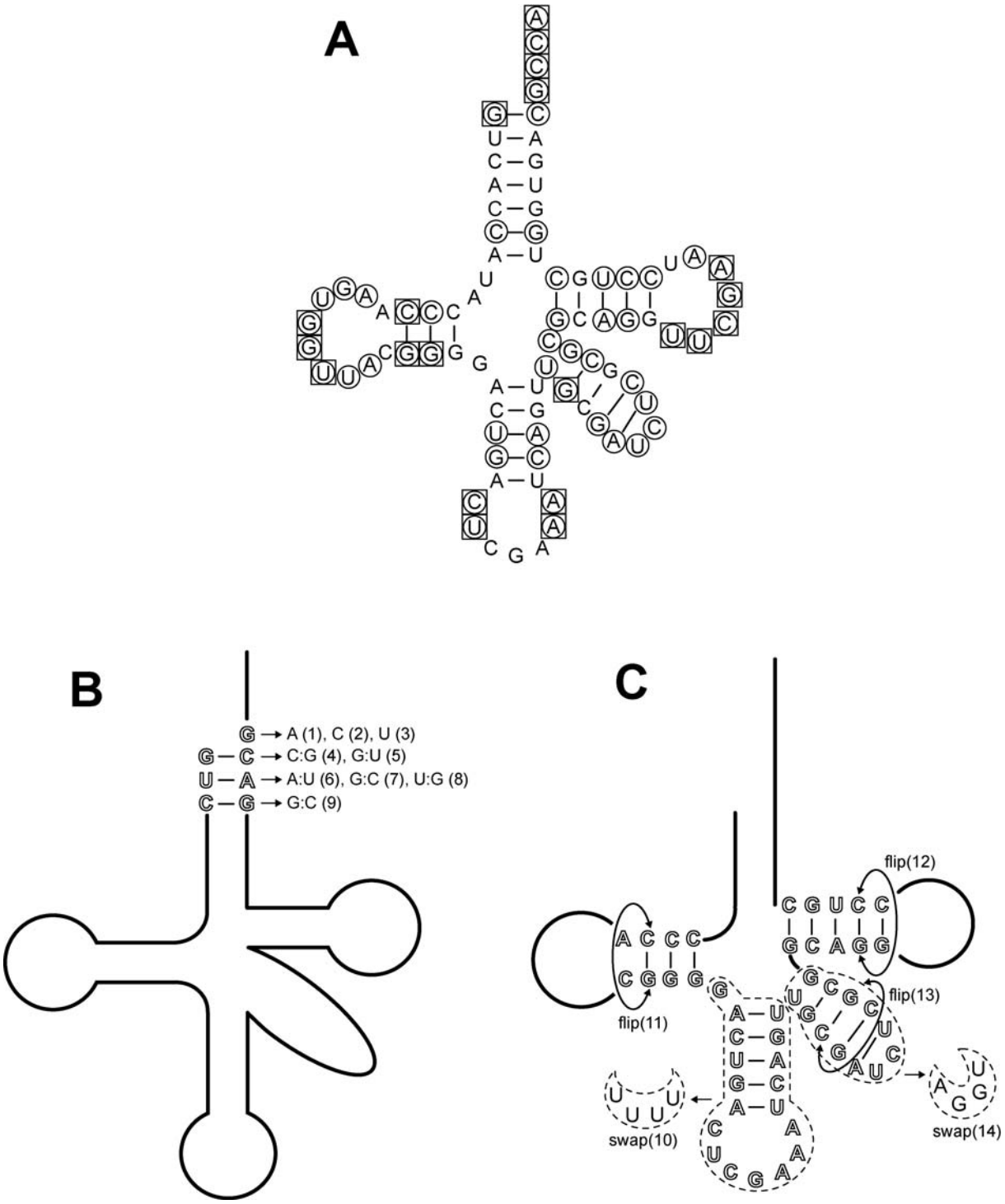
A
B
G → A (1), C (2), U (3)
G — C → C:G (4), G:U (5)
U — A → A:U (6), G:C (7), U:G (8)
C — G → G:C (9)
C
flip(12)
flip(13)
flip(11)
swap(10)
swap(14)

Figure 5

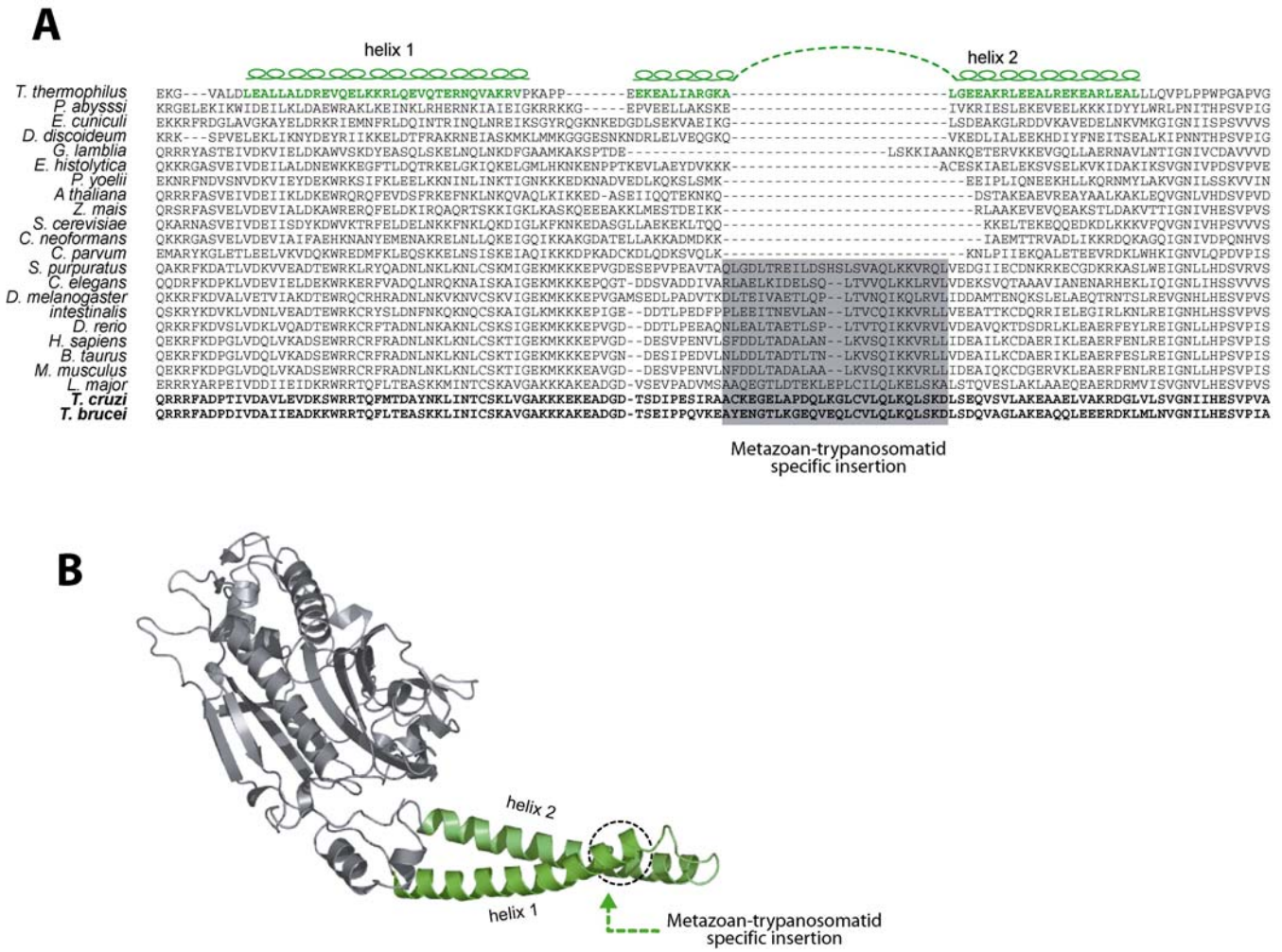
A
helix 1
helix 2
T. thermophilus
P. abysssi
E. cuniculi
D. discoideum
G. lamblia
E. histolytica
P. yoelii
A thaliana
Z. mais
S. cerevisiae
C. neoformans
C. parvum
S. purpuratus
C. elegans
D. melanogaster
intestinalis
D. rerio
H. sapiens
B. taurus
M. musculus
L. major
T. cruzi
T. brucei
Metazoan-trypanosomatid
specific insertion
B
helix 2
helix 1
Metazoan-trypanosomatid
specific insertion

Figure 6

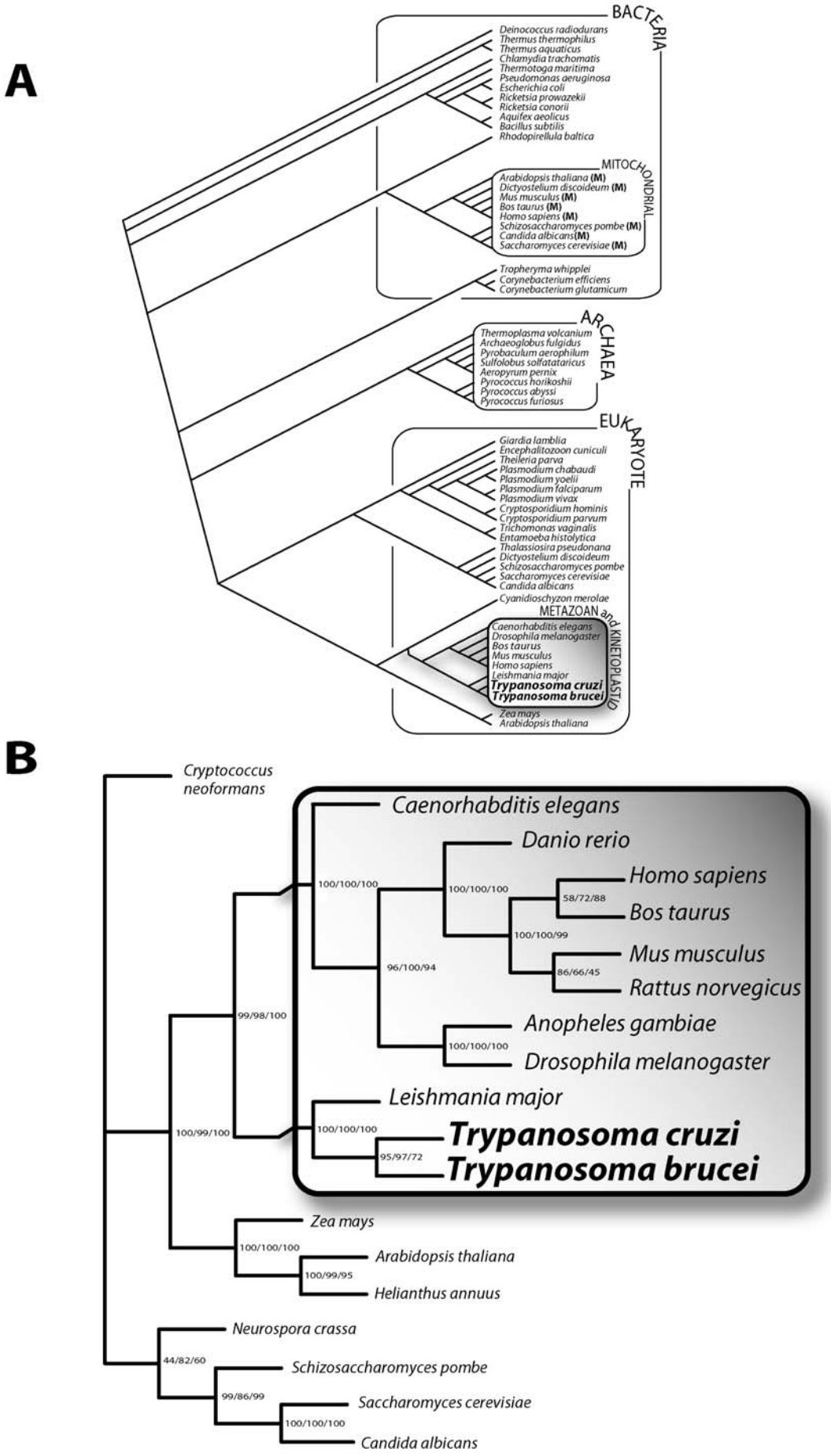
A
BACTERIA
Deinococcus radiodurans
Thermus thermophilus
Thermus aquaticus
Chlamydia trachomatis
Thermotoga maritima
Pseudomonas aeruginosa
Escherichia coli
Ricketsia prowazekii
Ricketsia canarii
Aquifex aeolicus
Bacillus subtilis
Rhodopirellula baltica
MITOCHONDRIAL
Arabidopsis thaliana (M)
Dictyostelium discoideum (M)
Mus musculus (M)
Bos taurus (M)
Homo sapiens (M)
Schizosaccharomyces pombe (M)
Candida albicans (M)
Saccharomyces cerevisiae (M)
Tropheryma whipplei
Corynebacterium efficiens
Corynebacterium glutamicum
ARCHAEA
Thermoplasma volcanium
Archaeoglobus fulgidus
Pyrobaculum aerophilum
Sulfolobus solfataricus
Aeropyrum pernix
Pyrococcus horikoshii
Pyrococcus abyssi
Pyrococcus furiosus
EUKARYOTE
Giardia lamblia
Encephalitozoon cuniculi
Theileria parva
Plasmodium chabaudi
Plasmodium yoelii
Plasmodium falciparum
Plasmodium vivax
Cryptosporidium hominis
Cryptosporidium parvum
Trichomonas vaginalis
Entamoeba histolytica
Thalassiosira pseudonana
Dictyostelium discoideum
Schizosaccharomyces pombe
Saccharomyces cerevisiae
Candida albicans
Cyanidioschyzon merolae
METAZOAN and KINETOPLASTID
Caenorhabditis elegans
Drosophila melanogaster
Bos taurus
Mus musculus
Homo sapiens
Leishmania major
Trypanosoma cruzi
Trypanosoma brucei
Zea mays
Arabidopsis thaliana
B
Cryptococcus neoformans
Caenorhabditis elegans
Danio rerio
Homo sapiens
Bos taurus
Mus musculus
Rattus norvegicus
Anopheles gambiae
Drosophila melanogaster
Leishmania major
Trypanosoma cruzi
Trypanosoma brucei
Zea mays
Arabidopsis thaliana
Helianthus annuus
Neurospora crassa
Schizosaccharomyces pombe
Saccharomyces cerevisiae
Candida albicans
100/100/100
100/100/100
58/72/88
100/100/99
86/66/45
96/100/94
100/100/100
99/98/100
100/99/100
100/100/100
95/97/72
100/100/100
100/99/95
44/82/60
99/86/99
100/100/100

Table 1

Transcripts	kcat (%)	Km (μM)	rel Km/kcat
Wild-type $tRNA^{Ser}_{CGA}$	100	3.2	1
Wild-type $tRNA^{Sec}_{UCA}$	91	0.4	0.1
G73→A (1)	16	4.7	9.1
G73→C (2)	1	13	416.6
G73→U (3)	0.01	[α]nd	[α]nd
G1:C72→C:G (4)	<0.001	[α]nd	[α]nd
G1:C72→G:U (5)	89	2.0	0.7
U2:A71→A:U (6)	82	0.9	0.3
U2:A71→G:C (7)	165	4	0.7
U2:A71→U:G (8)	114	2.6	0.7
C3:G70→G:C (9)	56	5.6	3.1
Δ anticodon domain (10)	15	2.5	5.3
D arm Flip (11)	152	3.5	0.7
T arm Flip (12)	101	3.9	1.2
Variable loop Flip (13)	85	6.4	2.4
Δ variable loop (14)	0.25	71	8 928

D

Conserved Motifs Reveal Details of Ancestry and Structure in the Small TIM Chaperones of the Mitochondrial Intermembrane Space.

Submitted

Ian E. Gentle[1,2], Andrew J. Perry[1,2], Felicity H. Alcock [3], Vladimir A. Likić[2], Pavel Dolezal[1,2], Ee Ting Ng[1,2], Malcolm McConnville[1,2], Thomas Naderer[1,2], Anne-Laure Chanez[4], Fabien Charrière[4], Caroline Aschinger[4], André Schneider[4], Kostas Tokatlidis[3,5] and Trevor Lithgow[1,2]

1 - Department of Biochemistry & Molecular Biology, University of Melbourne, Parkville 3010, Australia
2 - Bio21 Molecular Science and Biotechnology Institute, Parkville 3010, Australia
3- Institute of Molecular Biology & Biotechnology, Foundation for Research & Technology Hellas, Heraklion 71110, Crete, Greece
4 - Department of Biology/Zoology, University of Fribourg, Chemin du Musée 10, CH-1700 Fribourg, Switzerland
5- Department of Materials Science and Technology, University of Crete, PO Box 2208, 710 03 Heraklion, Crete, Greece

Conserved motifs reveal details of ancestry and structure in the small TIM chaperones of the mitochondrial intermembrane space.

Ian E. Gentle[1,2,#], Andrew J. Perry[1,2,#], Felicity H. Alcock [3], Vladimir A. Likić[2], Pavel Dolezal[1,2], Ee Ting Ng[1,2], Malcolm McConnville[1,2], Thomas Naderer[1,2], Anne-Laure Chanez[4], Fabien Charrière[4], Caroline Aschinger[4], André Schneider[4], Kostas Tokatlidis[3,5,*] and Trevor Lithgow[1,2,*]

1 - Department of Biochemistry & Molecular Biology, University of Melbourne, Parkville 3010, Australia

2 - Bio21 Molecular Science and Biotechnology Institute, Parkville 3010, Australia

3- Institute of Molecular Biology & Biotechnology, Foundation for Research & Technology Hellas, Heraklion 71110, Crete, Greece

4 - Department of Biology/Cell & Developmental Biology, University of Fribourg, Chemin du Musée 10, CH-1700 Fribourg, Switzerland

5- Department of Materials Science and Technology, University of Crete, PO Box 2208, 710 03 Heraklion, Crete, Greece

# - These authors contributed equally to this work.

* - To whom correspondence should be addressed:

email: t.lithgow@unimelb.edu.au, tokatlid@imbb.forth.gr

ABSTRACT

The mitochondrial inner and outer membranes are composed of a variety of integral membrane proteins, assembled into the membranes post-translationally. The small TIMs are a group of ~10 kDa proteins that function as chaperones to ferry imported membrane proteins across the mitochondrial intermembrane space. In yeast there are five small TIM proteins: Tim8, Tim9, Tim10, Tim12 and Tim13, with equivalent proteins reported in humans. Using hidden Markov models we find that many eukaryotes have proteins equivalent to the Tim8 and Tim13 and the Tim9 and Tim10 subunits. Some eukaryotes provide "snapshots" of evolution, with a single protein showing the features of both Tim8 and Tim13, suggesting that a single progenitor gene might have given rise to each of the small TIMs through duplication and modification. We show that no "Tim12" family of proteins exist, but rather that variant forms of the cognate small TIMs have been recently duplicated and modified to provide new functions: the yeast Tim12 is a modified form of Tim10, while in humans and some protists variant forms of Tim9, Tim8 and Tim13 are found instead. Sequence motif analysis reveals acidic residues conserved in the Tim10 substrate-binding tentacles, whereas more hydrophobic residues are found in the equivalent substrate-binding region of Tim13. The conserved features in the Tim10 and Tim13 subunits provide distinct binding surfaces to accommodate the broad range of substrate proteins delivered to the mitochondrial inner and outer membranes.

Keywords: mitochondria, protein import, hidden Markov model, protein translocase, molecular parasitology

Abbreviations: TOM, translocase of the outer mitochondrial membrane; TIM, translocase of the inner mitochondrial membrane; SAM, sorting and assembly machinery in the outer mitochondrial membrane; AAC, ATP/ADP carrier; HMM, hidden Markov model; DAPI, 4',6-diamidino-2-phenylindole

Mitochondria are found ubiquitously in eukaryotes where they house 10-20% of the cellular proteome (Sickmann, Reinders et al. 2003; Ohlmeier, Kastaniotis et al. 2004; Reichert & Neupert, 2004; Prokisch et al. 2004; Gabaldon & Huynen, 2004), with up to a thousand proteins of varying biochemical properties having to be imported into the organelle and sorted to one of the four sub-mitochondrial compartments. A series of four molecular machines in the outer and inner mitochondrial membranes are responsible for the import and assembly of mitochondrial proteins (Pfanner and Geissler 2001; Herrmann and Neupert 2003; Koehler 2004; Pfanner, Wiedemann et al. 2004; Dolezal, Likic et al. 2006). These machines: the TOM complex, SAM complex, TIM23 complex and TIM22 complex, are composed of thirty to forty subunit parts that function as distinct modules. Some of the modules found in the yeast protein import machinery are conserved in animals and plants, while others seem to be more restricted in their distribution suggesting they have arisen more recently (Dolezal, Likic et al. 2006). Comparative analysis of the protein import machinery from various eukaryotic groups provides a powerful means to address how the component parts combine to form functional machines, and how the machines handle the broad range of substrate proteins imported into mitochondria.

The several hundred membrane proteins imported into mitochondria enter an aqueous channel in the TOM complex, enabling their translocation across the outer membrane (Brix, Dietmeier et al. 1997; Dietmeier, Honlinger et al. 1997; Schatz 1997; Pfanner, Wiedemann et al. 2004). Those proteins destined for assembly into the outer membrane are then transferred to the SAM complex. Most of the proteins destined for the inner membrane, including the abundant metabolite carrier proteins, are transferred instead to the TIM22 complex. It remains unclear how a given substrate protein is recognized for specific delivery to either the SAM or TIM22 complex, but it is known that the transfer reaction requires the assistance of the small TIM chaperones (Rehling, Model et al. 2003; Koehler 2004; Koehler 2004; de Marcos-Lousa, Sideris et al. 2006). The small TIMs are a group of ~10 kDa proteins originally characterised by a unique arrangement of cysteines: two sequence motifs of CX_3C separated by 11-16 residues (Koehler 2004). This superfamily of proteins, referred to as zf-Tim10DDP (PF02953), is collected together as a single group by the Conserved Domain Database (Marchler-Bauer, Anderson et al. 2005) because of the common features centred around the conserved CX_3C sequences. The cysteines contribute to two pairs of

disulfide bonds that maintain the structural integrity of the proteins (Allen, Lu et al. 2003; Webb, Gorman et al. 2006).

In yeast there are five members of the zf-Tim10DDP family: according to their approximate molecular weight in kDa these proteins are called Tim8, Tim9, Tim10, Tim12 and Tim13. Three of these, Tim9, Tim10 and Tim12 are essential for cell viability while the genes encoding the other two, Tim8 and Tim13, can be deleted without obvious effects on cell growth (Koehler, Leuenberger et al. 1999). Tim9 and Tim10 combine to form a $\alpha_3\beta_3$ hexamer, and the function of this Tim9/Tim10 complex has been studied in detail (Koehler, Merchant et al. 1998; Adam, Endres et al. 1999; Luciano, Vial et al. 2001; Curran, Leuenberger et al. 2002; Curran, Leuenberger et al. 2002; Truscott, Wiedemann et al. 2002; Lu, Golovanov et al. 2004; Lu and Woodburn 2005; Webb, Gorman et al. 2006). The essential Tim12 sits as a peripheral subunit on the inner membrane TIM22 translocase, where it appears to help unload substrates delivered by the Tim9/Tim10 complex (Koehler, Jarosch et al. 1998; Sirrenberg, Endres et al. 1998; Bauer, Rothbauer et al. 1999; Endres, Neupert et al. 1999; Muhlenbein, Hofmann et al. 2004). It has not been clear why yeast also expresses the Tim8 and Tim13 members of this protein family, however it is known that these form a second $\alpha_3\beta_3$ hexameric complex which appears to perform analogously to the Tim9/Tim10 complex in delivering substrate proteins to the outer and inner membranes (Koehler, Leuenberger et al. 1999; Curran, Leuenberger et al. 2002).

Due to the sequence conservation in the small TIMs, BLAST searches with the yeast sequences revealed corresponding human proteins. The Tim9/Tim10 complex from humans is involved in inner membrane protein insertion (Bauer, Rothbauer et al. 1999; Muhlenbein, Hofmann et al. 2004) and its crystal structure was recently solved (Webb, Gorman et al. 2006). It consists of a ring-shaped hexamer formed from alternating Tim9 and Tim10 subunits. The Tim8/Tim13 complex is also found in humans and a mutation in one of the genes encoding Tim8 leads to Mohr-Tranebjaerg syndrome (Koehler, Leuenberger et al. 1999; Bauer and Neupert 2001; Roesch, Curran et al. 2002). This demonstrates that the Tim9/Tim10 complex can not subsume all the activities of the Tim8/Tim13 complex, although *in vitro* studies show the role

played by the Tim8/Tim13 complex to be a minor one in both humans and in yeast (Curran, Leuenberger et al. 2002; Curran, Leuenberger et al. 2002; Truscott, Wiedemann et al. 2002). We have taken a comparative genomics approach to assess the role of the small TIM proteins in delivery of substrates to the mitochondrial membranes, addressing three questions. Firstly, does a signature motif exist beyond the duplicate CX_3C sequence that defines each of the five small TIMs? Secondly, how do these defining motifs relate to the three dimensional structure of the small TIM proteins, in terms of subunit interactions and recognition of substrates? Thirdly, can these motifs be used to determine whether or not all organisms encode and rely on Tim12 and both the Tim9/Tim10 and Tim8/Tim13 complexes?

Using hidden Markov models (HMMs) we find that many eukaryotes have proteins equivalent to the Tim8 and Tim13 and the Tim9 and Tim10 subunits of yeast. We show that no "Tim12" family of proteins exist, but rather that different organisms have variant forms of one of the four cognate small TIMs: the yeast Tim12 is a modified form of Tim10, while in humans and some protists variant forms of Tim9, Tim8 and Tim13 are found instead. Many fungi, plants and other eukaryotes have no variant TIM that would serve the role of the yeast Tim12. Motifs of conserved residues that define each of the four small TIM families map to crucial inter-subunit contacts in the small TIM hetero-hexamers, and also to substrate-binding regions. Residues in the N-terminal segments are distinct in the Tim10 and Tim13 substrate-binding subunits: acidic residues are conserved in the Tim10 substrate-binding tentacles whereas more hydrophobic residues are found in the equivalent region of Tim13. The comprehensive sequence analysis made possible with the hidden Markov models shows some eukaryotes have a reduced number of small TIMs, with only two or three genes present. While some apicomplexan parasites like the malaria-causing *Plasmodium* have clear and distinct Tim9, Tim10, Tim8 and Tim13 subunits, the genome of a related apicomplexan, *Theileria parva*, encodes a Tim9 and a Tim10 and then has a third gene that encodes a hybrid Tim8-Tim13 protein. This work suggests that the small TIM chaperones were present in the last common ancestor to the eukaryote lineage, and that distinct features in the four types of small TIMs are critical: they have been maintained, or independently evolved, to be present in diverse eukaryotes and the distinct features in the Tim10 and Tim13 subunits provides for a

broad range of substrate proteins to be collected and ferried across the mitochondrial intermembrane space.

RESULTS

There are four, distinct small TIM families: Tim8, Tim9, Tim10 and Tim13

Tim9, Tim10, Tim8, Tim13 and Tim12 were first identified in yeast (Jarosch, Tuller et al. 1996; Koehler, Merchant et al. 1998; Sirrenberg, Endres et al. 1998) and a thorough characterization of the homologs of these proteins in humans has been done (Bauer, Rothbauer et al. 1999; Jin, Kendall et al. 1999). Starting with the functionally characterised small TIMs from yeast and humans, BLAST searches were used to gather an initial set of 53 small TIM sequences. From a phylogenetic analysis, these cluster into four groups with each of the groups containing at least one of the cognate small TIMs from yeast (data not shown). The Tim12 and Tim10 sequences from yeast sit in a single group.

The grouped sequences were then used to construct four hidden Markov models, one describing each of the small TIM sub-families. The HMMs were used to extract related sequences from UniProt 7.5 sequence data. Those sequences that had been used to construct the HMM were recognised in UniProt with scores of E >10e-40. This then constitutes a "perfect match" in this search. All of the novel sequences retrieved with scores above E = e-05 are proteins of 50-100 residues, carry the twin CX_3C motif and were therefore collected as members of the small TIM family. The 141 small TIM sequences discovered here come from a broad range of eukaryotes, but none were found in prokaryotes. A number of complete genome sequence data sets are present in UniProt, and the small TIM proteins discovered in these organisms are listed in Table 1.

Each of the four small TIM families was then analysed for motifs, in order to determine those features that distinguish each of the four families. The motifs are represented in Figure 1. In all Tim9 sequences, a single motif exists with fifteen residues situated between the two CX_3C sequences. Numerous key residues in the motif are highly conserved as judged by the height of the character in the sequence logo (Figure 1). In the other TIM families there are two motifs, which are broken by the insertion of a variable number of residues: in Tim10, there are 15-21 residues between the twin CX_3C sequences, in Tim8 there are 14-18 residues while the Tim13 sequences have 11-14 residues inserted between the twin CX_3C sequences. The region between the twin CX_3C sequences is known to form a flexible loop (Webb, Gorman et

al. 2006), which could accommodate the variable number of residues. The conserved, diagnostic motifs found here extend well beyond the twin CX_3C sequences, with the key residues conserved within each motif distinguishing the four families. For example, there are several conserved acidic residues in the N-terminal region of all the Tim10 sequences that are not found in the other small TIMs.

Tim12-type proteins are the result of recent gene duplication events

While only four characteristic families of small TIMs can be recognised, in many organisms for which complete sequence data is available, five distinct small TIM proteins were found: one corresponding to each of the cognate families and a fifth isoform that fits less well to the criteria shown in any of the conserved motifs. The best studied of these is the yeast Tim12, a peripheral component of the TIM22 complex (Koehler, Jarosch et al. 1998; Sirrenberg, Endres et al. 1998). Tim12 appears to serve as a docking point for the substrate-Tim9/Tim10 complex. Yeast Tim12 matches the Tim10 motif, though poorly compared to *bone fide* Tim10 homologues. A peripheral small TIM component of the TIM22 complex has also been described in humans (Muhlenbein, Hofmann et al. 2004), but this small TIM (Q9Y5J6) best matches the sequence criteria of the Tim9 HMM (E = 5.30e-46) rather than the Tim10 HMM (E = 6.00e-5). Thus it seems that the TIM22 complex subunit can be of either type of small TIM. Furthermore, the four species of *Plasmodium* for which complete genome data are available have a variant TIM that matches either the Tim8 or Tim13 HMM (E ~ e-05 to e-08 in all cases). This would suggest that the acquisition of a fifth, "Tim12" type, subunit might have occurred relatively recently and have come about independently in various lineages of eukaryotes. In keeping with this proposal plants, amoeba, kinetoplastids and filamentous fungi have no apparent variant form of small TIM available to fulfil this function. Presumably in these organisms the import pathway has evolved such that substrate-loaded small TIM complexes can dock to the TIM22 complex directly, without the assistance of a pre-bound Tim12 subunit.

Mapping the conserved residues onto the structural framework of the Tim9/Tim10 complex

The conserved residues discovered in the sequence motifs might be expected to form functionally important surfaces: either in subunit interfaces, as surfaces that dock to other components of the import machinery, or in substrate-binding features. The

structure of the Tim9/Tim10 complex from humans was recently solved by X-ray crystallography (Webb, Gorman et al. 2006) providing a framework to analyse the conserved features. Many of the highly conserved residues pinpointed in the motif analysis form contacts between the Tim9 and Tim10 subunits. For example, at the interface between the front face of Tim9 and the back face of Tim10: F29 and F36 of Tim9 form a conserved buried core with Y58, K32 and the C54-C29 disulphide bond of Tim10 (Figure 2A). Where the front face of Tim10 contacts the back face of Tim9, the most highly conserved interchain contacts are ionic interactions between D52 and R62 as well as E47 and K55 (Figure 2B). Thus conserved patches on both faces of Tim9 and Tim10 subunits contribute to the subunit interfaces of the hexamer.

As a result of these conserved inter-subunit contacts, a highly conserved surface can be seen at the top of the hexamer (Figure 2C). The surface would be continuous but for the poorly-conserved regions of the loops between the CX_3C motifs in each subunit. These loops break the conserved surface into two patches: the first is formed from Tim10 residues K32, G46, E47, C33-C50, R53 and the Tim9 residues F36 and K55, while the second, smaller patch is each formed from Tim9 residues E45 and C32-C48. It is possible these patches are purely a by-product of the conserved core being partially exposed at the surface; playing no functional role outside maintaining the structural integrity of the hexamer. However, the conserved surface would make an attractive means for the TIM complex to dock with other conserved components of the import machinery.

Substrate-binding regions in the Tim9/10 and the Tim8/Tim13 complexes

The first twenty-one residues of Tim10 are required for substrate binding (Vergnolle, Baud et al. 2005) and form three “tentacles” extending down from the inner ring of helices in the Tim9/Tim10 hexamer (Webb, Gorman et al. 2006). In the crystal structure, only one of these chains has all twenty-one residues defined, sitting in two contiguous helices (Figure 3A), the other two tentacles have N-terminal extensions that could not be resolved (Webb, Gorman et al. 2006). Mapping the conserved residues from the Tim10 motif onto the structure shows the various ways the acidic residues are displayed in the three tentacle conformations (Figure 3B), and none of the conserved residues in the tentacles appears to be involved in contacting neighbouring Tim9 subunits.

When Tim10 is purified in isolation from Tim9, it exists in a small soluble form that might be either a monomer or dimer (Vial, Lu et al. 2002; Webb, Gorman et al. 2006). The purified Tim10 subunit binds the inner membrane substrate AAC in a manner similar to the Tim9/Tim10 complex, whereas Tim9 alone does not bind at all. The N-terminal helix of the Tim10 subunit is required for substrate binding (Vergnolle, Baud et al. 2005).

Motif analysis also described a highly conserved N-terminal region in Tim13 (Figure 1) and we sought to determine if Tim13 might be the substrate binding subunit of the Tim8/Tim13 complex. A cellulose filter carrying 103 peptides representing the ADP/ATP carrier protein (AAC), a substrate of the small TIM chaperones, was incubated with purified Tim8 or Tim13. A discrete set of spots, highlighting the peptides bound by Tim13, can be seen on the filter (Figure 4A, upper panel). The peptides bound by Tim13 correspond to the hydrophobic transmembrane domains of AAC. These same regions of AAC are bound by Tim10 and the native Tim9/Tim10 complex (Curran, Leuenberger et al. 2002; Vasiljev, Ahting et al. 2004; Vergnolle, Baud et al. 2005). Binding of Tim8 to the same filter was barely detectable (Figure 4A, lower panel). To consolidate the idea that Tim13 functions as the substrate sensor in the Tim8/Tim13 complex, a second cellulose filter carrying peptides from the inner membrane protein Tim22 was tested in the same way. Again, Tim13 binds to discrete peptides on the membrane, while Tim8 bound weakly, to only one peptide spot (Figure 4B). As is the case for its binding to AAC, Tim13 binds peptides corresponding to the predicted transmembrane regions of the Tim22 substrate. This behaviour has also been demonstrated for the *Neurospora crassa* Tim9/Tim10 complex on a Tim22 peptide membrane (Vasiljev, Ahting et al. 2004). Both Tim10 and Tim13 therefore act as substrate sensors for their respective complexes, by binding to hydrophobic transmembrane segments of their substrate proteins.

Organisms lacking a Tim8/Tim13 complex?

Some organisms appear to lack genes that would encode Tim8 and Tim13 family members. *Dictyostelium discoideum* is a case in point where very clear Tim9 and Tim10 subunits are found while no other small TIM sequences are present in the completely sequenced genome (Table 1). Further species of eukaryotes for which

complete genome data is available also lack Tim8 and Tim13 proteins. However *Theileria parva, Leishmania major, Trypanosoma cruzi* and *Trypanosoma brucei* show intriguing sequences that might represent ancestral-type composite Tim8-13 proteins.

The kinetoplastida represents some of the earliest diverging forms of eukaryotes and include the human pathogens *L. major, T. cruzi* and *T. brucei*. Each of these organisms has three small TIMs. In *T. brucei* the first TIM matches both the Tim9 model and Tim10 model (E = 1.10e-06, E = 1.90e-07, respectively) and the second protein specifically matches the Tim10 HMM (E = 2.20e-05). The third sequence has limited conservation to any of the four TIM families, but conserved residues within the N-terminal half of the protein most closely match the signatures of Tim13, and conserved residues within the C-terminal half most closely match the signatures of Tim8.

Little is known about the protein import apparatus in the kinetoplastid mitochondrion. However, a few of the most conserved components of the protein import machinery have been annotated within the completely sequenced genomes (El-Sayed, Myler et al. 2005) including the inner membrane translocase *Tb*11.01.4870, a member of the Tim17/Tim22/Tim23 family of proteins (PF02466; (Marchler-Bauer, Anderson et al. 2005) that would serve as the core of the inner membrane (TIM) protein translocase. Depletion of this protein by RNAi in cultured procyclic form parasites gives a mitochondrial defect, with the normally reticular mitochondrion becoming a globular mass as judged from immunofluorescent staining of the mitochondrial matrix protein Hsp60 (Figure 5B). The defect, seen in 60-75% of cells after 72 hours of treatment (Figure 5C), might reflect the paucity of protein insertion into the mitochondrial membranes, and is distinct from the morphology after RNAi treatment of other essential proteins (Esseiva, Chanez et al. 2004; Smid, Horakova et al. 2006). Over the same timecourse, RNAi treatment to deplete the Tim8-13 of *T. brucei* yields the same mitochondrial defect, (Figure 5B, 5C) demonstrating that this small TIM protein functions as a crucial component in the mitochondria of these kinetoplastids.

Complete genome sequence data is also available for three groups of apicomplexan parasites, seven species in all from *Plasmodium*, *Cryptosporidium* and *Theileria*.

Cryptosporidium parvum and *Cryptosporidium hominis* have only relic mitochondria, the mitosome, with a greatly reduced set of proteins targeted to this organelle (Putignani, Tait et al. 2004; Henriquez, Richards et al. 2005); the genomes of these organisms encode only one small TIM, which has the characteristics of both Tim8 and Tim13 (Table 1). In *Theileria parva*, three proteins are encoded: the first matches the Tim9 HMM (E = 8.10e-41) and the second matches the Tim10 HMM (E = 9.10e-9). The third small TIM from *T. parva* matches both the HMM for Tim13 (E = 5.60e-07) and the HMM for Tim8 (E = 5.10e-41). In the genome sequence of the four diverse species of *Plasmodium*, four cognate small TIMs were detected. Each is remarkably similar to the Tim9, Tim10, Tim8 and Tim13 proteins found in humans and yeast (Table 1).

DISCUSSION

Delivery of substrates to the outer and to the inner membrane translocases

Recent functional analyses rule out the prospect that the two small TIM complexes selectively deliver substrates to either the outer membrane or to the inner membrane (Leuenberger, Bally et al. 1999; Davis, Sepuri et al. 2000; Curran, Leuenberger et al. 2002; Truscott, Wiedemann et al. 2002; Hoppins and Nargang 2004). Both Tim8/Tim13 and Tim9/Tim10 complexes are required for the efficient delivery of outer membrane substrates (Hoppins and Nargang 2004; Wiedemann, Truscott et al. 2004) and both complexes assist in the delivery of some inner membrane proteins. It seems that both chaperones bind predominantly to transmembrane segments of their substrate proteins. The identity of the residues conserved in the tentacles of Tim10 and the equivalent region of Tim13 differ, with numerous alanine residues diagnostic of the Tim13 substrate-binding segment. This might provide some differences in the range of peptide segments bound: we note that Tim13 binds best to the last transmembrane segment of the Tim22 substrate (Figure 4B) while Tim10 binds best to the second transmembrane segment (Vasiljev, Ahting et al. 2004). The N-terminal tentacle of both proteins predicts highly for propensity to form a coiled coil (data not shown). This structural feature may also contribute to substrate binding; in coils, the chaperone's α-helical tentacles might shield hydrophobic helical segments of substrate.

In yeast, the *TIM8* and *TIM13* genes are not essential for cell viability and *Dictyostelium discoideum* lacks Tim8 and Tim13 proteins. The Tim9 and Tim10 in *D. discoideum* are typical, with very high matches to the respective HMM (E = 1.70e-35 and 4.50e-44). This suggests that a single small TIM complex is sufficient to mediate targeting of all membrane protein substrates in this organism. Too little is known about mitochondrial protein targeting in *D. discoideum* yet, but its various substrate proteins might be less diverse in their sequence characteristics – which might in turn explain how a single small TIM complex could deliver all protein substrates to the outer and inner membranes. We suggest that the advantage to most organisms in having these distinct small TIM complexes comes in the increased range of substrates that can be bound; with the somewhat different substrate-binding tentacles in the

Tim13 and Tim10 subunits providing a broader capability for the substrates that can be recognized and delivered to the TIM22 and SAM complexes for assembly.

The primitive condition: where did small TIMs come from and how?

Our HMM analysis detects no proteins widely found in bacteria that might represent an ancestor chaperone from which the small TIMs have been derived, and we suggest that this family of chaperones was derived by the host cell in order to facilitate membrane protein transfer across the intermembrane space to the inner membrane; a pathway not pre-existing in the bacterial endosymbiont. The distinct "primitive" conditions, found in this study, each contribute something to a new understanding of how the small TIM proteins came about.

Firstly, some eukaryotes have no small TIMs, demonstrating that small TIMs are not essential for mitochondrial biogenesis *per se*. During the first phases of mitochondrial evolution, targeting of membrane proteins could have proceeded in the absence of small TIMs. *Encephalitozoon cuniculi* is a microsporidian, and these organisms diverged early from the animal and fungal lineage. Microsporidians have massively reduced genomes, and in particular have highly simplified mitochondria (referred to as "mitosomes") with no electron transport chain, no ATP synthase and no mitochondrial metabolite carriers in their inner membranes (Katinka, Duprat et al. 2001). The remnant mitochondrion in microsporidians probably houses relatively few proteins apart from the simplified mitochondrial protein import apparatus and FeS cluster biosynthetic machinery, and therefore has relatively few proteins assembled into the mitosomal membranes. The widespread distribution of small TIM proteins in other eukaryotes suggests an early origin for the family and that microsporidians have therefore lost their TIMs as part of their genome reduction. Microsporidians retain a Tom40 that must be assembled into the outer membrane and a vestigial SAM complex (Katinka, Duprat et al. 2001; Dolezal, Likic et al. 2006), and a TIM translocase that must be assembled in the inner membrane (Katinka, Duprat et al. 2001), thereby demonstrating that even in the absence of small TIMs mitochondrial membrane protein assembly can be achieved. A similar situation is seen in *Trichomonas vaginalis*, which might also have a reduced membrane protein complexity and shows an absence of small TIMs. While themselves being highly evolved organisms, these

eukaryotes provide a proof-of-principle for a situation in the earliest eukaryotes, when relatively few membrane proteins were coded on nuclear genes and in need of import.

The composite small TIM found in species of *Cryptosporidium*, *Theileria*, *Leishmania* and *Trypanosoma*, with the combined sequence characteristics of Tim8 and Tim13, supports our suggestion that a single gene might be enough to encode a functional chaperone. In particular, species of *Cryptosporidium* appear to have only this small TIM. *Leishmania* and *Trypanosoma* also have Tim9 and Tim10 proteins but the "Tim9" subunit shows strong similarity to both the Tim10 and Tim9 HMMs: we suggest this "Tim9" was derived from the Tim10 subunit by a gene duplication event but not modified so extensively as the Tim9s in other eukaryotes. Again, this represents a proof-of-principle example that in simple eukaryote a single gene encoding a suitable hybrid protein, such as Tim8-13 could form a functional chaperone. It also illustrates that, starting with a Tim9-10 hybrid protein, Tim9 and Tim10 subunits could come about through modification of duplicated genes.

We suggest that early eukaryotes carried a single small TIM, and that duplication of this gene gave rise to both the Tim10 and Tim13 type chaperones in the mitochondrial intermembrane space. Further gene duplications, and co-dependent mutations created the Tim9- and Tim8- type subunits, providing in each the necessary inter-subunit contacts to give rise to heteromeric complexes. Much more recently, gene duplication events have given rise to the "Tim12" subunit found attached to the TIM22 complex in the mitochondrial inner membrane. The development of Tim9/Tim10 and Tim8/Tim13 complexes may have occurred very early, so that all eukaryotes inherited a full set of the four cognate small TIMs. Alternatively, some of the duplication events may have occurred in parallel, in distinct lineages, with correlated mutations giving similar outcomes in the Tim9 and Tim8 families. With such small, simply structured proteins, this alternative represents a reasonable proposition.

METHODS

Hidden Markov models

The initial set of small TIM sequences gathered from BLAST searches were aligned using ClustalX (Jeanmougin, Thompson et al. 1998) and the alignment was used to generate a Neighbor-Joining phylogenetic tree that clustered the sequences into four main groups, with each of the cognate small TIMs from yeast sitting in one of the four groups. The sets representing Tim8, Tim9, Tim10, and Tim13 contained 16, 15, 13, and 9 sequences respectively. The grouped sequences were then used to construct HMMs which in turn were used to search the UniProt database for related proteins.

The HMMs were built with the program HMMER 2.3.2 (Durbin 1998). The best multiple alignment for each family of sequences was obtained with ClustalW (Thompson, Higgins et al. 1994) and t-coffee (Notredame, Holm et al. 1998). The two alignment programs produced different best alignments, and we built two sets of HMMs (corresponding to ClustalW and t-coffee alignments) for each family of sequences (Tim8, Tim9, Tim10 and Tim13). The resulting HMMs were used to scan UniProt database release 7.2 (Swiss-Prot release 49.2 and TrEMBL release 32.2) (Bairoch, Apweiler et al. 2005) and also to scan protein data sets from the *Trichomonas vaginalis* and *Encephalizoon cuniculi* genomes individually, as previously described (Dolezal, Likic et al. 2006). The results of all HMM searches were manually examined. The sequences used to construct the HMM were detected from within the UniProt search with scores better than E = e-40. Novel sequences retrieved with scores E< e-05 were proteins of 50-100 residues that carry the twin CX_3C motif and were considered members of the small TIM family. Sequences which scored poorer than E = e-04 were larger than 100 residues, did not carry the twin CX_3C motif, and were therefore discarded. Many of these were proteins of known function and have predicted (helix-rich) coiled-coil domain structures.

Motif analysis to distinguish four small TIM families

Proteins deemed to belong to one of the four small TIM families were used to define sequence motifs. Note, the hybrid Tim8-Tim13 sequences were not included for motif analysis. The program MEME version 3.5.2 (Bailey and Elkan 1994) was used and in the first step we searched each given protein family for the single strongest motif present in the sequences, the rationale being that if all sequences were correctly

assigned to a small TIM family they should have at least one common motif. Consequently, any sequence which did not have this motif was removed from further analysis. This resulted in the removal of one sequence from the initial Tim8, Tim9 and Tim10 sets. The resulting Tim8, Tim9, Tim10, and Tim13 sets containing 33, 40, 33 and 25 sequences, respectively, were used in further motif analysis. In the second step, we checked for possible motifs that occur as repetitions (MEME 'anr' distribution option). No such motifs were found in any of the four protein families. Finally, the three most prominent motifs in each family were searched for. The motifs were constrained to be between 5 and 128 residues, with the E-value not to exceed 1e-10. Motifs that were present in all sequences of a sub-family are represented in the logos in Figure 1 and have the following characteristics: Tim9 Motif (E-value = 2e-1115), Tim10 Motifs 1 and 2 (E-values = 1e-543 and = 4e-448), Tim8 Motifs 1 and 2 (E-values = 2e-400 and = 4e-211), Tim13 Motifs 1 and 2 (E-value = 8e-396 = 3e-335). No other characteristic motifs were found. From past experience we know that the output of a MEME motif search (including the exact beginning or end of a motif) may be affected by input parameters (V. Likić, unpublished). To test for reliability in the predicted motifs, we ran five repeats of motif elucidation with different input parameters. For each family of sequences the resulting motifs were confirmed.

In order to map the critical residues within the motifs onto the crystal structure of Tim9/10, the information content (Shannon uncertainty) (Schneider and Stephens, 1990) was calculated for each column in seperate multiple alignments of Tim9 and Tim10 using the Biopython tools (http://biopython.org) and assuming a uniform background symbol distribution. These values were mapped to the coordinates of the Tim9/Tim10 heterohexamer crystal structure (pdb accession 2BSK) (Webb et al, 2006) using the occupancy field of the pdb format and analysed using VMD (version 1.8.4) (Humphrey et al, 1999).

RNAi knockdowns of Tim8-13 and TIM translocase core in Trypanosoma brucei

RNAi-mediated ablation of the *T. brucei* Tim8-13 and TIM translocase core was performed using stem loop constructs containing the puromycine resistance gene as described (Bochud-Allemann and Schneider 2002). The constructs correspond to the sequence of the entire open-reading frame of *T. brucei* Tim8-13 and TIM translocase

genes. Transfection of *T. brucei* (strain 29-13), selection with antibiotics, cloning and induction with tetracycline were done as described (McCulloch, Vassella et al. 2004).

Binding assays with the yeast Tim8/Tim13 complex

PVDF membranes of 13mer peptides with a ten amino acid overlap were synthesised by automated spot synthesis (JPT Peptide Technologies, Berlin, Germany). Binding of Tim13 was performed as described (Vergnolle, Baud et al. 2005) with the following modifications: Tim13 antibodies were used to detect bound proteins, and signals were quantified using ImageQuant software (Molecular Dynamics). Transmembrane segments were predicted for Tim22 using DAS (Cserzo et al. 1997) and multiple sequence alignments as previously described (Chan, Likic et al. 2006) and for Aac2 by alignment with the bovine AAC crystal structure (Pebay-Peyroula, Dahout-Gonzalez et al. 2003).

ACKNOWLEDGEMENTS

This work was supported by grants from the Australian Research Council and NH&MRC (to TL) and funds from IMBB-FORTH, the University of Crete and the European Social Fund and national resources (to KT) and grant 3100-067906 of the Swiss National Foundation (to AS). IEG was supported by an Australian Postgraduate Award. FHA was supported by a BBSRC-UK studentship. We are grateful to MARCC for computer time. We thank … …. ……. for discussions and critical comments on the manuscript.

FIGURE LEGENDS

Figure 1. Motif representation of the four cognate small TIM families. Sequence Logos (Crooks et al. 2004) describing the conserved sequence motifs in each of the small TIMs are shown. These centre around the conserved twin CX_3C residues. In the case of Tim10, Tim8 and Tim13 the motif is broken in two due to a variable number of residues in the interhelical loop region. The highly conserved N-terminal region in the Tim10 sequences corresponds to the region of the protein that binds substrate (Vergnolle, Baud et al. 2005).

Figure 2. Conserved residues sit at the inter-subunit contacts of the Tim9/Tim10 hexamer. (A) The interface between the "front" face of Tim9 (cyan cylinders) and the "back" face of Tim10 (blue/white/red surface). The most conserved residues in contact across this interface are aromatics (Tim9-F29, Tim-F26 and Tim10-Y58), which pack against one of the two strictly conserved disulphide bonds in Tim10 (C54-C29) (B) Flipped 180^o, the view of the interface where the "back" face of Tim9 (transparent grey cylinders) contacts the "front" face of Tim10 (blue/white/red surface). In addition to the ionic interactions between Tim10-D52/Tim9-R62 and Tim10-E47/Tim9-K55, the conserved L43 of Tim10 packs against the acyl chain region of Tim9-K55 which "threads" through the loop of Tim10. The sidechains of the most conserved residues (>3.46 bits, 80^{th} percentile) in Tim9 are shown as orange spheres (C) The conserved core residues of the Tim9/Tim10 complex are also partially exposed on the top surface of the hexamer. Residues from Tim9 (grey labels) and Tim10 (orange labels) with side-chains contributing to the conserved patches are identified.

Figure 3. Conserved residues in the Tim10 tentacles. (A) Side view of the Tim9/Tim10 complex, with Tim9 subunits shaded dark grey and Tim10 shaded orange-gold. The length for which each of the "tentacles", formed from the N-terminal helices of the three Tim10 subunits, can be resolved varies in the crystal structure (Webb et al. 2006). The longest tentacle yielded electron density to define the structure of almost the full N-terminal segment. (B) The conserved residues in the first twenty residues of the N-terminal segments are mapped onto each of the three Tim10 subunits.

Figure 4. Substrate recognition by Tim13 and Tim8. Thirteen-mer peptide assemblies (see Methods) representing AAC (the Aac2 protein from *S. cerevisiae*) (left) and Tim22 from *S. cerevisiae* (right) were screened with purified Tim13 (upper panel) or Tim8 (lower panel) proteins. Bound protein was blotted to PVDF membranes and probed with antibodies that detect Tim13 or Tim8. Immunolocalisation of the respective small TIMs shows the pattern of peptides to which they bind, and the immunoblots are shown along with a graphical representation of relative amount of binding to each peptide spot. The positions of predicted transmembrane domains and loops, according to peptide number, are indicated below the graphs.

Figure 5. Depletion of TIM function leads to mitochondrial morphology defects and cell death in *T. brucei*. (A) Growth curves in the absence (-Tet) and presence (+Tet) of tetracycline of representative clonal *T. brucei* RNAi cell lines. Cell growth stops 50 hours after the addition of the tetracycline inducer. (B) Analysis of mitochondrial morphology in uninduced (0h) and induced (72h) TIM translocase core *Tb*11.01.4870 and Tim8-13 RNAi cell lines using immunofluorescence. Upper panel, Nomarski image. Lower panel, immunofluorescence staining with Hsp60 antiserum (red) and DAPI stain for nucleus (blue). Bar = 20 μm. (C) Time course of appearance and extent of mitochondrial fragmentation observed in induced TIM translocase core *Tb*11.01.4870 and Tim8-13 RNAi cell lines (n > 200 cells for each time point).

TABLE LEGEND

Table 1. Patterns of distribution of the small TIMs in eukaryotes. Hidden Markov models were built to describe Tim9, Tim10, Tim8 and Tim13 and used to search genome sequence data. The organisms listed each have completely sequenced genomes. The column "other" includes the Tim12 protein from yeast and humans, both of which have been shown to be located on the surface of the TIM22 translocase ([8] - weak similarity to Tim8, [9] - strong similarity to Tim9, [10] - weak similarity to Tim10, [13] - weak similarity to Tim13).

~~REFERENCES~~

Adam, A., M. Endres, et al. (1999). "Tim9, a new component of the TIM22.54 translocase in mitochondria." Embo J **18**(2): 313-9.

Allen, S., H. Lu, et al. (2003). "Juxtaposition of the two distal CX3C motifs via intrachain disulfide bonding is essential for the folding of Tim10." J Biol Chem **278**(40): 38505-13.

Bailey, T. L. and C. Elkan (1994). "Fitting a mixture model by expectation maximization to discover motifs in biopolymers." Proc Int Conf Intell Syst Mol Biol **2**: 28-36.

Bairoch, A., R. Apweiler, et al. (2005). "The Universal Protein Resource (UniProt)." Nucleic Acids Res **33**(Database issue): D154-9.

Bauer, M. F. and W. Neupert (2001). "Import of proteins into mitochondria: a novel pathomechanism for progressive neurodegeneration." J Inherit Metab Dis **24**(2): 166-80.

Bauer, M. F., U. Rothbauer, et al. (1999). "The mitochondrial TIM22 preprotein translocase is highly conserved throughout the eukaryotic kingdom." FEBS Lett **464**(1-2): 41-7.

Bochud-Allemann, N. and A. Schneider (2002). "Mitochondrial substrate level phosphorylation is essential for growth of procyclic Trypanosoma brucei." J Biol Chem **277**(36): 32849-54.

Brix, J., K. Dietmeier, et al. (1997). "Differential recognition of preproteins by the purified cytosolic domains of the mitochondrial import receptors Tom20, Tom22, and Tom70." J Biol Chem **272**(33): 20730-5.

Chan, N. C., V. A. Likic, et al. (2006). "The C-terminal TPR domain of Tom70 defines a family of mitochondrial protein import receptors found only in animals and fungi." J Mol Biol **358**(4): 1010-22.

Curran, S. P., D. Leuenberger, et al. (2002). The Tim9p-Tim10p complex binds to the transmembrane domains of the ADP/ATP carrier. Embo J. **21**.

Curran, S. P., D. Leuenberger, et al. (2002). The role of the Tim8p-Tim13p complex in a conserved import pathway for mitochondrial polytopic inner membrane proteins. J Cell Biol. **158**.

Cserzo, E. Wallin, I. et al. (1997). Prediction of transmembrane alpha-helices in procariotic membrane proteins: the Dense Alignment Surface method; Prot. Eng. 10(6): 673-6.

Davis, A. J., N. B. Sepuri, et al. (2000). "Two intermembrane space TIM complexes interact with different domains of Tim23p during its import into mitochondria." J Cell Biol **150**(6): 1271-82.

de Marcos-Lousa, C., D. P. Sideris, et al. (2006). "Translocation of mitochondrial inner-membrane proteins: conformation matters." Trends Biochem Sci **31**(5): 259-67.

Dietmeier, K., A. Honlinger, et al. (1997). "Tom5 functionally links mitochondrial preprotein receptors to the general import pore." Nature **388**(6638): 195-200.

Dolezal, P., V. Likic, et al. (2006). "Evolution of the molecular machines for protein import into mitochondria." Science **313**(5785): 314-8.

Durbin, R., S.R. Eddy, A. Krogh, G. Mitchison (1998). Biological Sequence Analysis: Probabilistic Models of Proteins and Nucleic Acids, Cambridge University Press.

El-Sayed, N. M., P. J. Myler, et al. (2005). "Comparative genomics of trypanosomatid parasitic protozoa." Science **309**(5733): 404-9.

Endres, M., W. Neupert, et al. (1999). "Transport of the ADP/ATP carrier of mitochondria from the TOM complex to the TIM22.54 complex." Embo J **18**(12): 3214-21.
Esseiva, A. C., A. L. Chanez, et al. (2004). "Temporal dissection of Bax-induced events leading to fission of the single mitochondrion in Trypanosoma brucei." EMBO Rep **5**(3): 268-73.
Gabaldon T, Huynen MA. Shaping the mitochondrial proteome. Biochim Biophys Acta. 2004 Dec 6;1659(2-3):212-20
Henriquez, F. L., T. A. Richards, et al. (2005). "The unusual mitochondrial compartment of Cryptosporidium parvum." Trends Parasitol **21**(2): 68-74.
Herrmann, J. M. and W. Neupert (2003). "Protein insertion into the inner membrane of mitochondria." IUBMB Life **55**(4-5): 219-25.
Hoppins, S. C. and F. E. Nargang (2004). "The Tim8-Tim13 complex of Neurospora crassa functions in the assembly of proteins into both mitochondrial membranes." J Biol Chem **279**(13): 12396-405.
Humphrey, W., Dalke, A. and Schulten, K., (1999) "VMD - Visual Molecular Dynamics", J. Molec. Graphics, 4: 33-38.
Jarosch, E., G. Tuller, et al. (1996). "Mrs5p, an essential protein of the mitochondrial intermembrane space, affects protein import into yeast mitochondria." J Biol Chem **271**(29): 17219-25.
Jeanmougin, F., J. D. Thompson, et al. (1998). "Multiple sequence alignment with Clustal X." Trends Biochem Sci **23**(10): 403-5.
Jin, H., E. Kendall, et al. (1999). "The human family of Deafness/Dystonia peptide (DDP) related mitochondrial import proteins." Genomics **61**(3): 259-67.
Katinka, M. D., S. Duprat, et al. (2001). "Genome sequence and gene compaction of the eukaryote parasite Encephalitozoon cuniculi." Nature **414**(6862): 450-3.
Koehler, C. M. (2004). "New developments in mitochondrial assembly." Annu Rev Cell Dev Biol **20**: 309-35.
Koehler, C. M. (2004). "The small Tim proteins and the twin Cx3C motif." Trends Biochem Sci **29**(1): 1-4.
Koehler, C. M., E. Jarosch, et al. (1998). "Import of mitochondrial carriers mediated by essential proteins of the intermembrane space." Science **279**(5349): 369-73.
Koehler, C. M., D. Leuenberger, et al. (1999). "Human deafness dystonia syndrome is a mitochondrial disease." Proc Natl Acad Sci U S A **96**(5): 2141-6.
Koehler, C. M., S. Merchant, et al. (1998). "Tim9p, an essential partner subunit of Tim10p for the import of mitochondrial carrier proteins." Embo J **17**(22): 6477-86.
Leuenberger, D., N. A. Bally, et al. (1999). "Different import pathways through the mitochondrial intermembrane space for inner membrane proteins." Embo J **18**(17): 4816-22.
Lu, H., A. P. Golovanov, et al. (2004). "The structural basis of the TIM10 chaperone assembly." J Biol Chem **279**(18): 18959-66.
Lu, H. and J. Woodburn (2005). "Zinc binding stabilizes mitochondrial Tim10 in a reduced and import-competent state kinetically." J Mol Biol **353**(4): 897-910.
Luciano, P., S. Vial, et al. (2001). Functional reconstitution of the import of the yeast ADP/ATP carrier mediated by the TIM10 complex. Embo J. **20**.
Marchler-Bauer, A., J. B. Anderson, et al. (2005). "CDD: a Conserved Domain Database for protein classification." Nucleic Acids Res **33**(Database issue): D192-6.

McCulloch, R., E. Vassella, et al. (2004). "Transformation of monomorphic and pleomorphic Trypanosoma brucei." Methods Mol Biol **262**: 53-86.
Muhlenbein, N., S. Hofmann, et al. (2004). "Organization and function of the small Tim complexes acting along the import pathway of metabolite carriers into mammalian mitochondria." J Biol Chem **279**(14): 13540-6.
Notredame, C., L. Holm, et al. (1998). "COFFEE: an objective function for multiple sequence alignments." Bioinformatics **14**(5): 407-22.
Ohlmeier, S., A. J. Kastaniotis, et al. (2004). "The yeast mitochondrial proteome, a study of fermentative and respiratory growth." J Biol Chem **279**(6): 3956-79.
Pebay-Peyroula, E., C. Dahout-Gonzalez, et al. (2003). "Structure of mitochondrial ADP/ATP carrier in complex with carboxyatractyloside." Nature **426**(6962): 39-44.
Pfanner, N. and A. Geissler (2001). Versatility of the mitochondrial protein import machinery. Nat Rev Mol Cell Biol. **2**.
Pfanner, N., N. Wiedemann, et al. (2004). "Assembling the mitochondrial outer membrane." Nat Struct Mol Biol **11**(11): 1044-8.
Prokisch H, Scharfe C, Camp DG 2nd, Xiao W, David L, Andreoli C, Monroe ME, Moore RJ, Gritsenko MA, Kozany C, Hixson KK, Mottaz HM, Zischka H, Ueffing M, Herman ZS, Davis RW, Meitinger T, Oefner PJ, Smith RD, Steinmetz LM. Integrative analysis of the mitochondrial proteome in yeast. PLoS Biol. 2004 Jun;2(6):e160
Putignani, L., A. Tait, et al. (2004). "Characterization of a mitochondrion-like organelle in Cryptosporidium parvum." Parasitology **129**(Pt 1): 1-18.
Rehling, P., K. Model, et al. (2003). "Protein insertion into the mitochondrial inner membrane by a twin-pore translocase." Science **299**(5613): 1747-51.
Reichert AS, Neupert W. Mitochondriomics or what makes us breathe. Trends Genet. 2004 Nov;20(11):555-62
Roesch, K., S. P. Curran, et al. (2002). "Human deafness dystonia syndrome is caused by a defect in assembly of the DDP1/TIMM8a-TIMM13 complex." Hum Mol Genet **11**(5): 477-86.
Schatz, G. (1997). "Just follow the acid chain." Nature **388**(6638): 121-2.
Schneider TD, Stephens RM. (1990) “Sequence logos: a new way to display consensus sequences.” Nucleic Acids Res. 18(20): 6097-100.
Sickmann, A., J. Reinders, et al. (2003). "The proteome of Saccharomyces cerevisiae mitochondria." Proc Natl Acad Sci U S A **100**(23): 13207-12.
Sirrenberg, C., M. Endres, et al. (1998). "Carrier protein import into mitochondria mediated by the intermembrane proteins Tim10/Mrs11 and Tim12/Mrs5." Nature **391**(6670): 912-5.
Smid, O., E. Horakova, et al. (2006). "Knock-downs of iron-sulfur cluster assembly proteins ISCS and ISCU down-regulate the active mitochondrion of procyclic trypanosoma brucei." J Biol Chem.
Thompson, J. D., D. G. Higgins, et al. (1994). "CLUSTAL W: improving the sensitivity of progressive multiple sequence alignment through sequence weighting, position-specific gap penalties and weight matrix choice." Nucleic Acids Res **22**(22): 4673-80.
Truscott, K. N., N. Wiedemann, et al. (2002). "Mitochondrial import of the ADP/ATP carrier: the essential TIM complex of the intermembrane space is required for precursor release from the TOM complex." Mol Cell Biol **22**(22): 7780-9.

Vasiljev, A., U. Ahting, et al. (2004). "Reconstituted TOM core complex and Tim9/Tim10 complex of mitochondria are sufficient for translocation of the ADP/ATP carrier across membranes." Mol Biol Cell **15**(3): 1445-58.

Vergnolle, M. A., C. Baud, et al. (2005). "Distinct domains of small Tims involved in subunit interaction and substrate recognition." J Mol Biol **351**(4): 839-49.

Vial, S., H. Lu, et al. (2002). "Assembly of Tim9 and Tim10 into a functional chaperone." J Biol Chem **277**(39): 36100-8.

Webb, C. T., M. A. Gorman, et al. (2006). "Crystal structure of the mitochondrial chaperone TIM9.10 reveals a six-bladed alpha-propeller." Mol Cell **21**(1): 123-33.

Wiedemann, N., K. N. Truscott, et al. (2004). Biogenesis of the protein import channel Tom40 of the mitochondrial outer membrane: intermembrane space components are involved in an early stage of the assembly pathway. J Biol Chem. **279**.

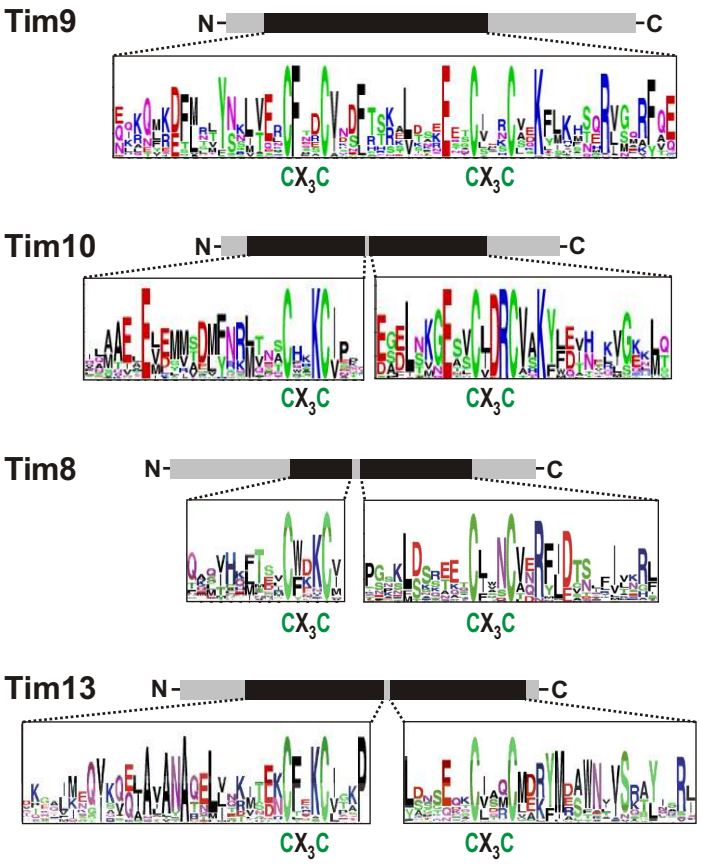
Tim9
N-
-C
CX3C
CX3C
Tim10
N-
-C
CX3C
CX3C
Tim8
N-
-C
CX3C
CX3C
Tim13
N-
-C
CX3C
CX3C

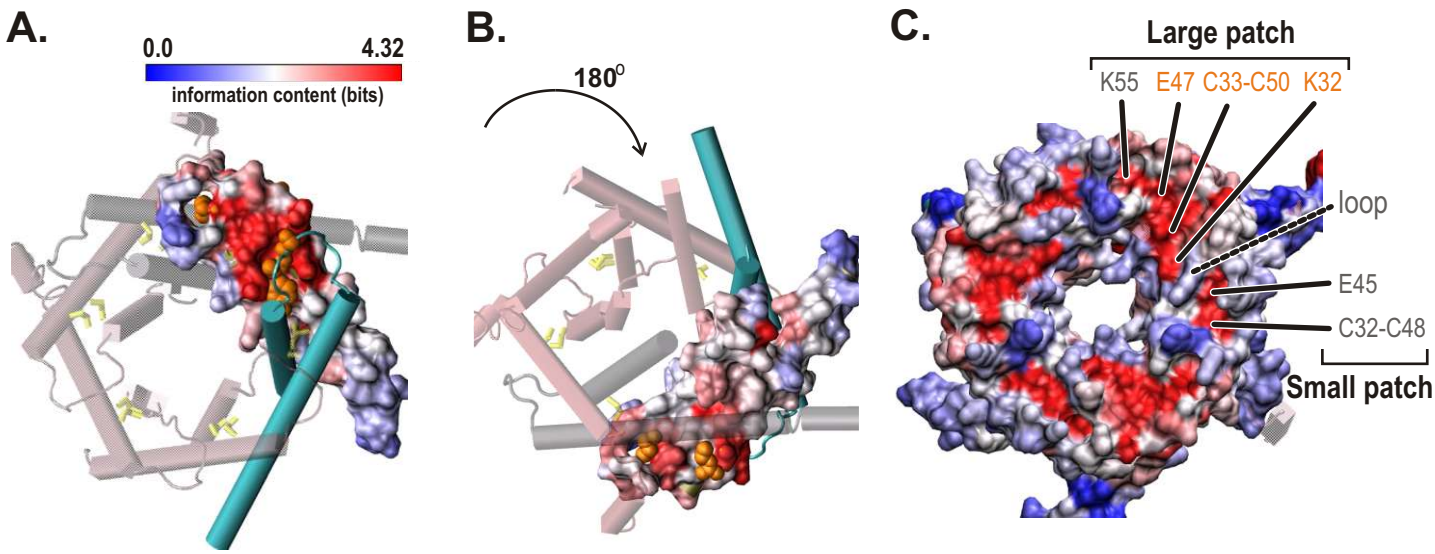
A.
0.0
4.32
information content (bits)
B.
180°
C.
Large patch
K55
E47
C33-C50
K32
loop
E45
C32-C48
Small patch

A.

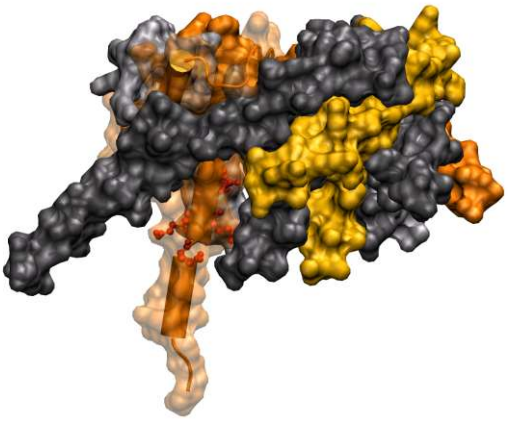

B.

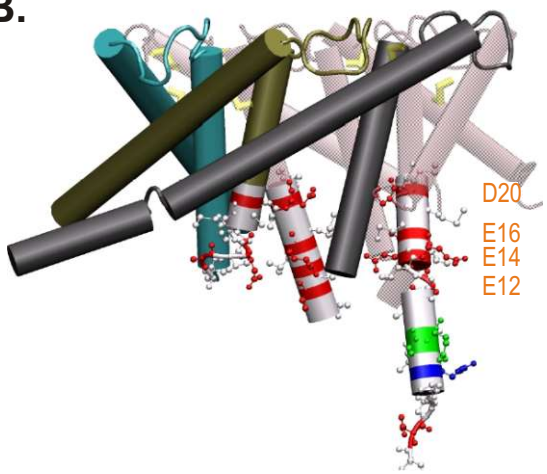

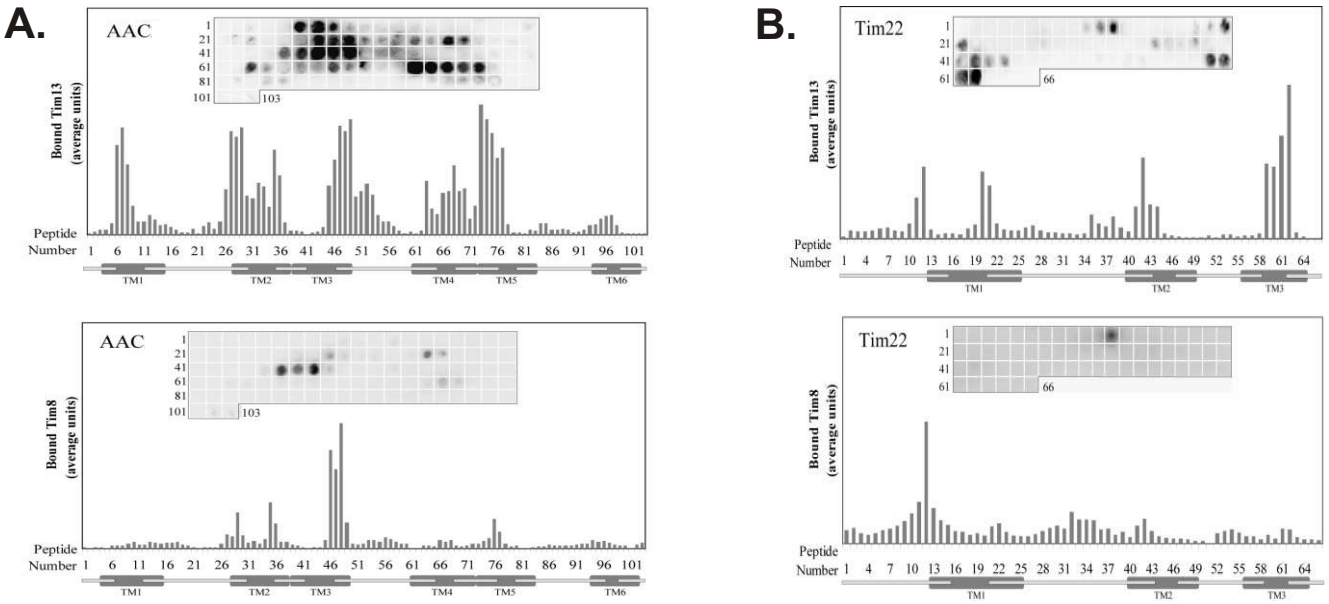
A.
AAC
Bound Tim13 (average units)
Peptide Number
TM1
TM2
TM3
TM4
TM5
TM6
AAC
Bound Tim8 (average units)
Peptide Number
B.
Tim22
Bound Tim13 (average units)
Peptide Number
Tim22
Bound Tim8 (average units)
Peptide Number

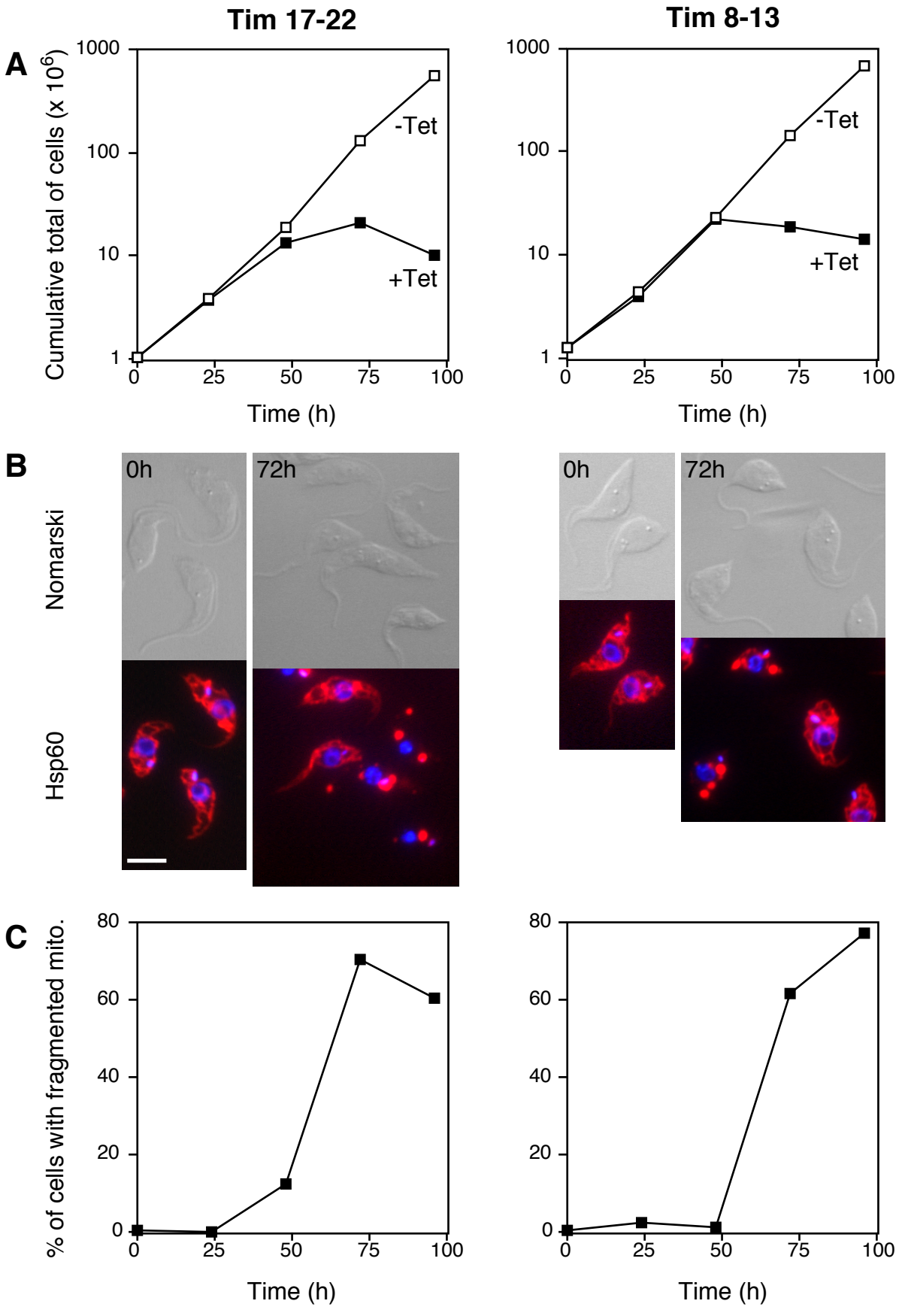
A
Tim 17-22
Tim 8-13
Cumulative total of cells (x 10^6)
1000
100
10
1
-Tet
+Tet
0
25
50
75
100
Time (h)
B
Nomarski
Hsp60
0h
72h
C
% of cells with fragmented mito.
80
60
40
20
0

	Tim9	Tim10	Tim8	Tim13	other
Fungi					
Saccharomyces cerevisiae	O74700	P87108	P57744	P53299	P32830[10]
Neurospora crassa	Q8J1Z1	Q9C0N3	Q9Y8C0	Q7SBR3	none
Eremothecium gossypii	Q757S0	Q759W7	Q75DU7	Q75F72	AAS51609[10]
Encephalitozoon cuniculi	none	none	none	none	none
Animals					
Homo sapiens	Q9Y5J7	P62072	O60220 Q9Y5J9	AAF15101 AAF15102	Q9Y5J6[9]
Mus musculus	Q9WV98	P62073	Q9WVA2 P62077	P62075 BAB22536	Q9WV96[9]
Danio rerio	Q9W762	Q6DI06	Q6DEM5	Q6DGJ3	Q568N4
Caenorhabditis elegans	Q17754	Q9Y0V6	Q9N408	O45319	Q9Y0V2[9]
Drosophila melanogaster	Q9VYD7	Q9W2D6	Q9Y1A3	Q9VTN3	Q9Y0V3[9]
Plants					
Arabidopsis thaliana	Q9XGX9	Q9ZW33	Q9XGY4	Q9XH48	none
Oryza sativa	Q9XGX7	Q7XI32	Q6Z1H2	Q7XUM9	none
Protists					
Dictyostelium discoideum	EAL71103	EAL64919	none	none	none
Plasmodium falciparum	Q8ID24	Q8I5W2	Q8ILN5	Q8I500	Q8I472[13]
Plasmodium bergheii	Q4YMY2	Q4YCZ6	Q4Z7J2	Q4Z4Q5	Q4Z7B6[13]
Plasmodium chabaudi	Q4XVQ0	Q4XF82	CAH85260	Q4XDV1	Q4Y1F0[8]
Plasmodium yoelli	Q7RCS2	Q7RBI2	Q7R8G4	Q7RH88	Q7RFP3[8]
Theileria parva	EAN34037	EAN34123	EAN30577		none
Cryptosporidium parvum	none	none	EAK90166		none
Cryptosporidium hominis	none	none	EAL36478		none
Leishmania major	CAJ03937	CAJ05328	CAJ04425		none
Trypanosoma brucei	AAX69615	AAX80231	EAN79502		none
Trypanosoma cruzi	EAN98593	EAN94952	EAN92571		none
Trichomonas vaginalis	none	none	none	none	none

Hidden Markov models were built to describe Tim9, Tim10, Tim8 and Tim13 and used to sift the data in UniProt. The listed organisms have complete genome sequences represented in UniProt.

[8] - weak similarity to Tim8
[9] - strong similarity to Tim9, functional studies reveal the protein to be located on the inner membrane and part of the TIM22 complex in humans (ref)
[10] - weak similarity to Tim10, functional studies show the protein to be located on the inner membrane and part of the TIM22 complex in yeast (ref)
[13] - weak similarity to Tim13

Remerciements

Au terme de cette thèse de doctorat, je tiens à remercier tout particulièrement André Schneider pour sa grande disponibilité. Sans lui ce travail n'aurait pas été possible. En plus des connaissances relatives à mes projets de doctorat, André m'a enseigné l'attitude à avoir face à la recherche scientifique, dont les maîtres mots sont la rigueur, la patience, le sens critique, l'humilité, et la bonne humeur même dans les moments difficiles.

Je voudrais également remercier tous les membres du "Trypsli lab" pour leur précieuse aide et leur sourire: Eric Aeby, Nabile Bouzaidi-Tiali, Mascha Pusnik, Anne-Laure Chanez, Anne Crausaz-Esseiva, Stephan Nicolet, Martin Spicher, Dani Thut, Elke K. Horn et Laurence Bulliard.

Un grand merci également à tous les membres de l'institut de Zoologie.

Merci aussi à ma famille qui m'a beaucoup soutenu dans l'entreprise de cette thèse.

Je tiens surtout à remercier Catherine qui m'a énormément encouragé pendant ce travail.

Curriculum Vitae

Fabien Charrière
Russalet 7
1630 Bulle
Switzerland
Date of birth: August 9th 1978

Single
E-mail: fabien.charriere@unifr.ch
Mobile: 0041 (0)79 427 18 32
Phone (Lab): 0041 (0)26 300 88 93

EDUCATION AND PROFESSIONAL EXPERIENCE

11. 2003 - Present	PhD in molecular cell biology / biochemistry, Institute of Zoology, **University of Fribourg**, under the direction of Prof. André Schneider
02. – 06. 2003	Visiting fellow in the Plant Cell Biology group, **Australian National University** of Canberra, supervised by Prof. Adrienne Hardham
10. 1998 – 12. 2002	Master in biology with emphasis on biochemistry, cell and molecular biology, Plant Cell Biology Institute, **University of Fribourg,** supervised by Prof. Felix Mauch - 04. 2002: Teaching of biology, Collège du Sud (Gymnasium), Bulle - 09. - 10. 2001: Summer student in the Agrochemical company **Syngenta** in Stein/BS

PUBLICATIONS

Charrière F, Helgadóttir S, Horn EK, Söll D, Schneider A: Dual targeting of a single tRNA(Trp) requires two different tryptophanyl-tRNA synthetases in *Trypanosoma brucei*. *Proc Natl Acad Sci U S A* 2006, 103(18):6847-6852.

Charrière F, Tan TH, Schneider A: Mitochondrial initiation factor 2 of *Trypanosoma brucei* binds imported formylated elongator-type tRNA(Met). *J Biol Chem* 2005, 280(16):15659-15665.

Schneider A, **Charrière F**, Pusnik M, Horn EK: Isolation of mitochondria from procyclic *Trypanosoma brucei, Methods Mol Biol* 2006, vol. 372.

Geslain R, Aeby E, Guitart T, Jones TE, de Moura MC, **Charrière F**, Schneider A, Ribas de Pouplana L: *Trypanosoma* seryl-tRNA synthetase is a metazoan-like enzyme with high affinity for $tRNA^{Sec}$. Submitted

Gentle IE, Perry AJ, Alcock FH, Likić VA, Dolezal P, Ng ET, McConnville M, Naderer T, Chanez AL, **Charrière F**, Aschinger C, Schneider A, Tokatlidis K and Lithgow T: Conserved motifs reveal details of ancestry and structure in the small TIM chaperones of the mitochondrial intermembrane space. Submitted

TALKS AND CONFERENCES

(Glasgow, August 2006) : "International Congress of Parasitology". Title: *Cytosolic and mitochondrial aminoacylation of nucleus-encoded $tRNA^{Trp}$ of Trypanosoma brucei requires distinct enzymes* (poster presentation).

(Leysin, February 2006): Annual "Swiss trypanosomatid meeting". Title: *Why two tryptophanyl-tRNA synthetases in Trypanosoma brucei ?* (poster presentation).

(Bern, October 2005) : "Swiss RNA workshop". Title: *Tryptophanyl-tRNA formation in Trypanosoma brucei* (oral presentation).

(Leysin, January 2005): Annual "Swiss trypanosomatid meeting". Title: *Mitochondrial translation initiation in Trypanosoma brucei: the role of Initiation Factor 2* (oral presentation).

(Rome, October 2004): "Third Joint Workshop of WP4 and WP5" about mitochondrial transcription, RNA processing, and translation. Title: *Mitochondrial translation initiation in Trypanosoma brucei: the role of initiation factor 2* (oral presentation).

(Strasbourg, July 2004): "Miteuro training course WP6" about RNA transport into mitochondria. Title: *Consequences of tRNA import in T. brucei for the mitochondrial translation initiation* (oral presentation).

LANGUAGES

French : first language
English : very good knowledge, written and spoken
German : good knowledge

REFERENCES

André Schneider (Professor)
Department of Biology, University of Fribourg
Chemin du Musée 10
1700 Fribourg
Switzerland
Phone: 0041 (0)26 300 88 77
E-mail: andre.schneider@unifr.ch

Dieter Söll (Professor, Member of the National Academy of Sciences of the USA)
Department of Molecular Biophysics and Biochemistry,
Yale University
266 Whitney Avenue
New Haven, CT 06520-8114, USA
Phone: 001 203 432 6200
E-mail: soll@trna.chem.yale.edu